

Supplement

for

**Zwitterionic biphenyl quinone methides in
photodehydration reactions of 3-hydroxybiphenyl
derivatives: laser flash photolysis and
antiproliferation study**

By

Nikola Basarić,*^a Damir Bobinac,^a Nikola Cindro,^a Lidija Uzelac,^b Kata Mlinarić-Majerski,^a Marijeta Kralj,^b Peter Wan^c

^a Department of Organic Chemistry and Biochemistry, Ruđer Bošković Institute,
Bijenička cesta 54, 10 000 Zagreb, Croatia.

Fax: + 385 1 4680 195; Tel: +385 1 4561 141; E-mail: nbasaric@irb.hr

^b Department of Molecular Medicine, Ruđer Bošković Institute, Bijenička cesta 54,
10000 Zagreb, Croatia

^c Department of Chemistry, University of Victoria, Box 3065 Stn CSC, Victoria BC,
V8W3V6, Canada.

Table of contents:

1. Experimental procedures and characterization of compounds	S3
2. Irradiations of 4-8 under different conditions	S6
3. UV-vis and Fluorescence spectra of 4-8	S9
4. Laser Flash Photolysis of 4-8	S17
5. Antiproliferative investigation	S24
6. Cross-linking and cleavage of Plasmid DNA	S25
7. ^1H and ^{13}C NMR spectra	S28

1. Experimental procedures and characterization of compounds

General

^1H and ^{13}C NMR spectra were recorded on a Bruker AV- 300, 500 or 600 MHz. The NMR spectra were taken in CDCl_3 or $\text{DMSO}-d_6$ at rt using TMS as a reference and chemical shifts were reported in ppm. Melting points were determined using an original Köfler Mikroheiztisch apparatus (Reichter, Wien) and were not corrected. UV-VIS spectra were recorded on a Varian Cary 100 Bio spectrophotometer at rt. IR spectra were recorded on a FT-IR-ABB Bomem MB 102 spectrophotometer in KBr. Deuterium content was determined by MS recorded on an Agilent 6410 Triple Quadrupole Mass Spectrometer by use of the electrospray ionization technique. The spectra were obtained in the positive and negative mode in the presence of formic acid. HRMS were obtained on an Applied Biosystems 4800 Plus MALDI TOF/TOF instrument (AB, Foster City, CA). For the sample analysis a Shimadzu HPLC equipped with a Diode-Array detector and a Phenomenex Luna 3u C18(2) column was used. Mobile phase was $\text{CH}_3\text{OH}-\text{H}_2\text{O}$ (20 %). For the chromatographic separations silica gel (Merck 0.05-0.2mm) was used. Analytical thin layer chromatography was performed on Polygram® SILG/UV₂₅₄ (Machery-Nagel) plates. Irradiation experiments were performed in a Rayonet reactor equipped with 16 lamps with the output at 254 nm or a Luzchem reactor equipped with 8 lamps. During irradiations in the Rayonet, the irradiated solutions were continuously purged with Ar and cooled by a tap-water finger-condenser. Solvents for irradiation were of HPLC purity. Chemicals (dibromobenzenes, bromoanisoles, 2-adamantanone, solution of BBr_3) were purchased from the usual commercial sources and were used as received. Solvents for chromatographic separations were purified by distillation.

Suzuki reaction, general procedure

A two neck flask (100 mL) equipped with a condenser and a nitrogen inlet was charged with a methanol solution (15 mL) of 3-methoxyphenyl boronic acid (1.50 g, 10 mmol) and a toluene solution (35 mL) of dibromobenzene (2.33 g, 10 mmol). To the mixture was added anhydrous potassium carbonate (2.73 g, 19.72 mmol) and *tetrakis*-

triphenylphosphine palladium $\text{Pd}(\text{PPh}_3)_4$ (0.17 g, 0.148 mmol), and the mixture was heated at the temperature of reflux for 24 h. The next day, to the cooled mixture H_2O (50 mL) was added and the layers were separated. The aqueous layer was extracted with CH_2Cl_2 (3×30 mL), the organic layers were combined and dried over anhydrous MgSO_4 . After filtration, the solvent was removed on a rotary evaporator to afford crude product that was purified on a column of silica gel using hexane- CH_2Cl_2 (2:1) as an eluent.

2-bromo-3'-methoxybiphenyl

From 3-methoxyphenyl boronic acid (1.5 g, 10 mmol) and *o*-dibromobenzene (2.35 g, 10 mmol), in the presence of potassium carbonate (2.74 g, 20 mmol) and $\text{Pd}(\text{PPh}_3)_4$ (0.14 g, 0.12 mmol), the reaction furnished 1.03 g (40%) of the product in the form of yellowish oil.

^1H NMR (CDCl_3 , 300 MHz) δ/ppm 7.66 (d, 1H, $J = 8.0$ Hz), 7.30-7.38 (m, 3H), 7.20 (dd, 1H, $J = 8.0$ Hz, $J = 3.1$ Hz), 6.98 (dt, 1H, $J = 7.7$ Hz, $J = 1.2$ Hz), 6.90-6.96 (m, 2H), 3.84 (s, 3H, OCH_3); ^{13}C NMR (CDCl_3 , 75 MHz) δ/ppm 159.00 (s), 142.31 (s), 133.00 (d), 131.08 (d), 128.88 (d), 128.65 (d), 127.20 (d), 122.49 (s), 121.71 (d), 114.94 (d), 113.12 (d), 55.18 (q), one singlet was not observed.

3-bromo-3'-methoxybiphenyl

From 3-methoxyphenyl boronic acid (1.5 g, 10 mmol) and *m*-dibromobenzene (2.35 g, 10 mmol), in the presence of potassium carbonate (2.74 g, 20 mmol) and $\text{Pd}(\text{PPh}_3)_4$ (0.14 g, 0.12 mmol), the reaction furnished 1.64 g (62%) of the product in the form of yellowish oil.

^1H NMR (CDCl_3 , 300 MHz) δ/ppm 7.72 (t, 1H, $J = 1.7$ Hz), 7.44-7.52 (m, 2H), 7.36 (t, 1H, $J = 7.9$ Hz), 7.29 (t, 1H, $J = 7.9$ Hz), 7.13 (d, 1H, $J = 7.7$ Hz), 7.07 (t, 1H, $J = 2.0$ Hz), 6.91 (dd, 1H, $J = 0.7$ Hz, $J = 8.2$ Hz), 3.86 (s, 3H, OCH_3); ^{13}C NMR ($\text{DMSO}-d_6$, 150 MHz) δ/ppm 159.75 (s), 142.49 (s), 140.04 (s), 130.91 (d), 130.27 (d), 130.04 (d), 129.33 (d), 125.89 (d), 122.27 (s), 119.10 (d), 113.85 (d), 112.18 (d), 55.17 (q).

4-bromo-3'-methoxybiphenyl

From 3-methoxyphenyl boronic acid (1.5 g, 10 mmol) and *p*-dibromobenzene (2.35 g, 10 mmol), in the presence of potassium carbonate (2.74 g, 20 mmol) and Pd(PPh₃)₄ (0.14 g, 0.12 mmol), the reaction furnished 1.35 g (51%) of the product in the form of yellowish oil.

¹H NMR (CDCl₃, 600 MHz) δ/ppm 7.54 (d, 2H, *J* = 8.5 Hz), 7.44 (d, 2H, *J* = 8.5 Hz), 7.34 (t, 1H, *J* = 7.9 Hz), 7.13 (d, 1H, *J* = 7.9 Hz), 7.07 (t, 1H, *J* = 2.0 Hz), 6.90 (d, 1H, *J* = 7.9 Hz), 3.85 (s, 3H, OCH₃); ¹³C NMR (CDCl₃, 150 MHz) δ/ppm 159.95 (s), 141.42 (s), 139.91 (s), 131.73 (d, 2C), 129.80 (d), 128.66 (d, 2C), 121.55 (s), 119.33 (d), 112.87 (d), 112.70 (d), 55.22 (q).

2. Irradiations of 4-8 in CH₃OH-H₂O under different conditions.

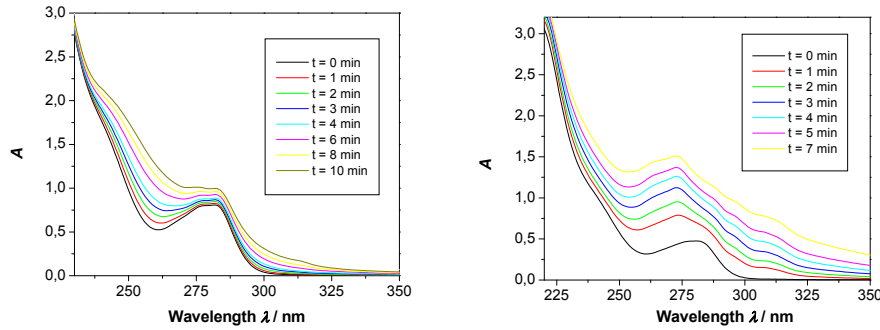


Fig 1. UV-Vis spectra after photolyses (16 lamps 254 nm) of **4** in a UV-vis cuvette in CH₃CN (left) and CH₃CN-H₂O (1:1) (right).

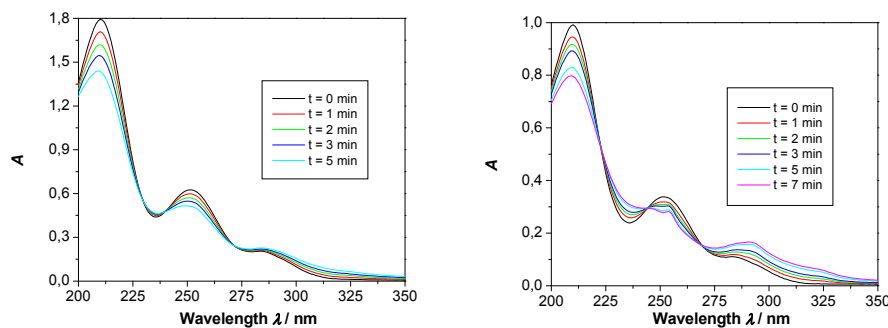


Fig 2. UV-Vis spectra after photolyses (16 lamps 254 nm) of **5** in a UV-vis cuvette in CH₃CN (left) and CH₃CN-H₂O (1:1) (right)

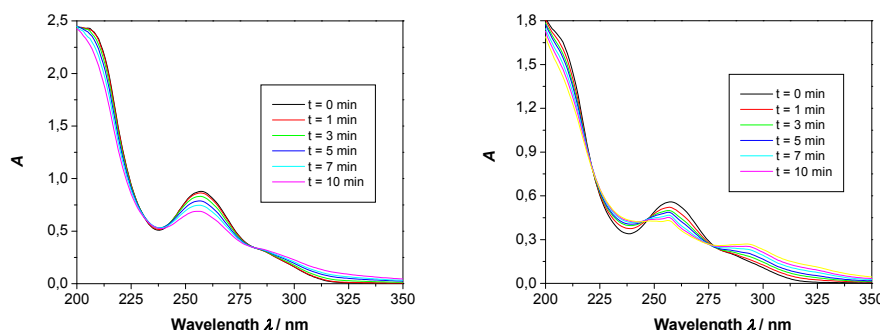


Fig 3. UV-Vis spectra after photolyses (16 lamps 254 nm) of **8** in a UV-vis cuvette in CH₃CN (left) and CH₃CN-H₂O (1:1) (right)

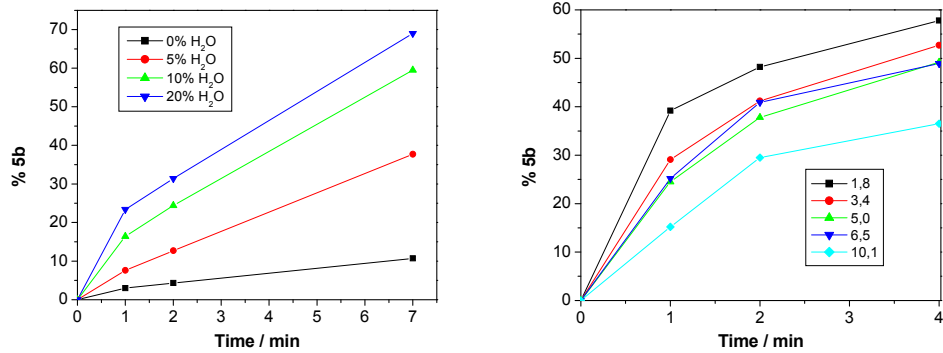


Fig. 4. Conversion of **5** to **5b** on photolysis (8 lamps, 254 nm) in CH₃OH-H₂O with different H₂O content (left) and in CH₃OH-H₂O (1:1) at different pH (right).

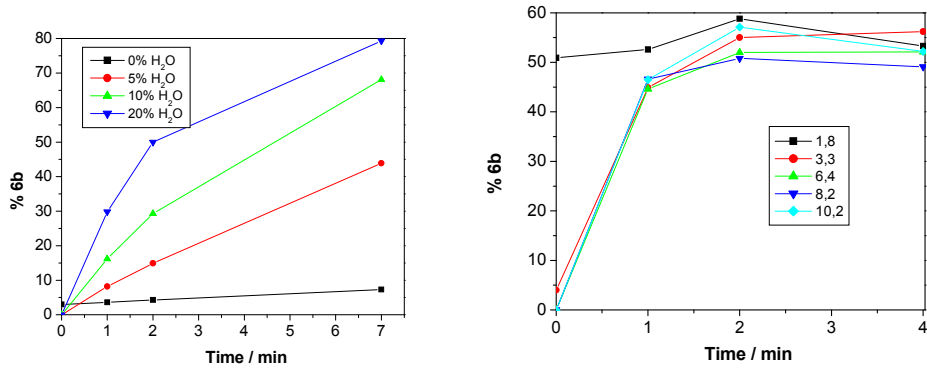


Fig. 5. Conversion of **6** to **6b** on photolysis (8 lamps, 254 nm) in CH₃OH-H₂O with different H₂O content (left) and in CH₃OH-H₂O (1:1) at different pH (right).

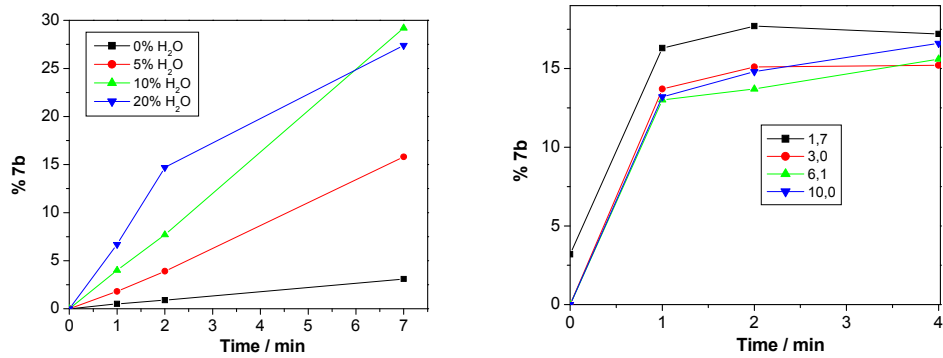


Fig. 6. Conversion of **7** to **7b** on photolysis (8 lamps, 254 nm) in CH₃OH-H₂O with different H₂O content (left) and in CH₃OH-H₂O (1:1) at different pH (right).

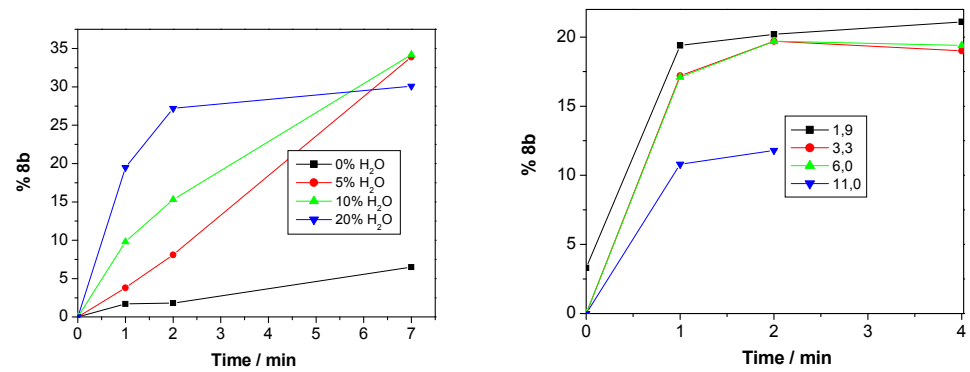


Fig. 7. Conversion of **8** to **8b** on photolysis (8 lamps, 254 nm) in CH₃OH-H₂O with different H₂O content (left) and in CH₃OH-H₂O (1:1) at different pH (right).

3. UV-vis and Fluorescence Spectra of 4-8.

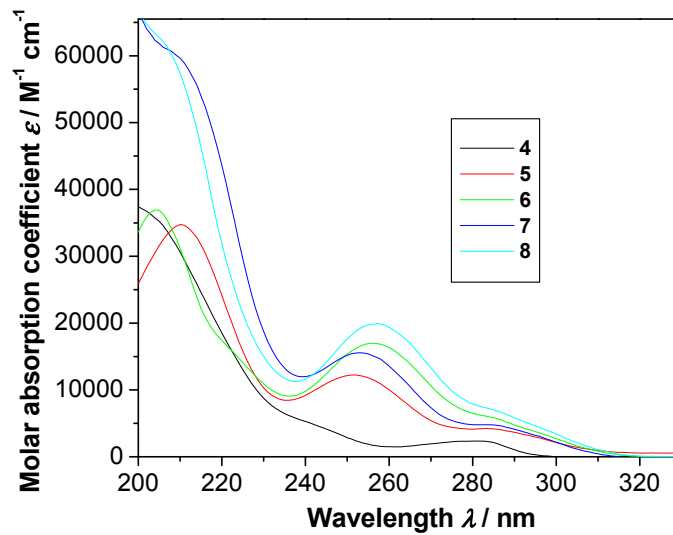


Fig. 8. Absorption spectra of **4-8** in CH_3CN .

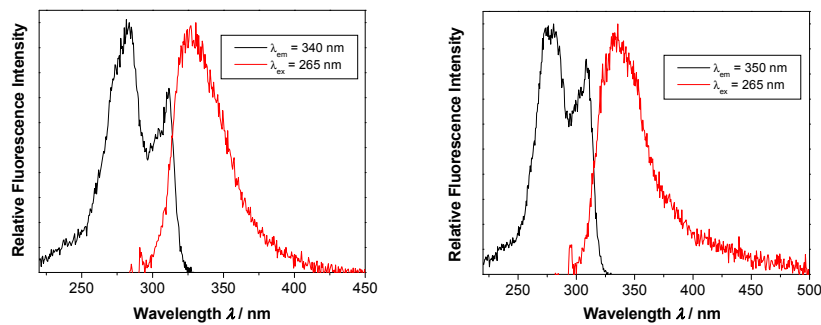


Fig. 9. Normalized excitation and emission spectra of **4** in CH_3CN (left) and $\text{CH}_3\text{CN}-\text{H}_2\text{O}$ (1:4) (right).

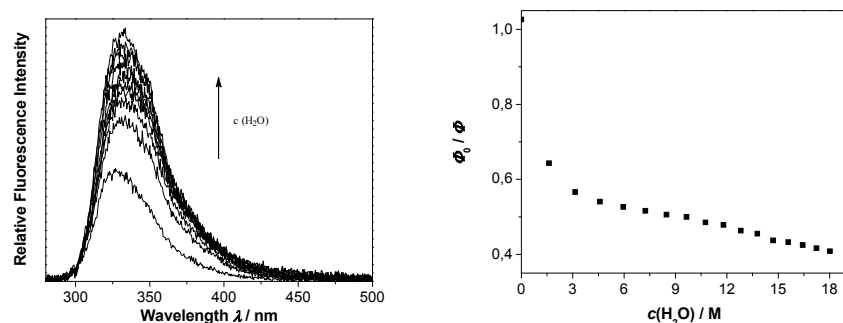


Fig. 10. Fluorescence spectra of **4** in CH_3CN on addition of H_2O (left) and Stern-Volmer quenching plot of fluorescence of **4** in CH_3CN by addition of H_2O (right).

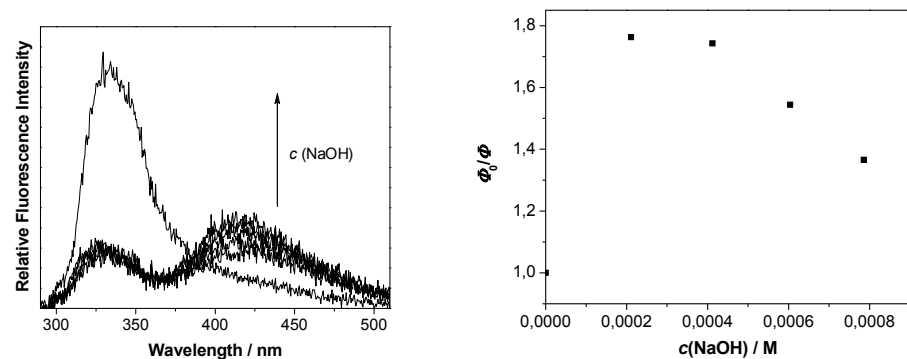


Fig. 11. Fluorescence spectra of **4** in $\text{CH}_3\text{CN}-\text{H}_2\text{O}$ (1:4) on addition of NaOH (left), and Stern-Volmer quenching plot of fluorescence of **4** in $\text{CH}_3\text{CN}-\text{H}_2\text{O}$ (1:4) by addition of NaOH (right).

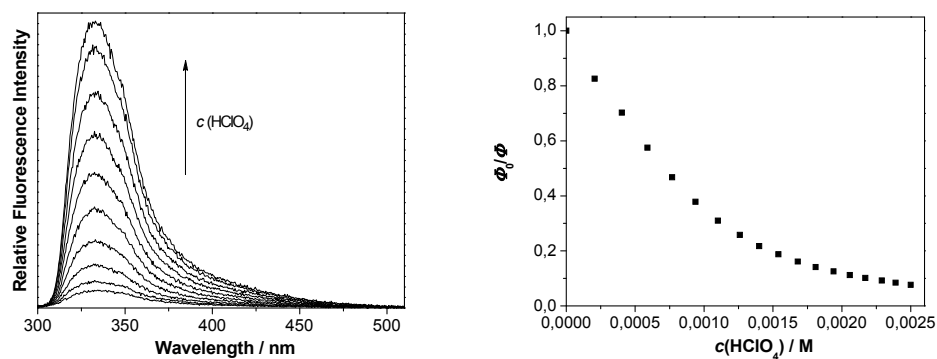


Fig. 12. Fluorescence spectra of **4** in $\text{CH}_3\text{CN}-\text{H}_2\text{O}$ (1:4) on addition of HClO_4 (left), and Stern-Volmer quenching plot of fluorescence of **4** in $\text{CH}_3\text{CN}-\text{H}_2\text{O}$ (1:4) by addition of HClO_4 (right).

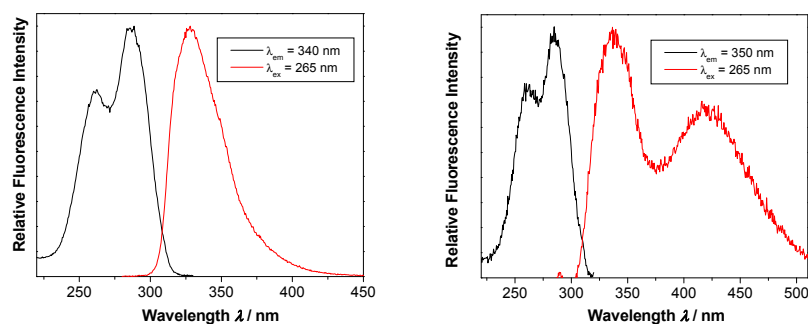


Fig. 13. Normalized excitation and emission spectra of **5** in CH_3CN (left) and $\text{CH}_3\text{CN}-\text{H}_2\text{O}$ (1:4) (right).

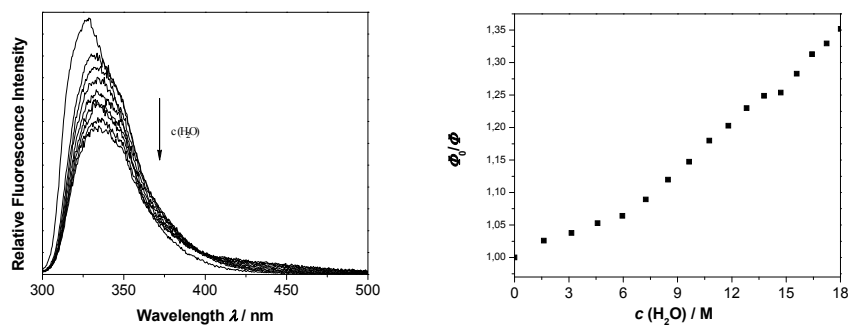


Fig. 14. Fluorescence spectra of **5** in CH_3CN on addition of H_2O (left) and Stern-Volmer quenching plot of fluorescence of **5** in CH_3CN by addition of H_2O (right).

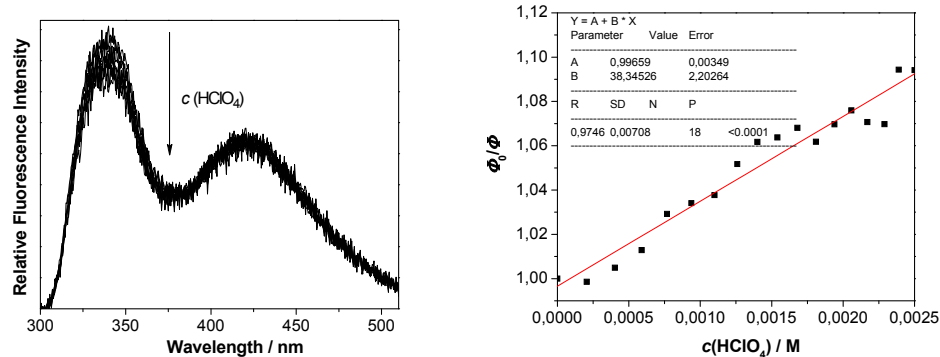


Fig. 15. Fluorescence spectra of **5** in $\text{CH}_3\text{CN}-\text{H}_2\text{O}$ (1:4) on addition of HClO_4 (left), and Stern-Volmer quenching plot of fluorescence of **5** in $\text{CH}_3\text{CN}-\text{H}_2\text{O}$ (1:4) by addition of HClO_4 (right).

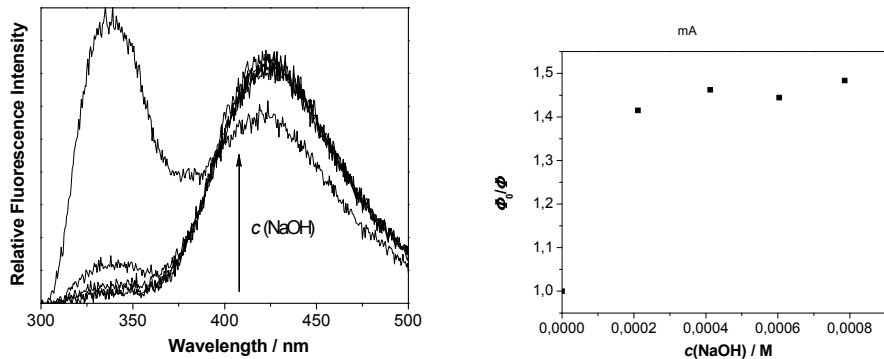


Fig. 16. Fluorescence spectra of **5** in $\text{CH}_3\text{CN}-\text{H}_2\text{O}$ (1:4) on addition of NaOH (left), and Stern-Volmer quenching plot of fluorescence of **5** in $\text{CH}_3\text{CN}-\text{H}_2\text{O}$ (1:4) by addition of NaOH (right).

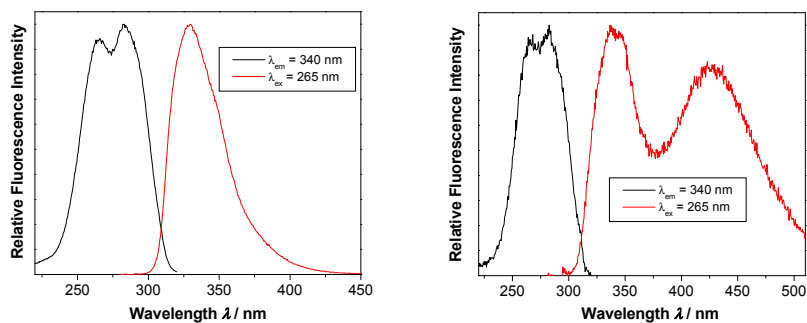


Fig. 17. Normalized excitation and emission spectra of **6** in CH_3CN (left) and $\text{CH}_3\text{CN}-\text{H}_2\text{O}$ (1:4) (right).

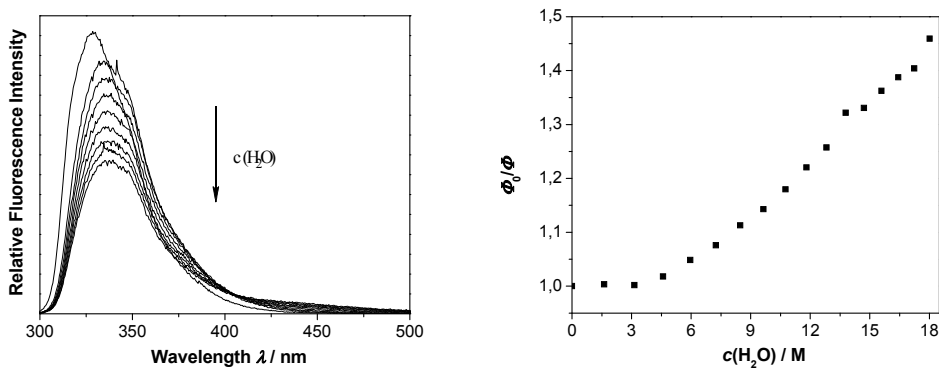


Fig. 18. Fluorescence spectra of **6** in CH_3CN on addition of H_2O (left) and Stern-Volmer quenching plot of fluorescence of **6** in CH_3CN by addition of H_2O (right).

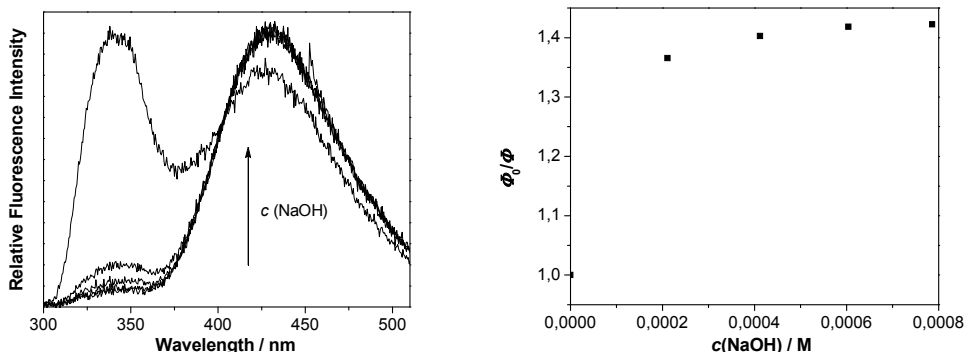


Fig. 19. Fluorescence spectra of **6** in $\text{CH}_3\text{CN}-\text{H}_2\text{O}$ (1:4) on addition of NaOH (left), and Stern-Volmer quenching plot of fluorescence of **6** in $\text{CH}_3\text{CN}-\text{H}_2\text{O}$ (1:4) by addition of NaOH (right).

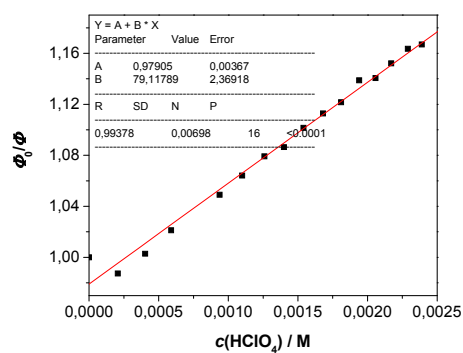


Fig. 20. Stern-Volmer quenching plot of fluorescence of **6** in $\text{CH}_3\text{CN}-\text{H}_2\text{O}$ (1:4) by addition of HClO_4 .

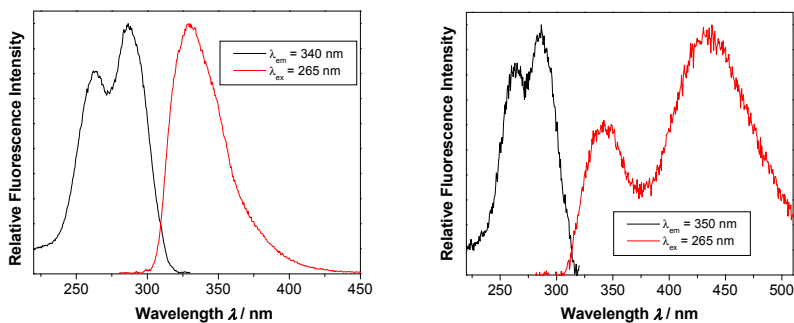


Fig. 21. Normalized excitation and emission spectra of **7** in CH_3CN (left) and $\text{CH}_3\text{CN}-\text{H}_2\text{O}$ (1:4) (right).

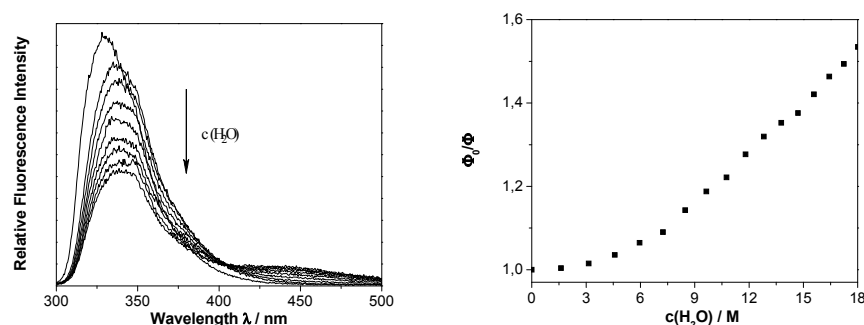


Fig. 22. Fluorescence spectra of 7 in CH_3CN on addition of H_2O (left) and Stern-Volmer quenching plot of fluorescence of 7 in CH_3CN by addition of H_2O (right).

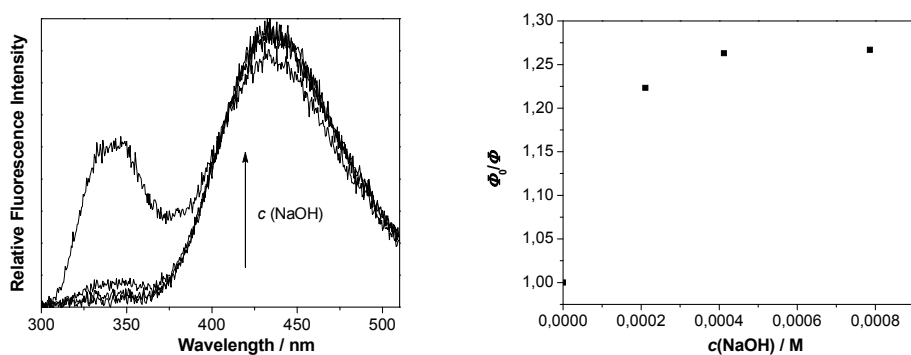


Fig. 23. Fluorescence spectra of 7 in $\text{CH}_3\text{CN}-\text{H}_2\text{O}$ (1:4) on addition of NaOH (left), and Stern-Volmer quenching plot of fluorescence of 7 in $\text{CH}_3\text{CN}-\text{H}_2\text{O}$ (1:4) by addition of NaOH (right).

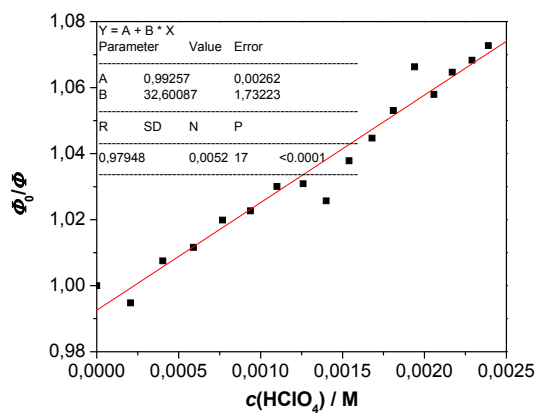


Fig. 24. Stern-Volmer quenching plot of fluorescence of 7 in $\text{CH}_3\text{CN}-\text{H}_2\text{O}$ (1:4) by addition of HClO_4 .

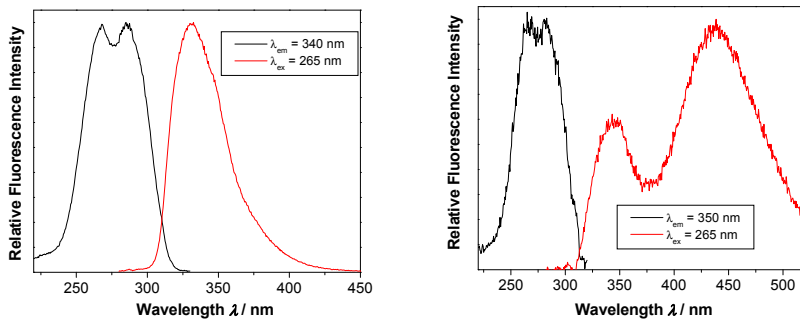


Fig. 25. Normalized excitation and emission spectra of **8** in CH_3CN (left) and $\text{CH}_3\text{CN}-\text{H}_2\text{O}$ (1:4) (right).

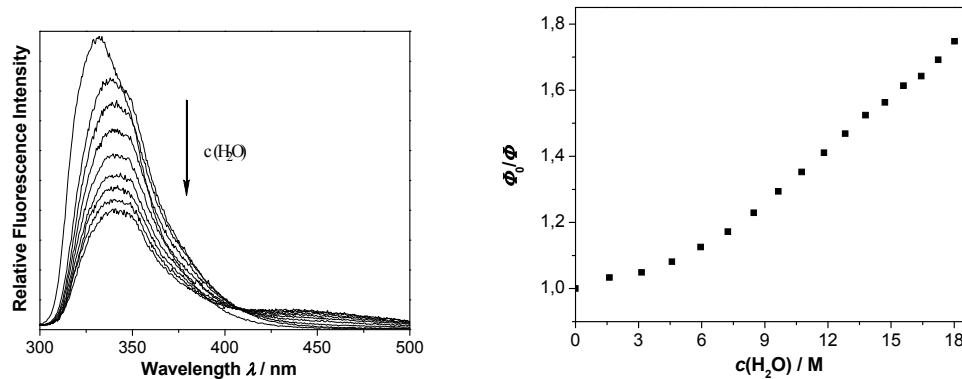


Fig. 26. Fluorescence spectra of **8** in CH_3CN on addition of H_2O (left) and Stern-Volmer quenching plot of fluorescence of **8** in CH_3CN by addition of H_2O (right).

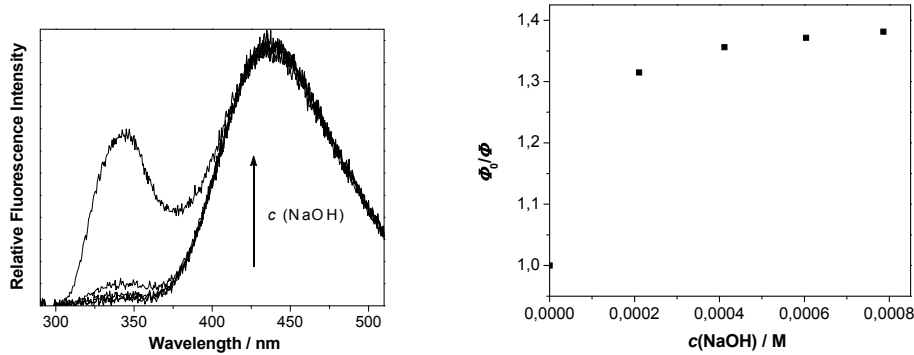


Fig. 27. Fluorescence spectra of **8** in $\text{CH}_3\text{CN}-\text{H}_2\text{O}$ (1:4) on addition of NaOH (left), and Stern-Volmer quenching plot of fluorescence of **8** in $\text{CH}_3\text{CN}-\text{H}_2\text{O}$ (1:4) by addition of NaOH (right).

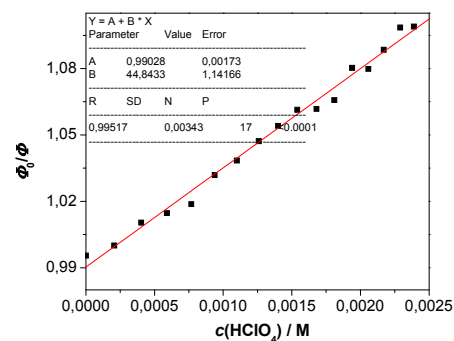


Fig. 28. Stern-Volmer quenching plot of fluorescence of **8** in $\text{CH}_3\text{CN}-\text{H}_2\text{O}$ (1:4) by addition of HClO_4 .

4. Laser Flash Photolysis

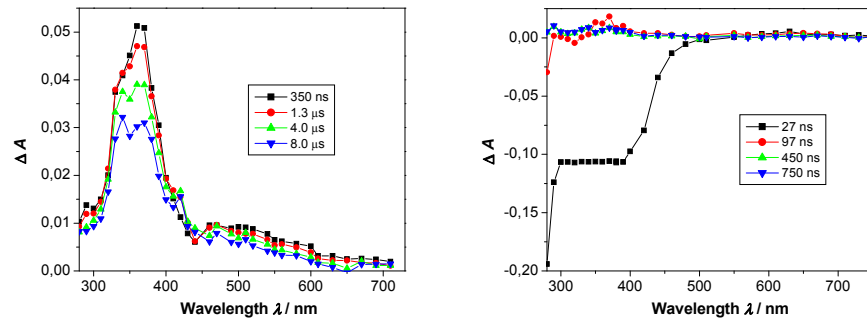


Fig. 29. Transient absorption spectra of N₂-purged TFE solution of **4** (left) and O₂-purged TFE solution of **4** (right).

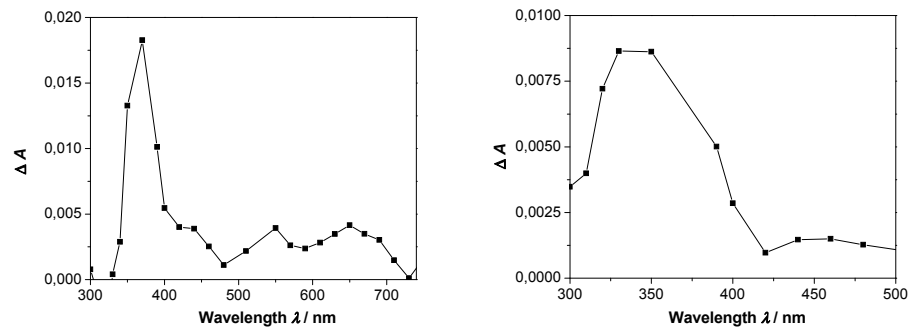


Fig. 30. Transient absorption spectra of O₂-purged TFE solution of **4**, 97 ns (left) and 450 ns (right) after the laser pulse.

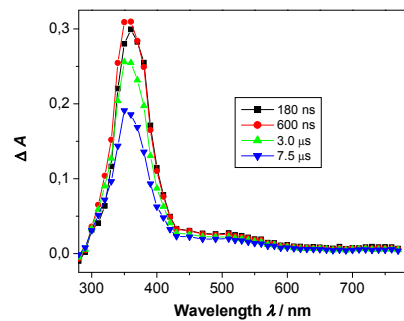


Fig. 31. Transient absorption spectra of N₂-purged TFE solution of **5**.

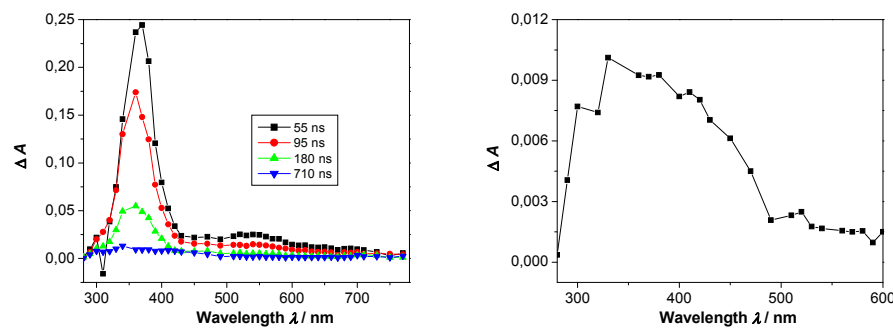


Fig. 32. Transient absorption spectra of O_2 -purged TFE solution of **5** (left) and O_2 -purged TFE solution of **5**, 710 ns after the laser pulse (right).

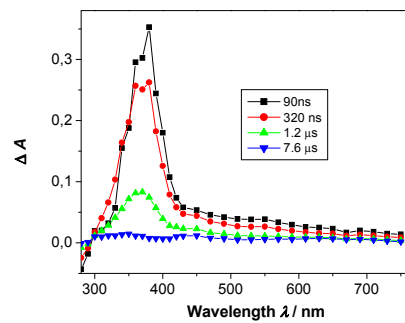


Fig. 33. Transient absorption spectra of N_2 -purged TFE solution of **6**.

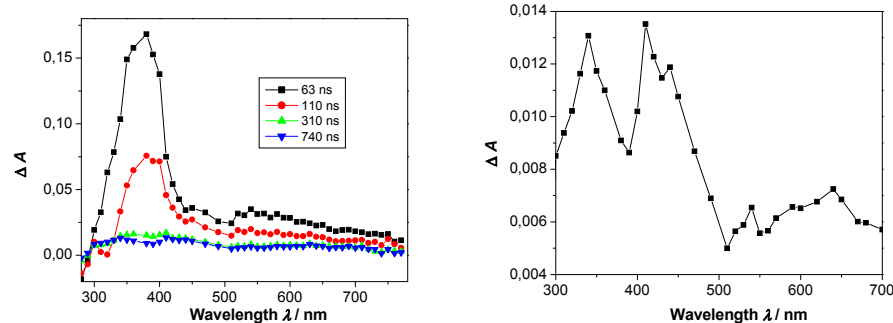


Fig. 34. Transient absorption spectra of O_2 -purged TFE solution of **6** (left) and O_2 -purged TFE solution of **6**, 740 ns after the laser pulse (right).

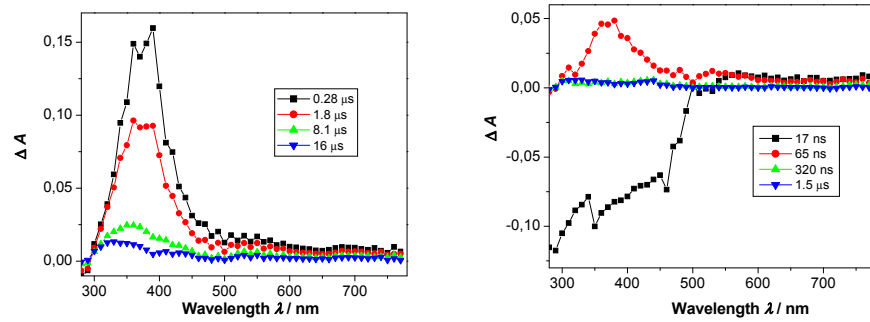


Fig. 35. Transient absorption spectra of N₂-purged (left) and O₂-purged (right) CH₃CN solution of 7.

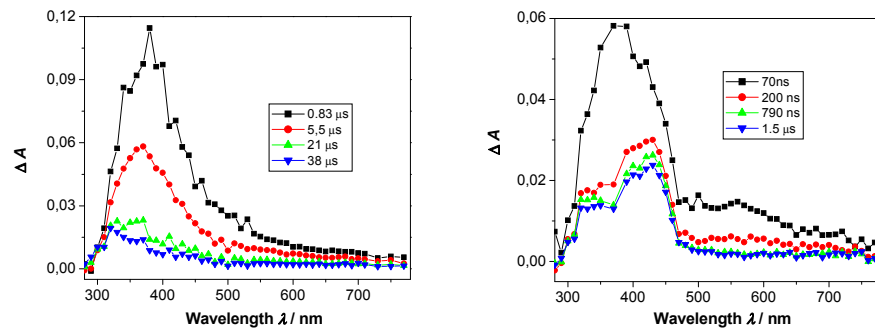


Fig. 36. Transient absorption spectra of N₂-purged and O₂-purged (right) CH₃CN-H₂O (1:1) solution of 7.

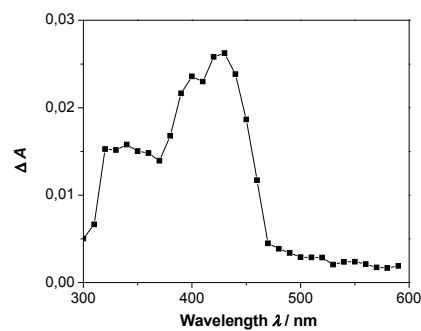


Fig. 37. Transient absorption spectrum of O₂-purged CH₃CN-H₂O (1:1) solution of 7, 790 ns after the laser pulse.

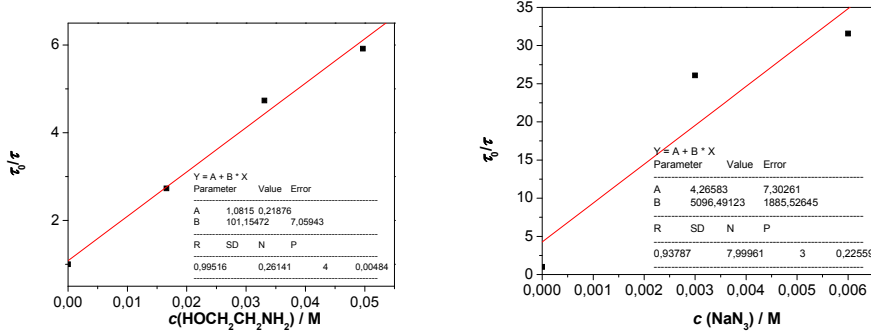


Fig. 38. Stern-Volmer plots for the quenching of the transient absorption of $\text{CH}_3\text{CN}-\text{H}_2\text{O}$ (1:1) solution of 7 by ethanolamine (left) and NaN_3 (right).

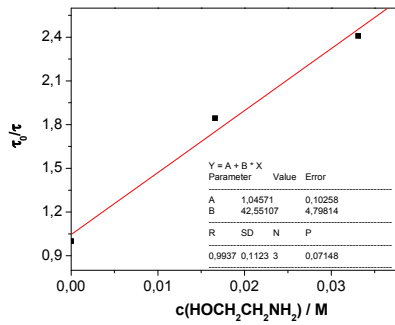


Fig. 39. Stern-Volmer plots for the quenching of the transient absorption at 600 nm of $\text{CH}_3\text{CN}-\text{H}_2\text{O}$ (1:1) solution of 7 by ethanolamine.

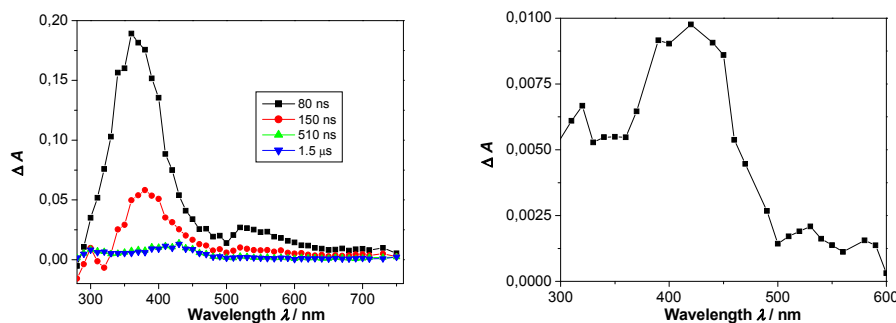


Fig. 40. Transient absorption spectra of O_2 -purged TFE solution of 7 (left) and O_2 -purged TFE solution of 7, 1.5 μs after the laser pulse (right).

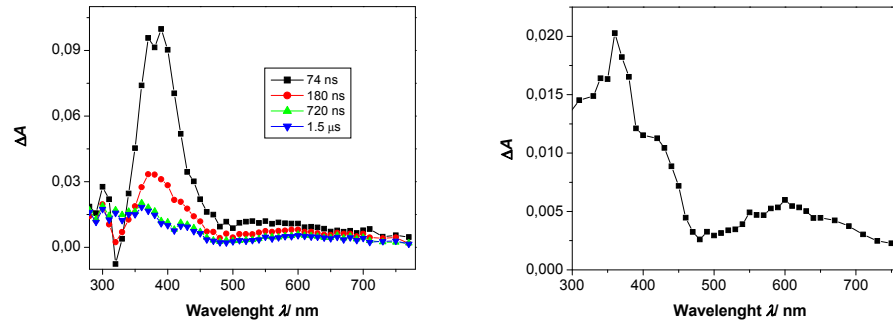


Fig. 41. Transient absorption spectra of O_2 -purged CH_3CN - H_2O (1:1) solution of **7a** (left) and O_2 -purged CH_3CN - H_2O (1:1) solution of **7a**, 720 ns after the laser pulse (right).

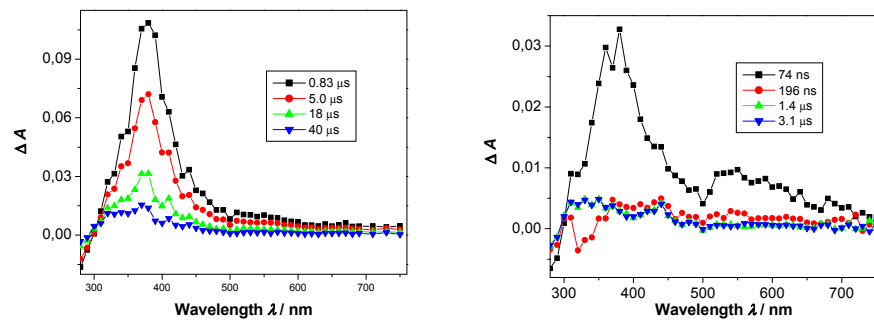


Fig. 42. Transient absorption spectra of N_2 -purged (left) and O_2 -purged (right) CH_3CN solution of **8**.

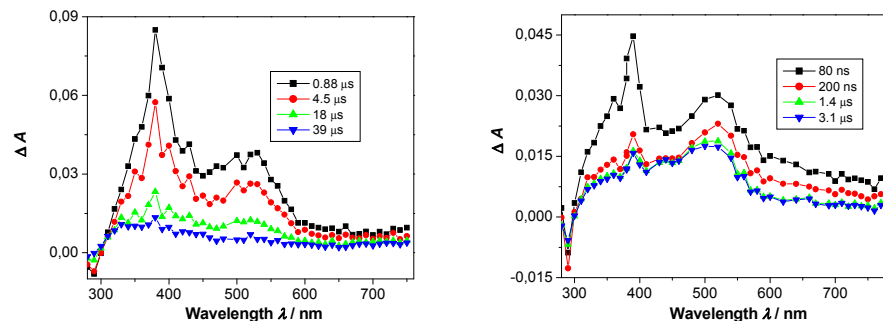


Fig. 43. Transient absorption spectra of N_2 -purged (left) and O_2 -purged (right) CH_3CN - H_2O (1:1) solution of **8**.

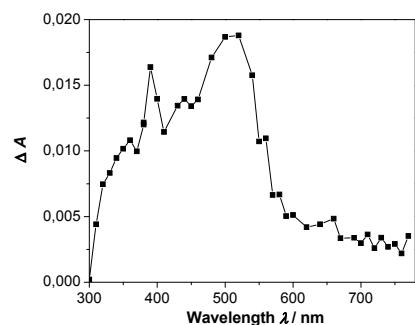


Fig. 44. Transient absorption spectrum of O_2 -purged $\text{CH}_3\text{CN}-\text{H}_2\text{O}$ (1:1) solution of **8**, 1.4 μs after the laser pulse.

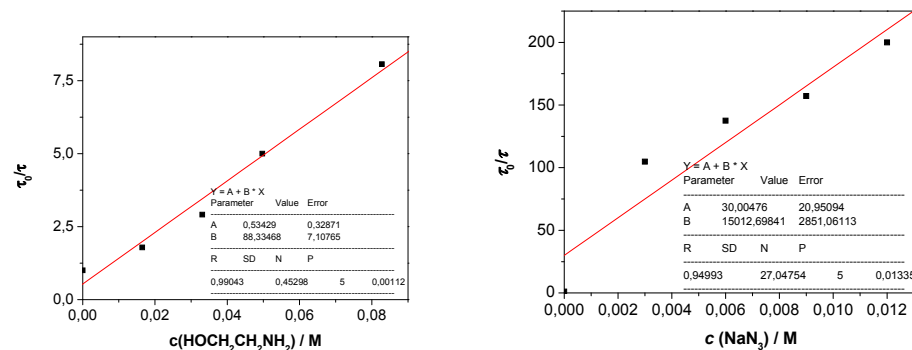


Fig. 45. Stern-Volmer plots for the quenching of the transient absorption of $\text{CH}_3\text{CN}-\text{H}_2\text{O}$ (1:1) solution of **8** by ethanolamine (left) and NaN_3 (right).

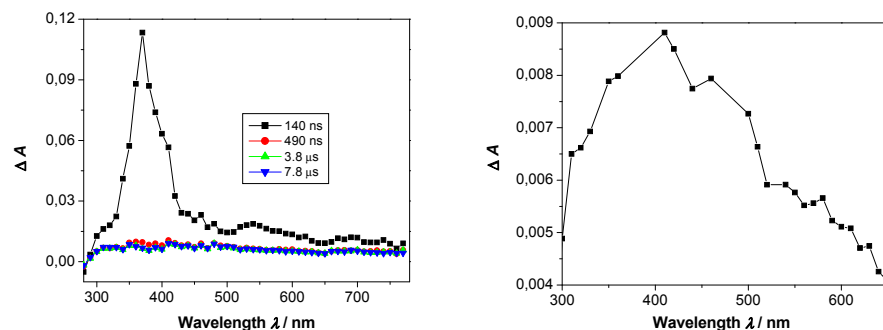


Fig. 46. Transient absorption spectra of O_2 -purged TFE solution of **8** (left) and O_2 -purged TFE solution of **8**, 4 μs after the laser pulse (right).

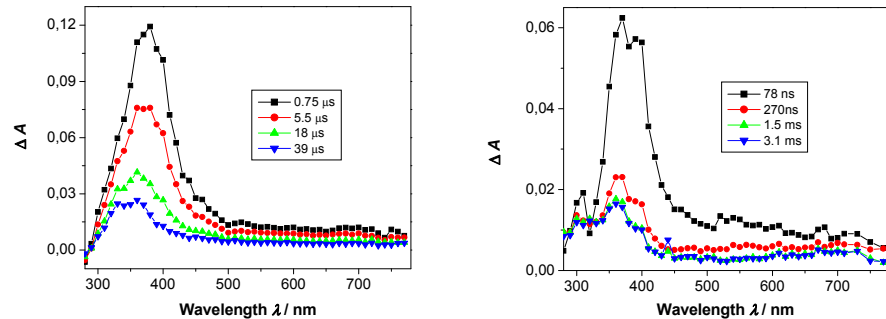


Fig. 47. Transient absorption spectra of N_2 -purged (left) and O_2 -purged (right) $\text{CH}_3\text{CN}-\text{H}_2\text{O}$ (1:1) solution of **8a**.

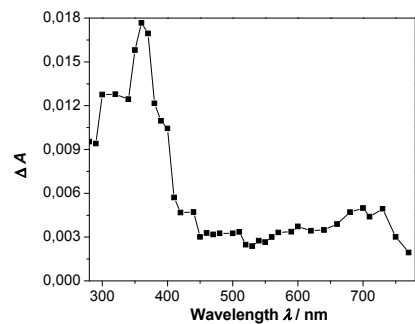
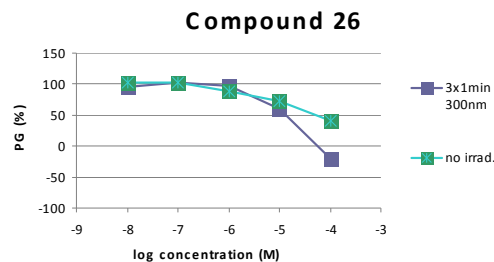


Fig. 48. Transient absorption spectrum of O_2 -purged $\text{CH}_3\text{CN}-\text{H}_2\text{O}$ (1:1) solution of **8a**, 1.5 μs after the laser pulse.

Radical cation at 600 nm 23 μs , quenched by ethanolamine, $k_{\text{q}} = 3 \times 10^8 \text{ M}^{-1} \text{ s}^{-1}$.

5. Antiproliferative investigation

A



B

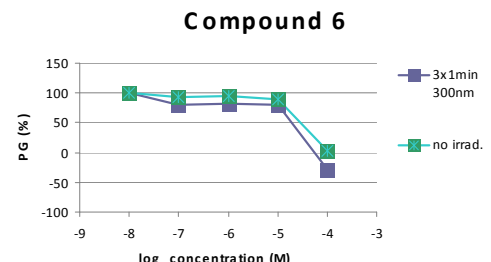


Fig 49. An example of dose-response profiles for compounds **26** and **6**, after irradiation 3×1 min at 300 nm and without irradiation, tested *in vitro* on MCF-7 cell line.

6. Cross-Linking and cleavage of Plasmid DNA

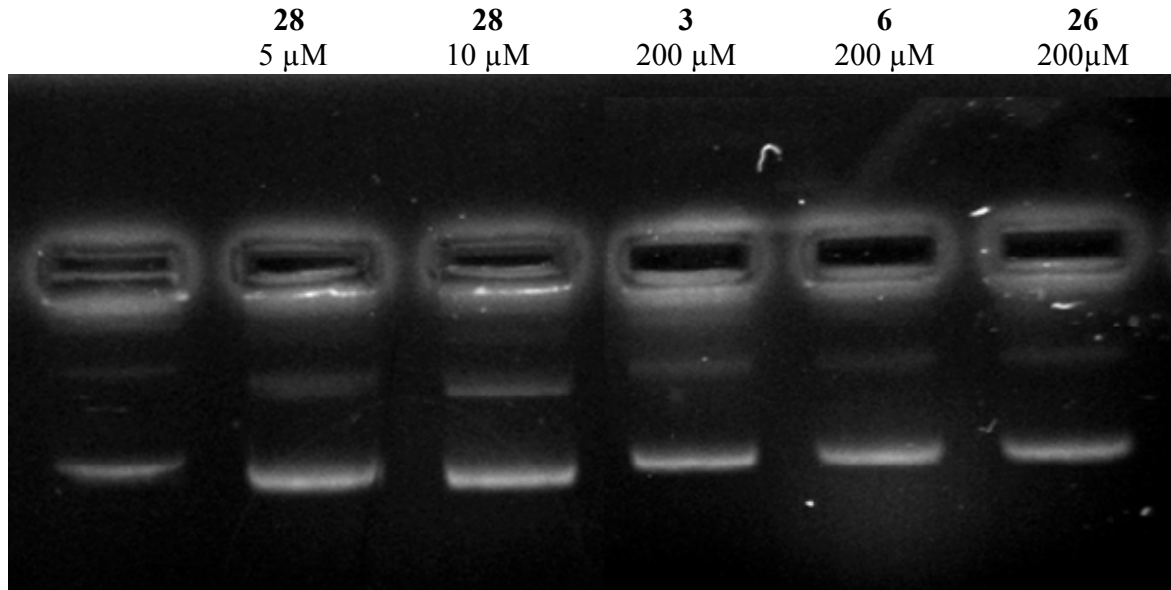


Fig. 50. Influence of selected test compounds on plasmid DNA cross-linking ability by compounds **3**, **6** and **26**, along with psoralen **28** as a positive control. Plasmid (pCI DNA (0.8 μ g) lane 1) DNA was mixed with psoralen (5 μ M), lane 2; (10 μ M), lane 3, compound **3** (200 μ M), lane 4, **6** (200 μ M), lane 5 and **26** (200 μ M), lane 6. Reaction mixtures were irradiated at 300 nm for 3 minutes and loaded on 1% alkaline agarose gel. Gels were stained with ethidium bromide and the resulting products were visualized and documented with UV light at 254 nm (Image Master VDS, Pharmacia Biotech, Sweden).

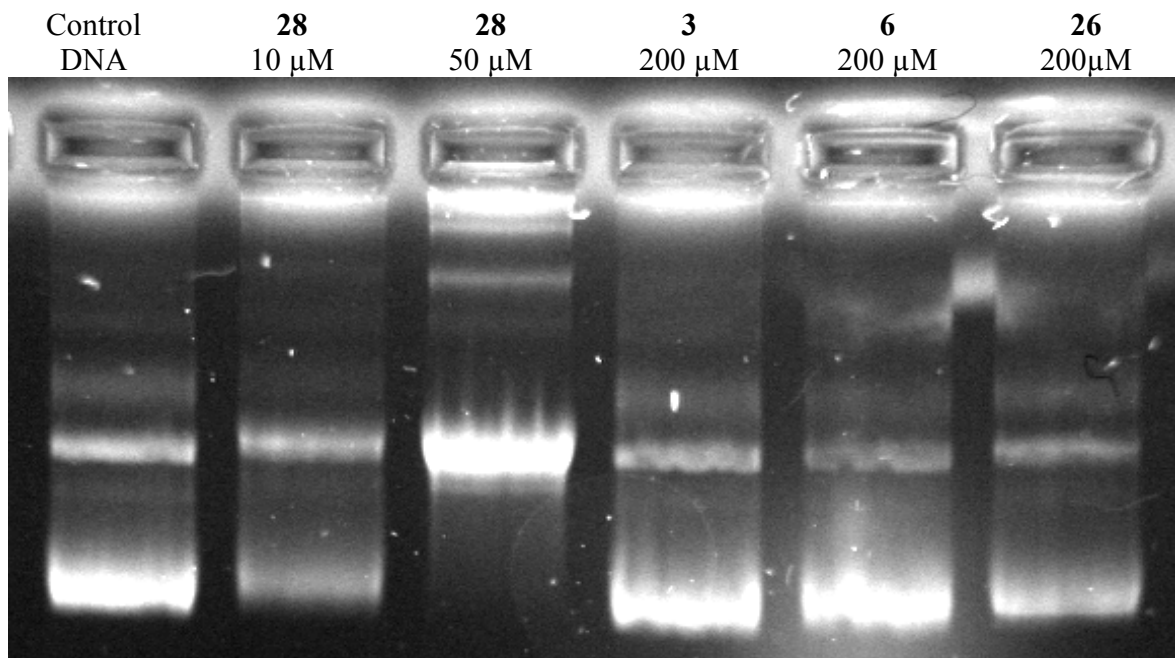


Fig. 51. Influence of selected test compounds on plasmid DNA cross-linking ability by compounds **3**, **6** and **26**, along with psoralen **28** as a positive control. Plasmid (pCI DNA (0.8 µg) lane 1) DNA was mixed with psoralen (10 µM), lane 2; (50 µM), lane 3, compound **3** (200 µM), lane 4, **6** (200 µM), lane 5 and **26** (200 µM), lane 6. Reaction mixtures were irradiated at 300 nm for 3 minutes and loaded on 1% alkaline agarose gel. Gels were stained with ethidium bromide and the resulting products were visualized and documented with UV light at 254 nm (Image Master VDS, Pharmacia Biotech, Sweden).

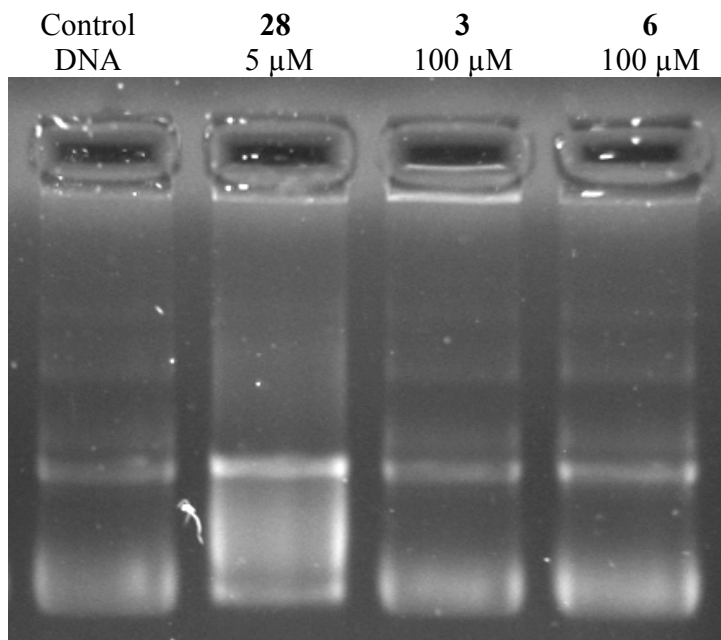
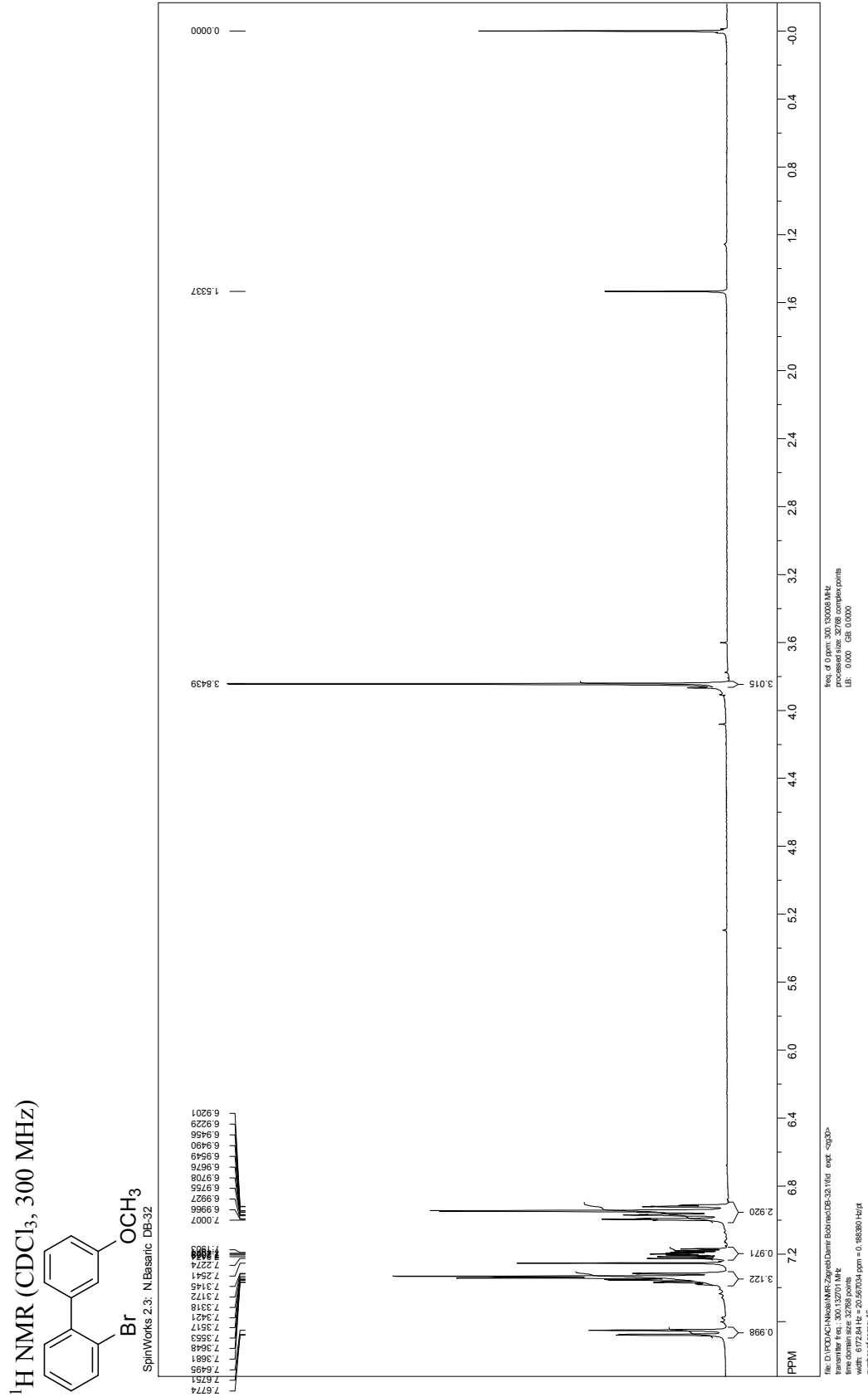
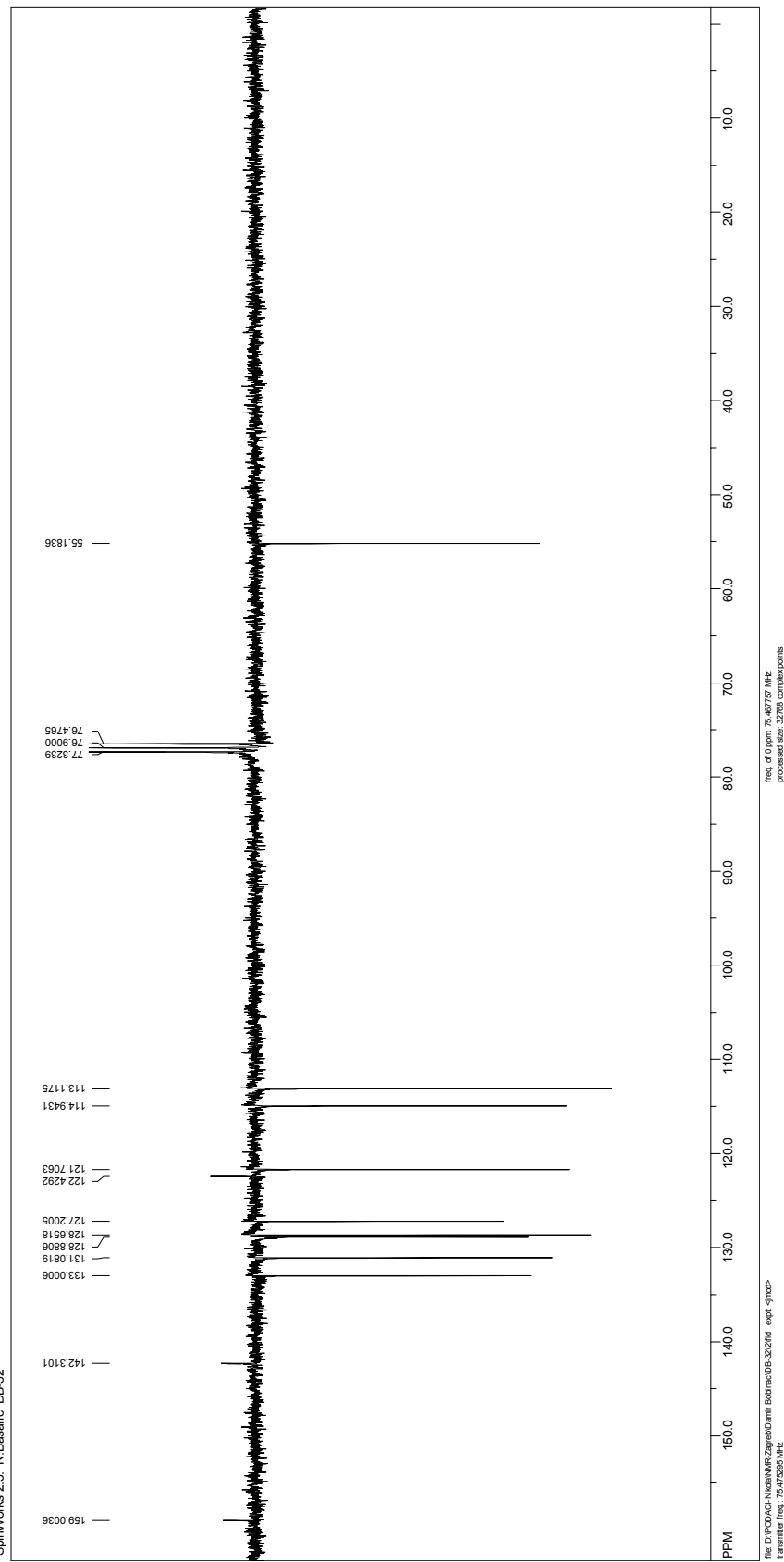
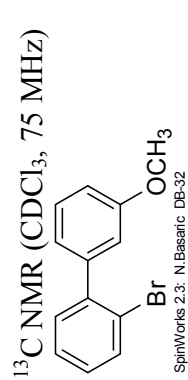
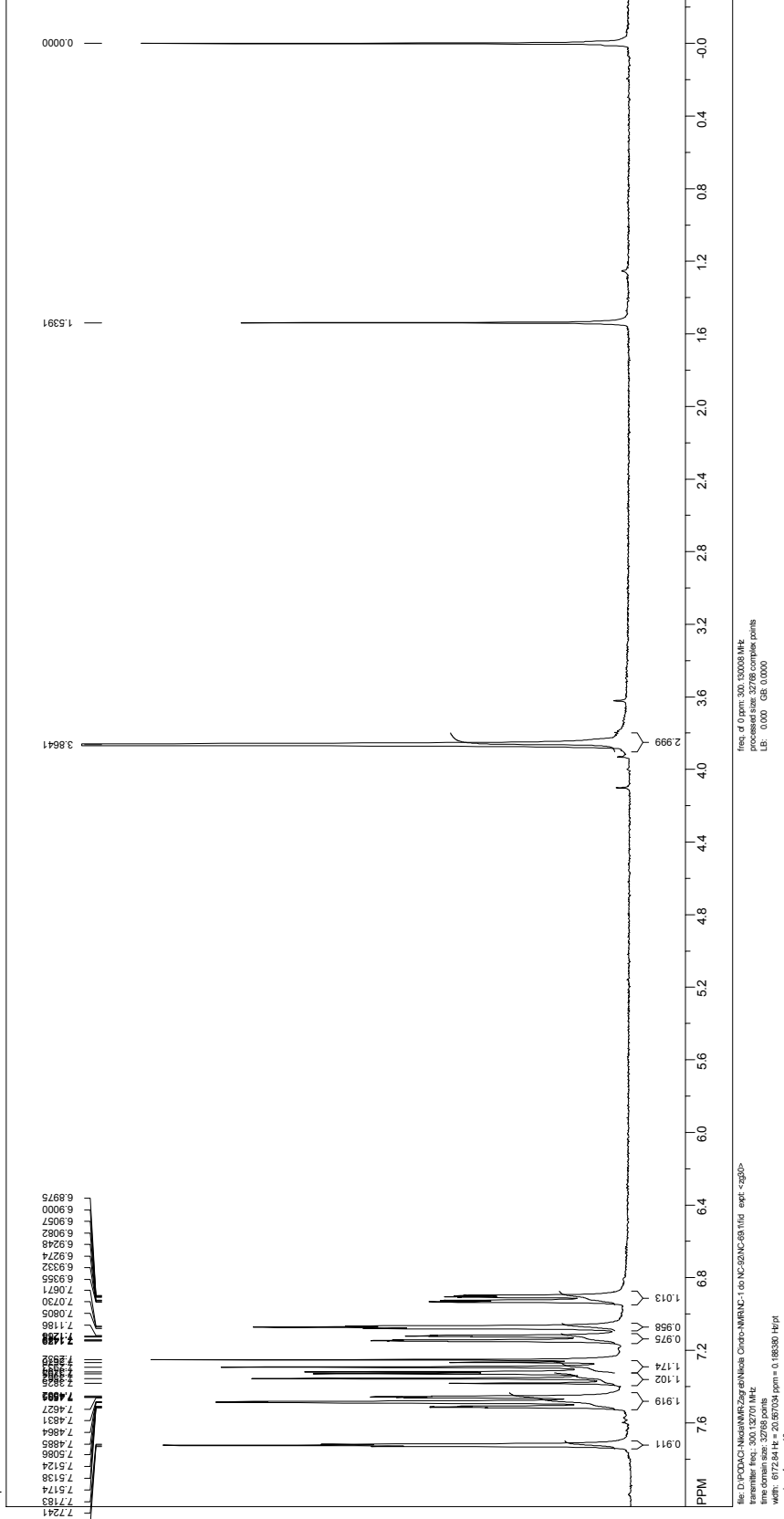
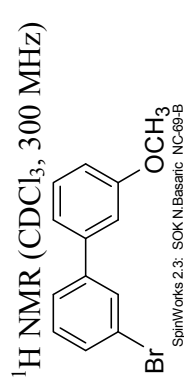
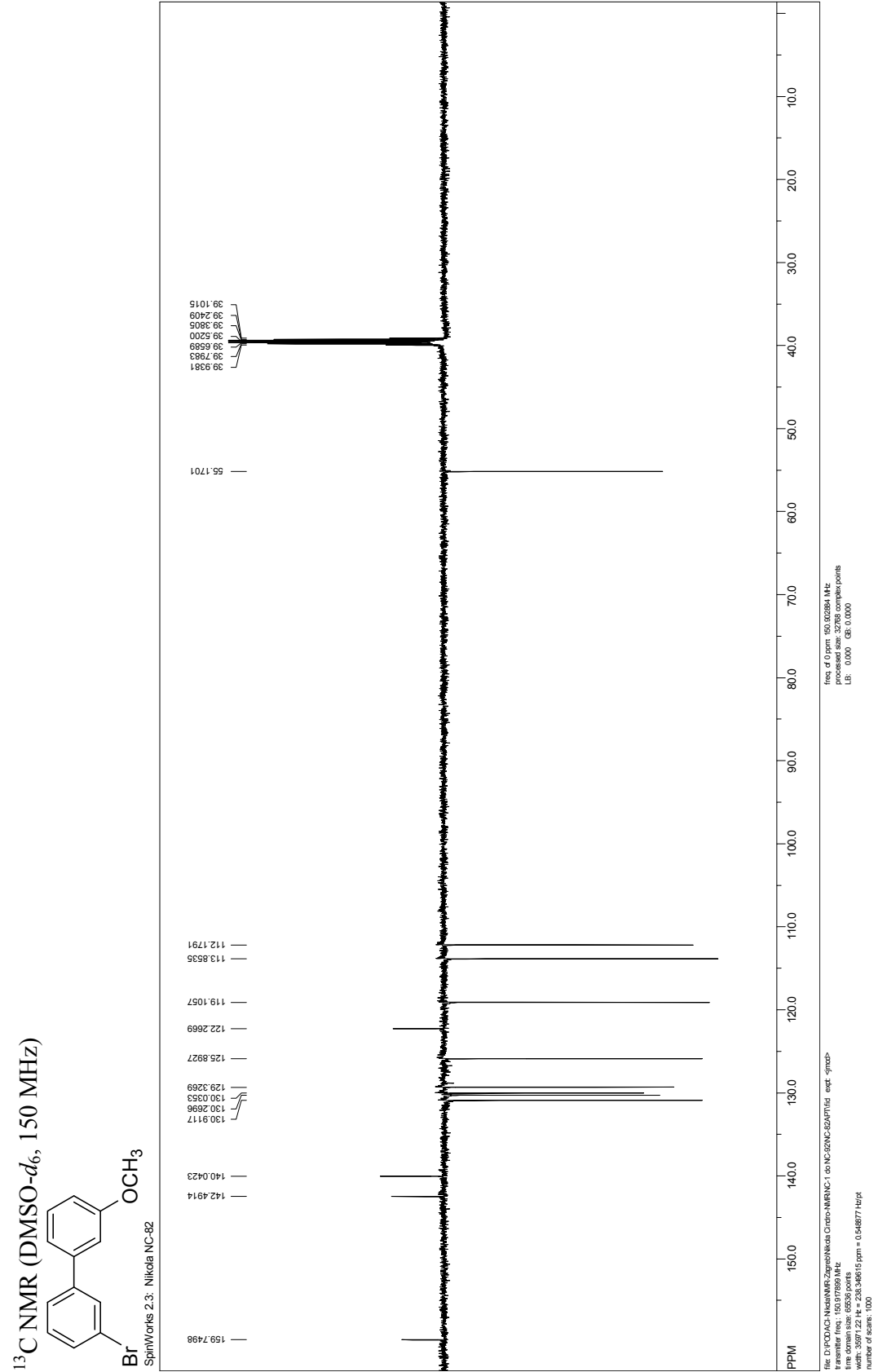


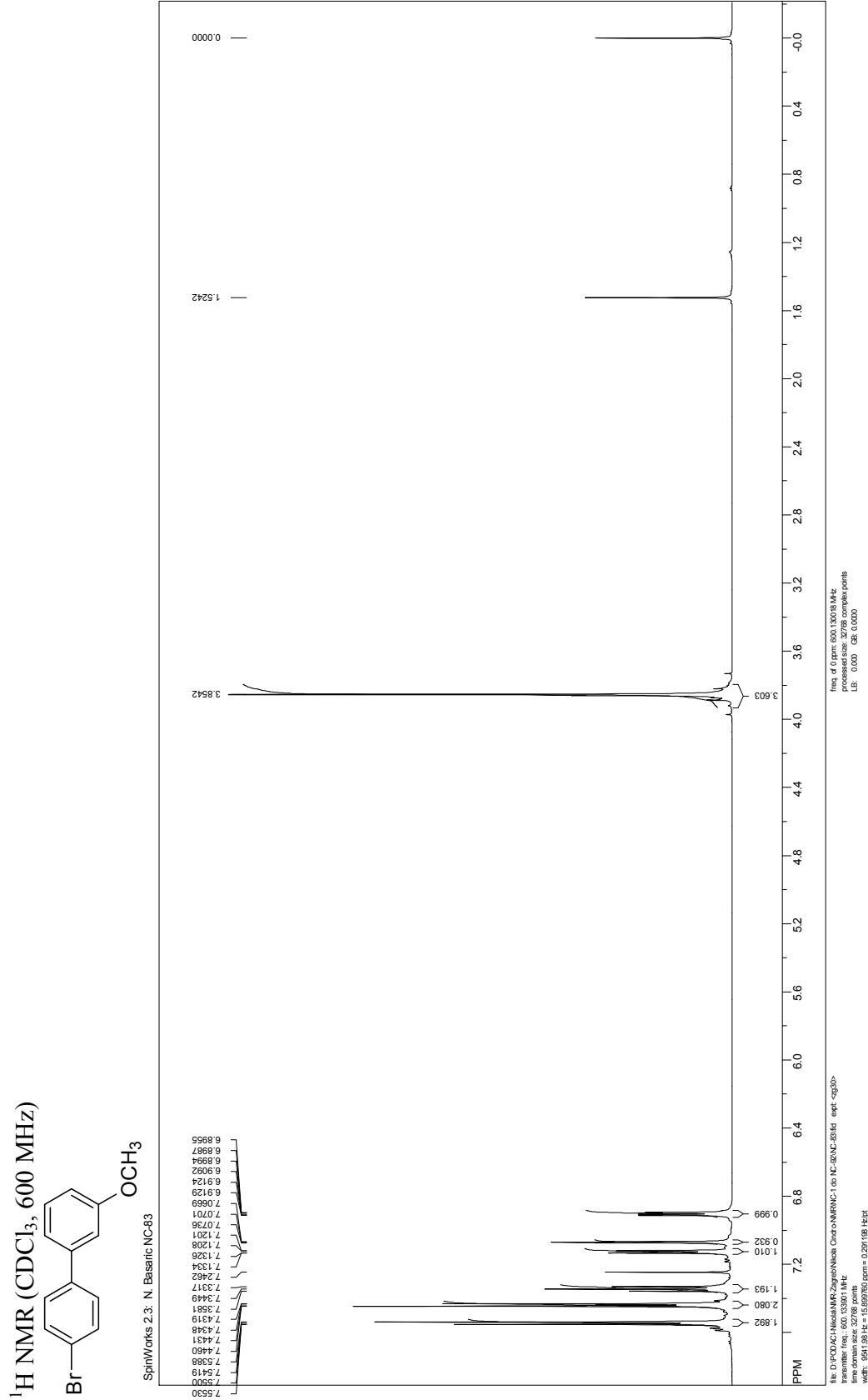
Fig. 52. Influence of selected test compounds on plasmid DNA unwinding/cleavage ability by compounds **3** and **6**, along with psoralen **28** as a positive control. Plasmid (pCI DNA (0.8 μ g), lane 1) DNA was mixed with psoralen (5 μ M), lane 2, compound **3** (100 μ M), lane 3, **6** (100 μ M), lane 4. Reaction mixtures were irradiated at 300 nm for 3 minutes and loaded on 1% agarose gel. Gels were stained with ethidium bromide and the resulting products were visualized and documented with UV light at 254 nm (Image Master VDS, Pharmacia Biotech, Sweden).

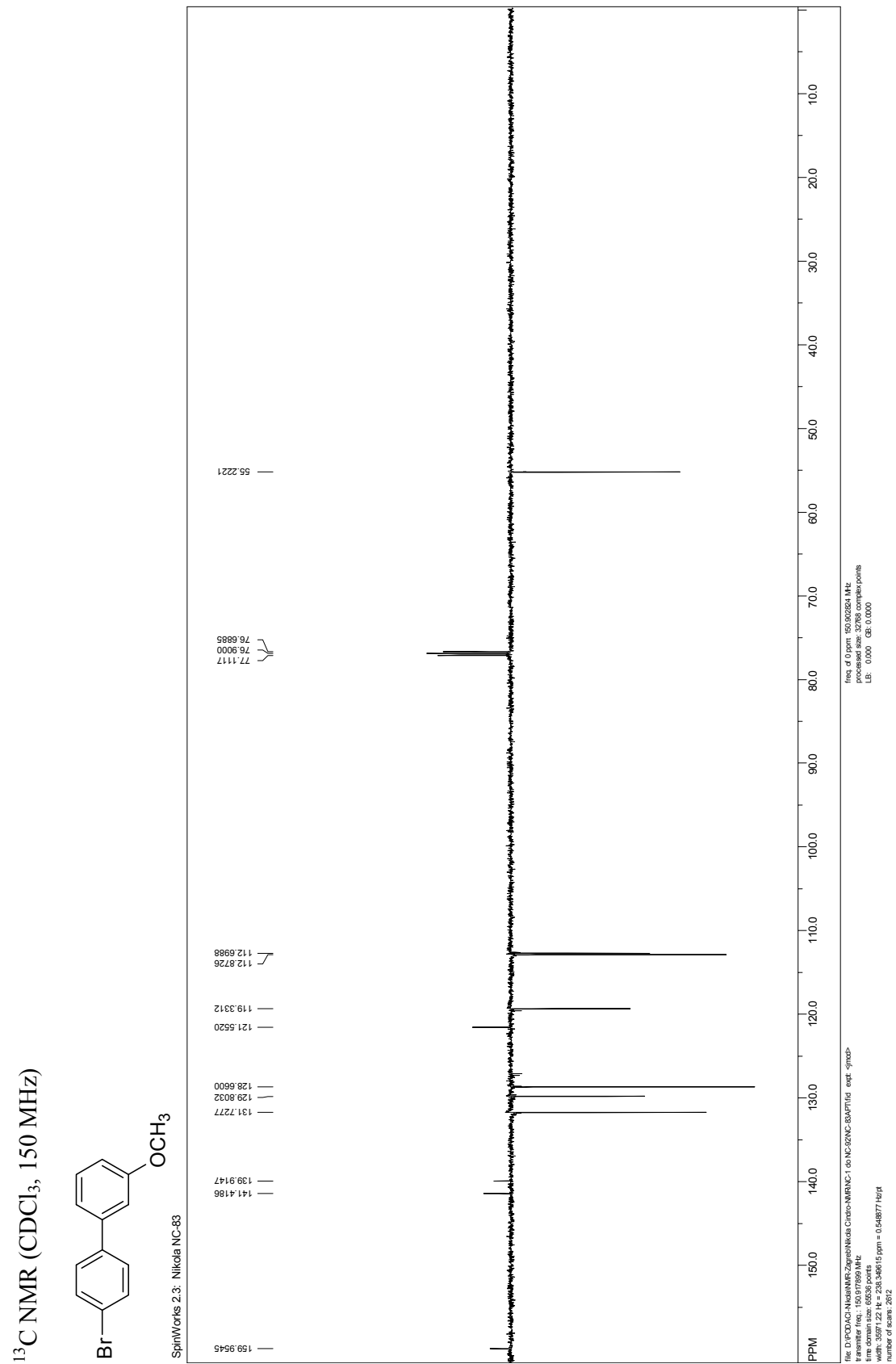




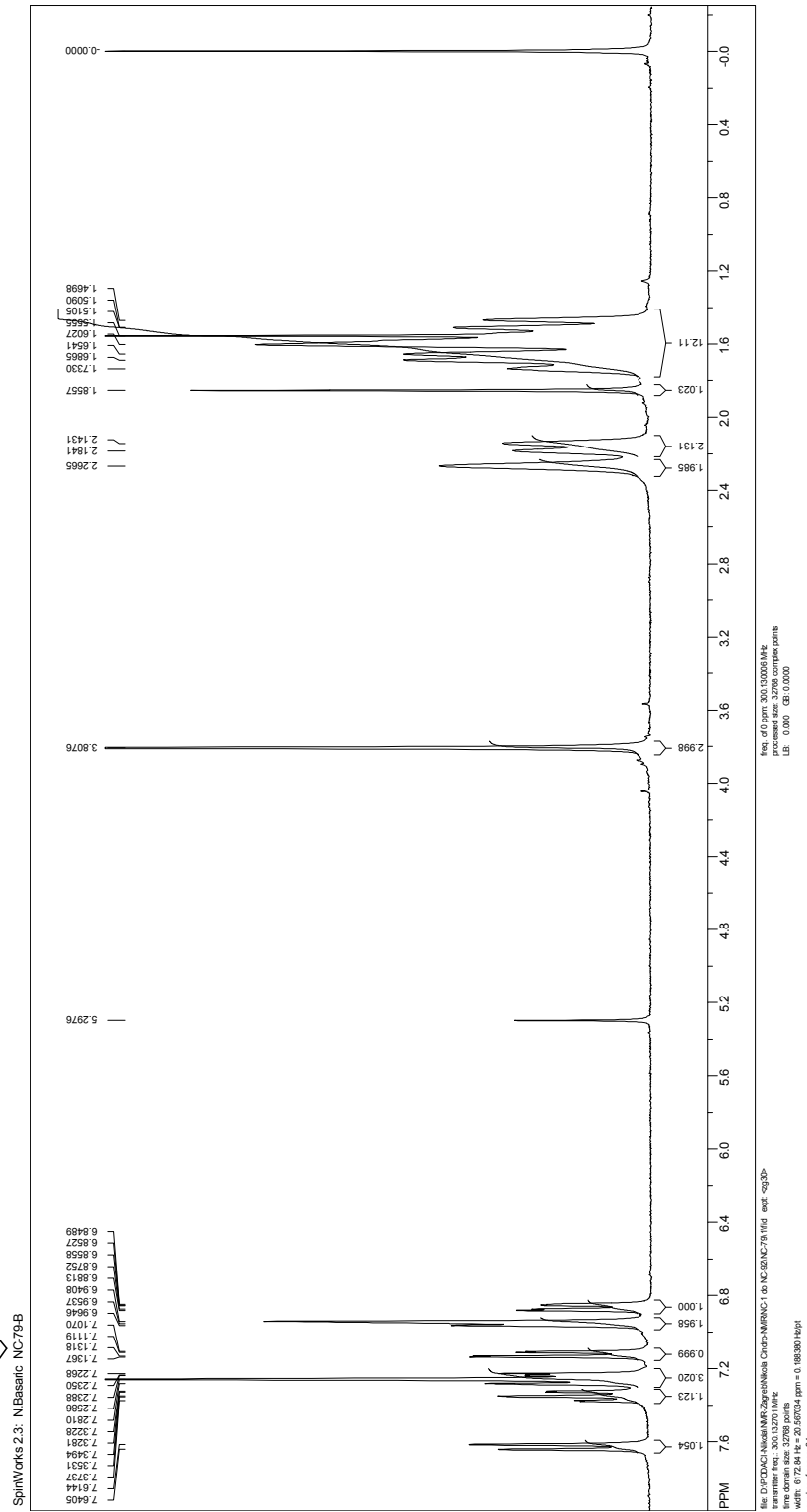
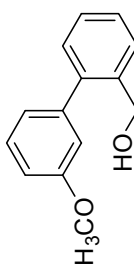




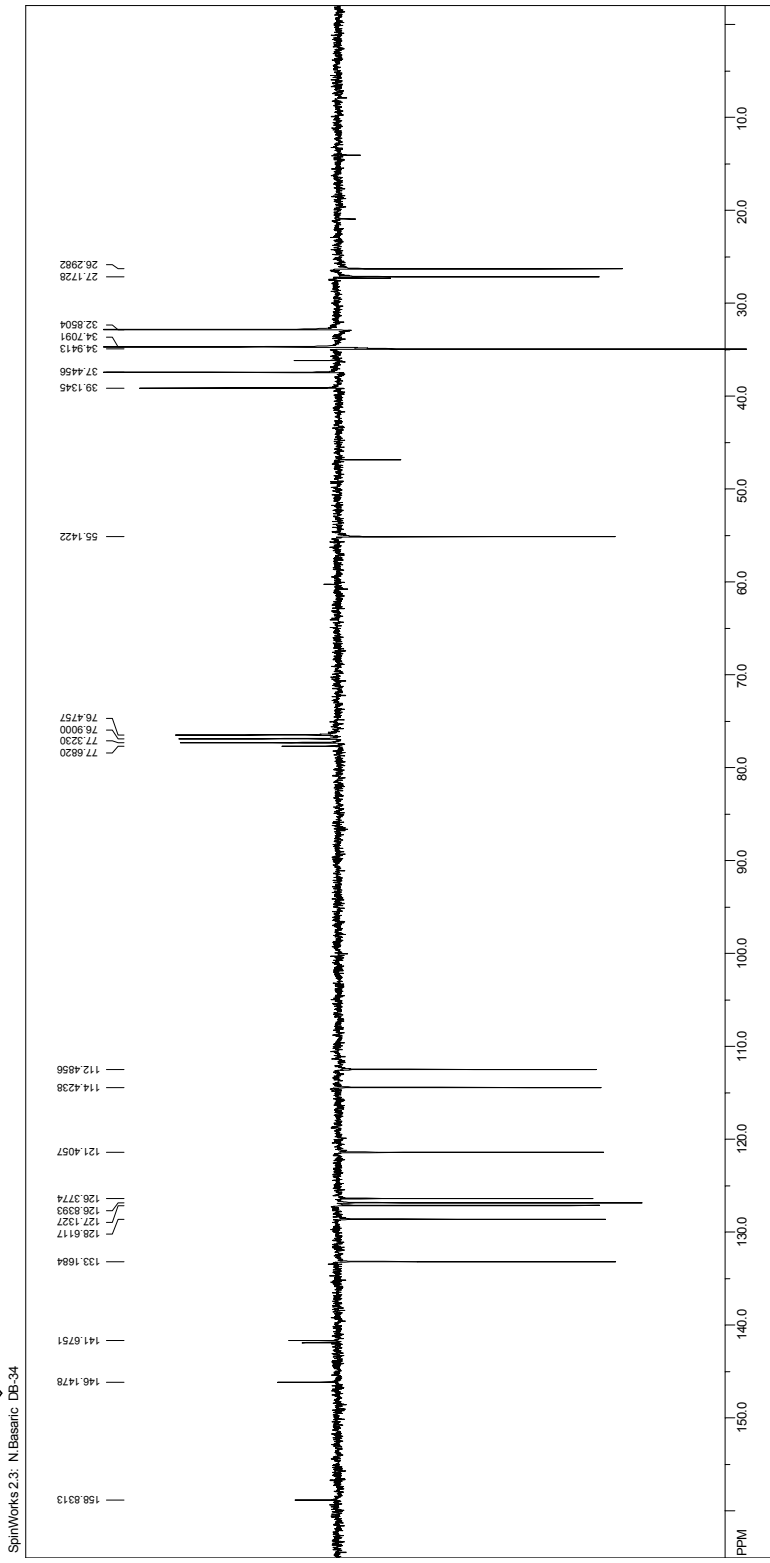
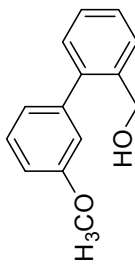


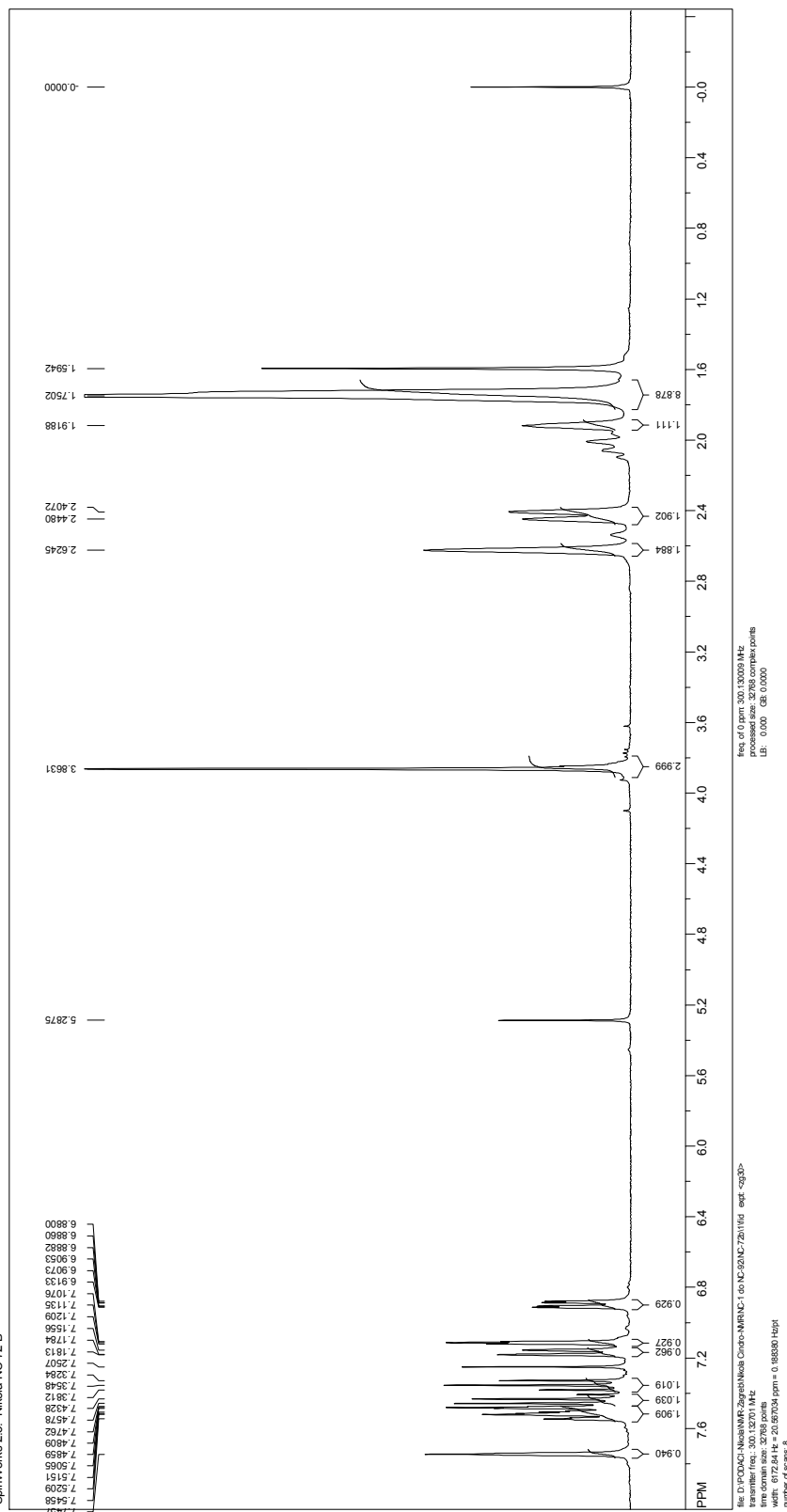
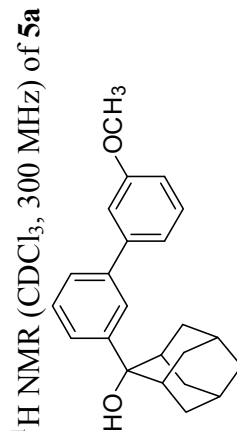


^1H NMR (CDCl_3 , 300 MHz) of 4a

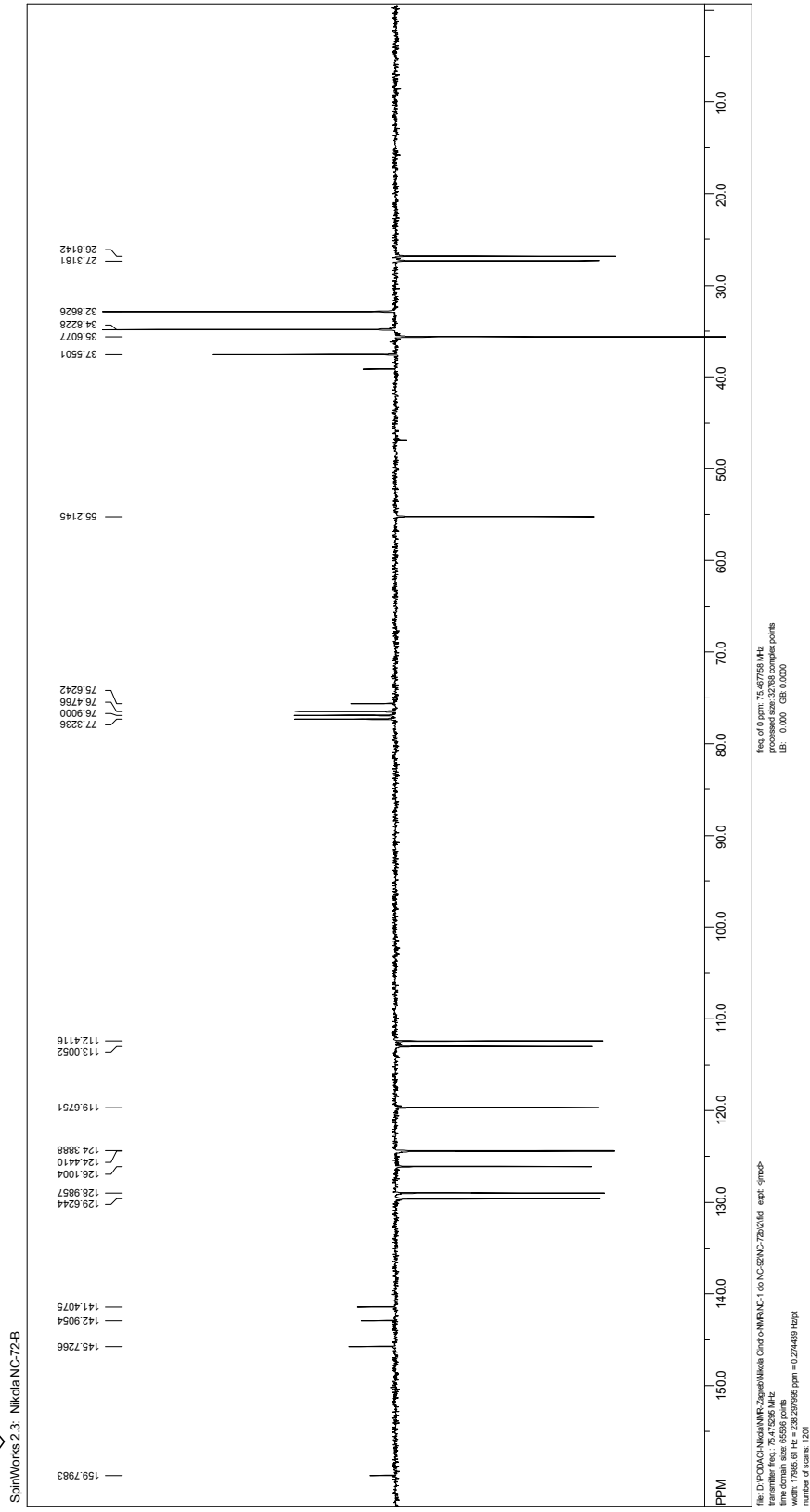
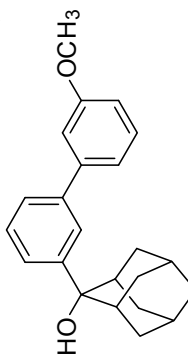


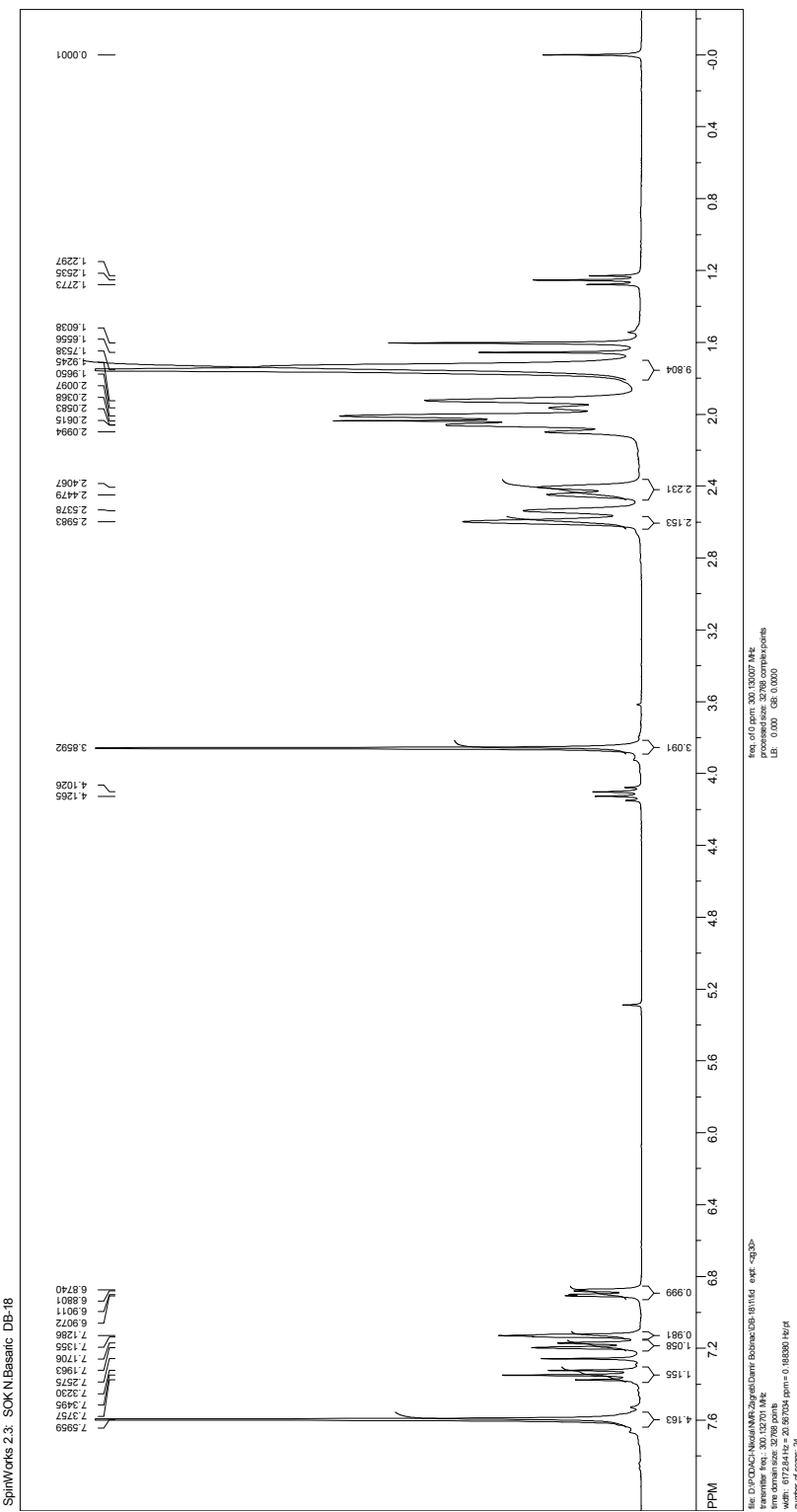
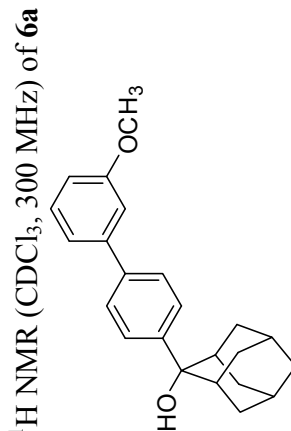
^{13}C NMR (CDCl_3 , 75 MHz) of 4a



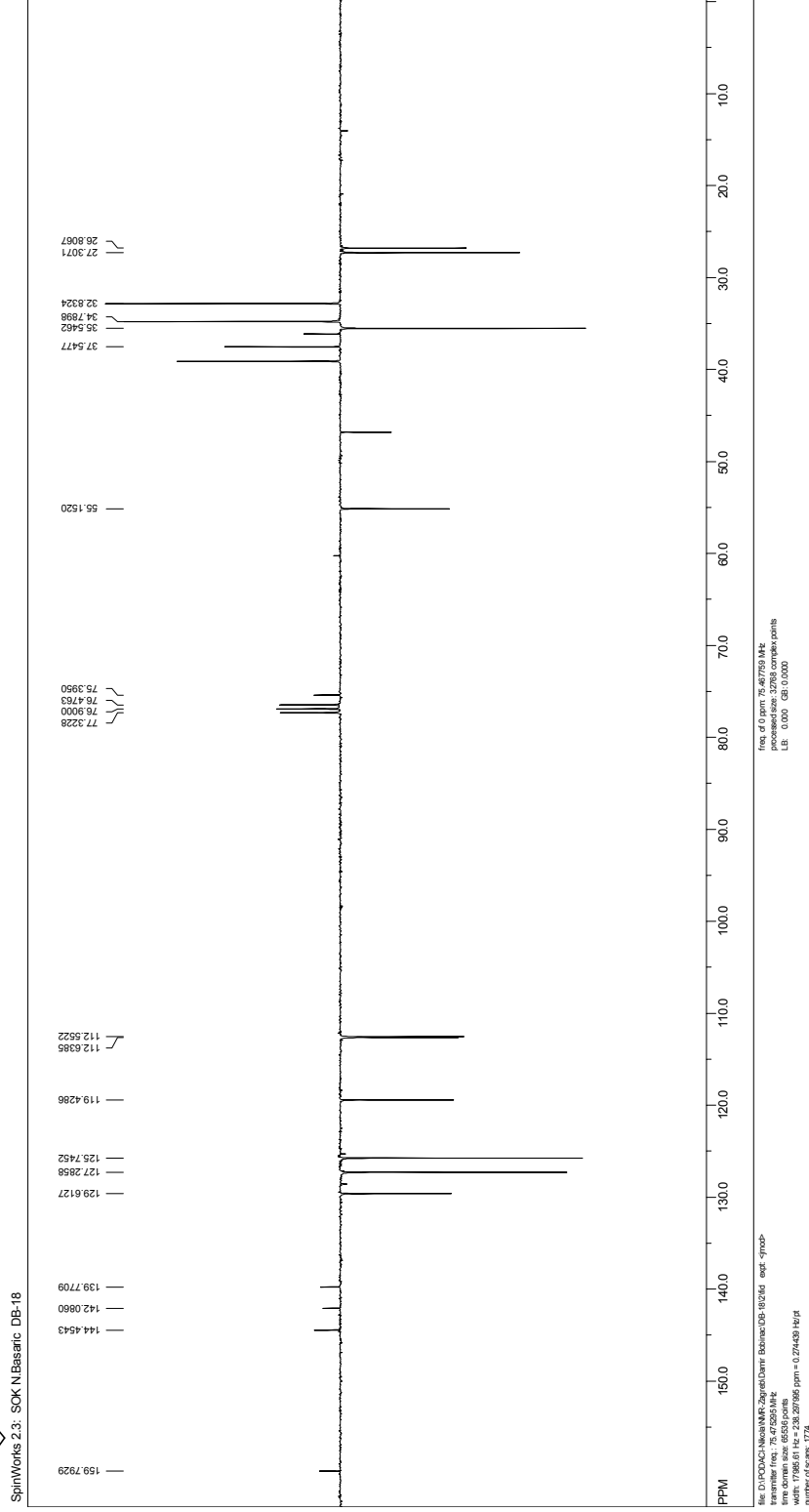
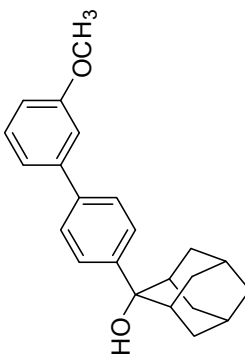


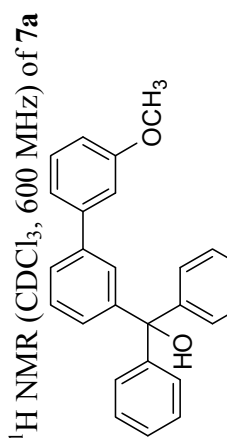
^{13}C NMR (CDCl_3 , 75 MHz) of 5a



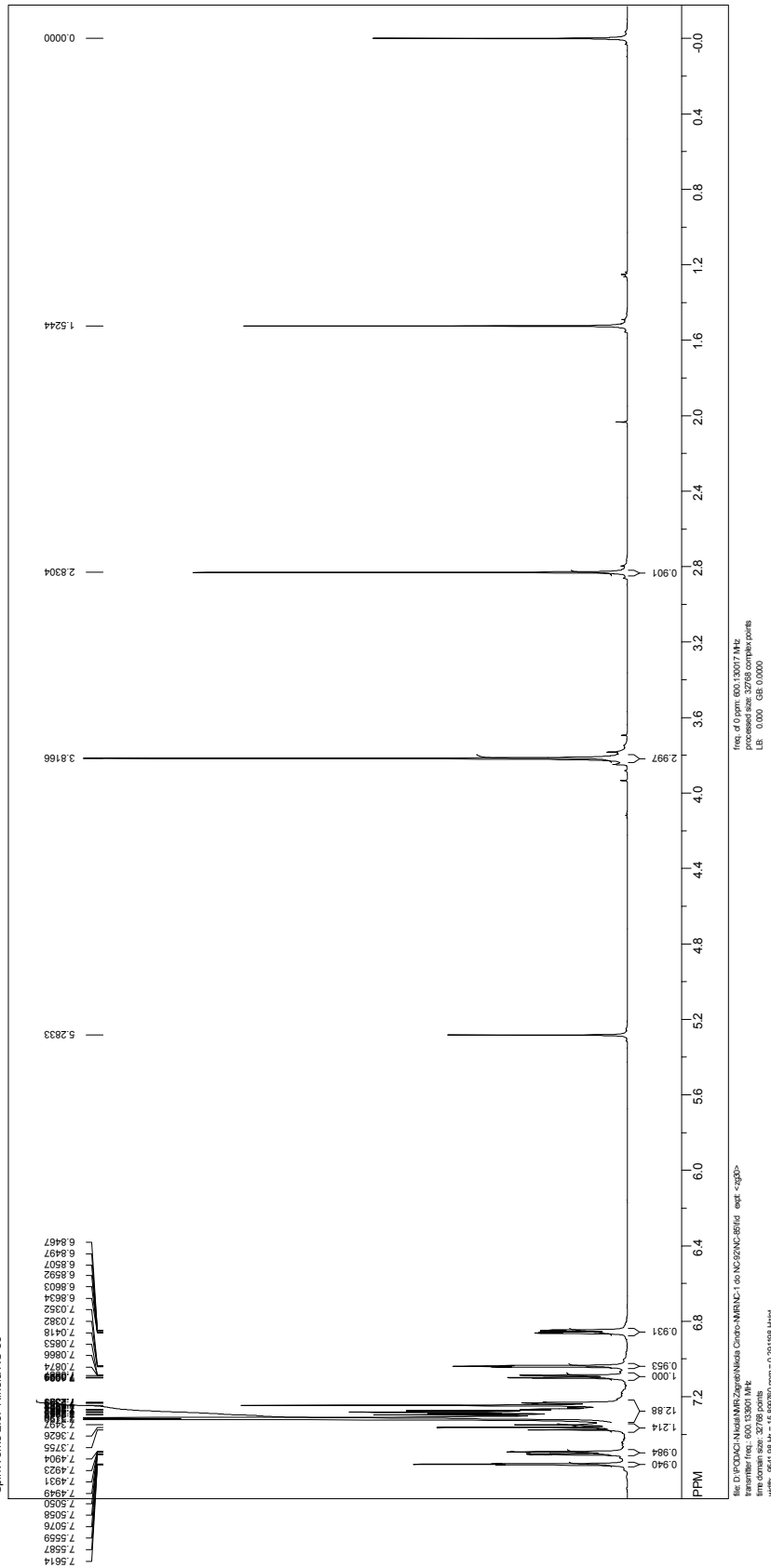


^{13}C NMR (CDCl_3 , 75 MHz) of **6a**

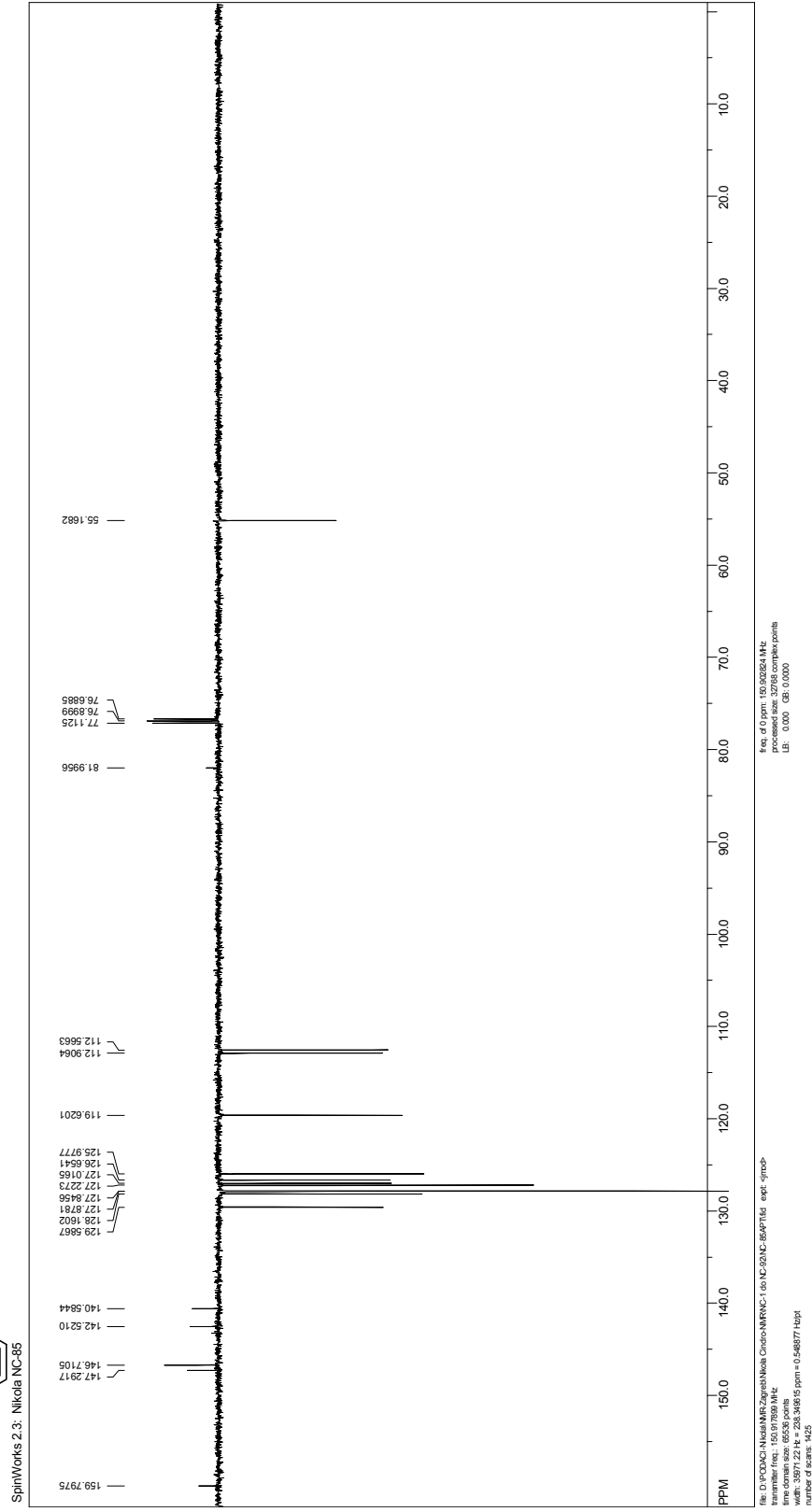
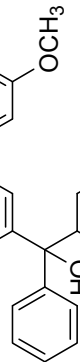


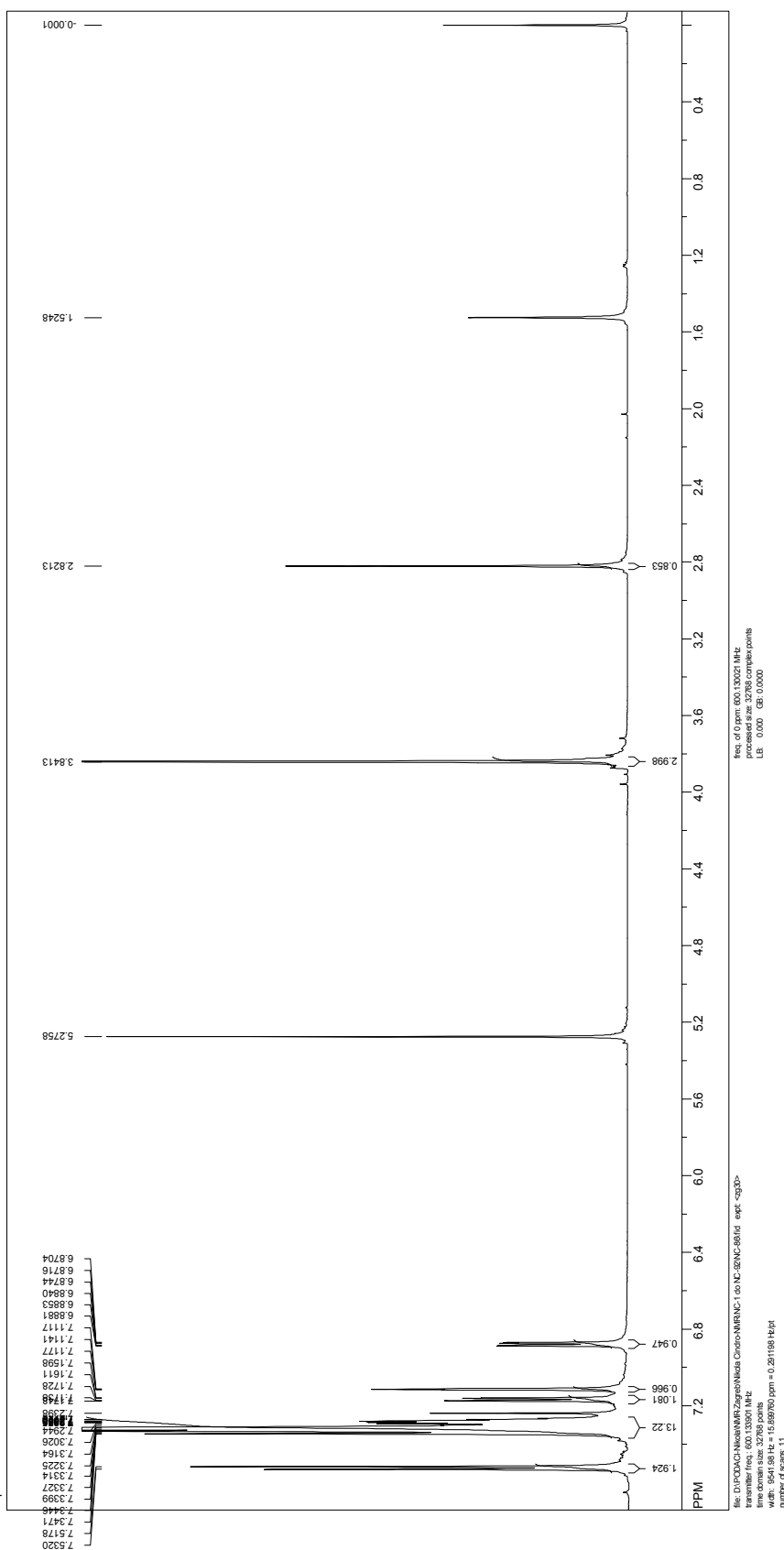
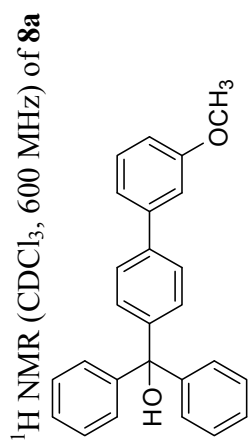


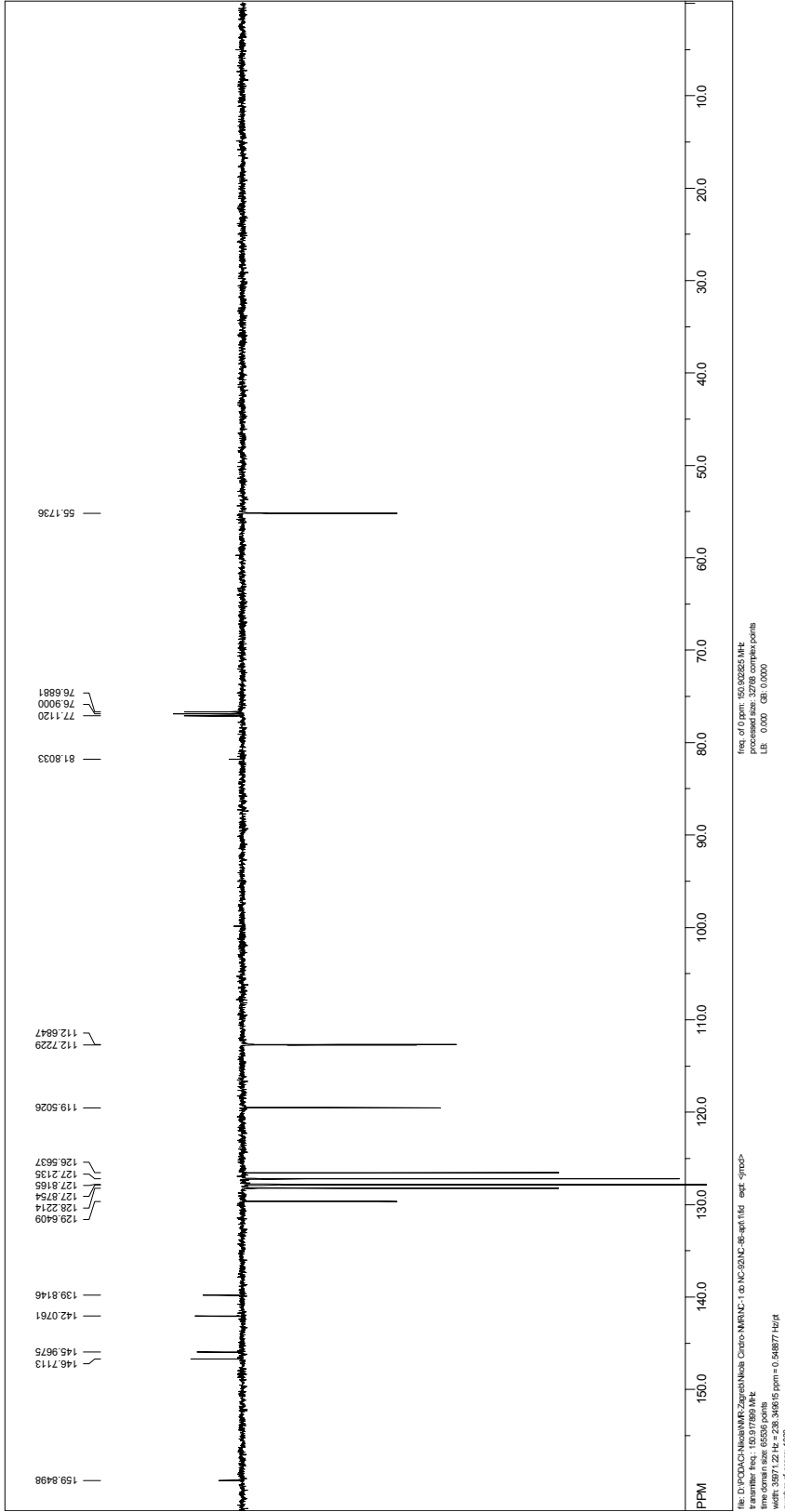
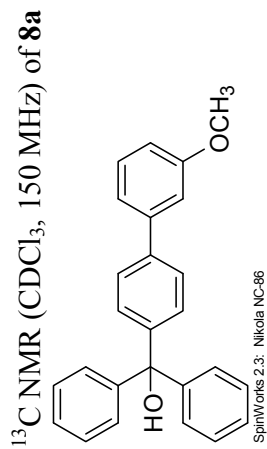
^1H NMR (CDCl_3 , 600 MHz) of 7a



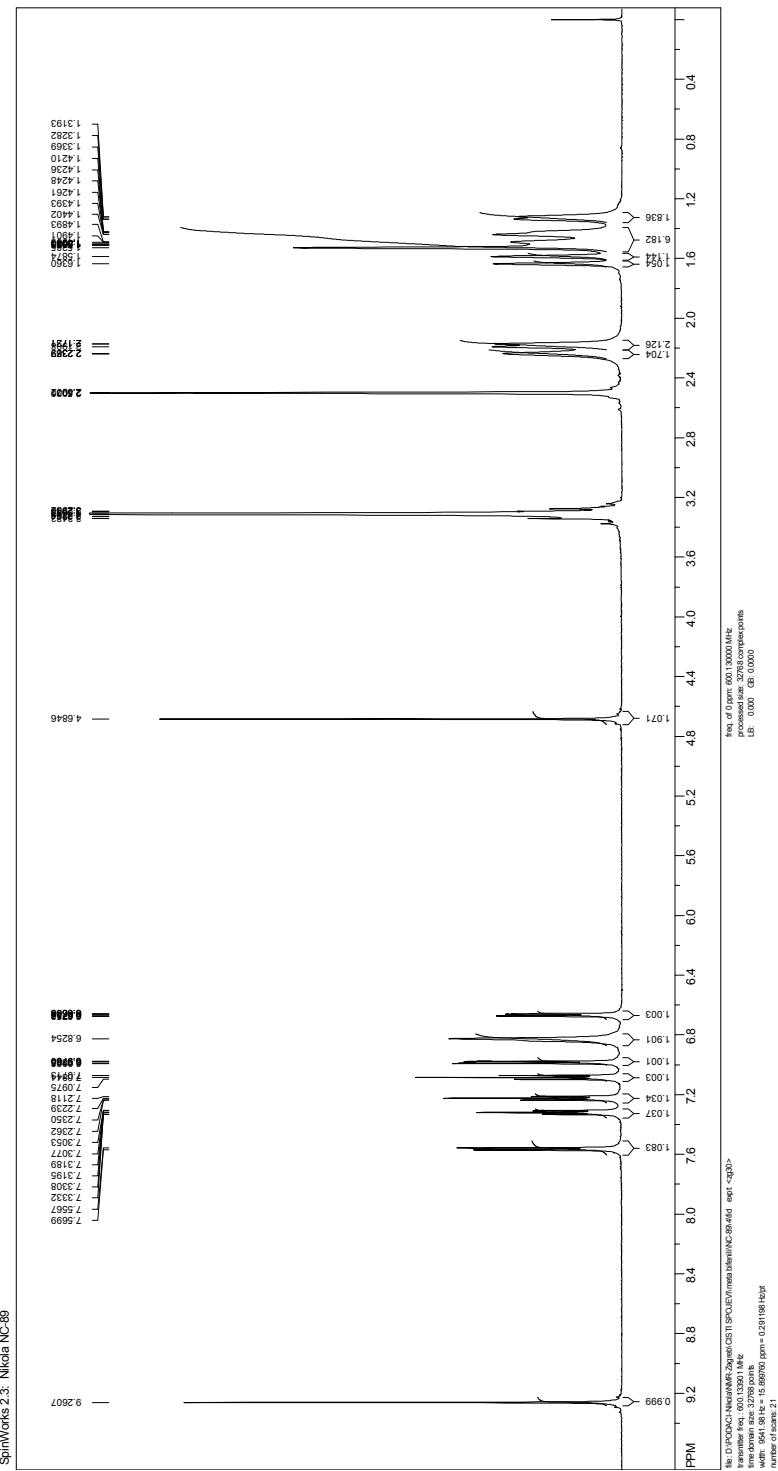
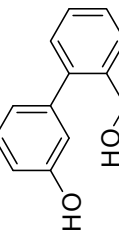
^{13}C NMR (CDCl_3 , 150 MHz) of 7a

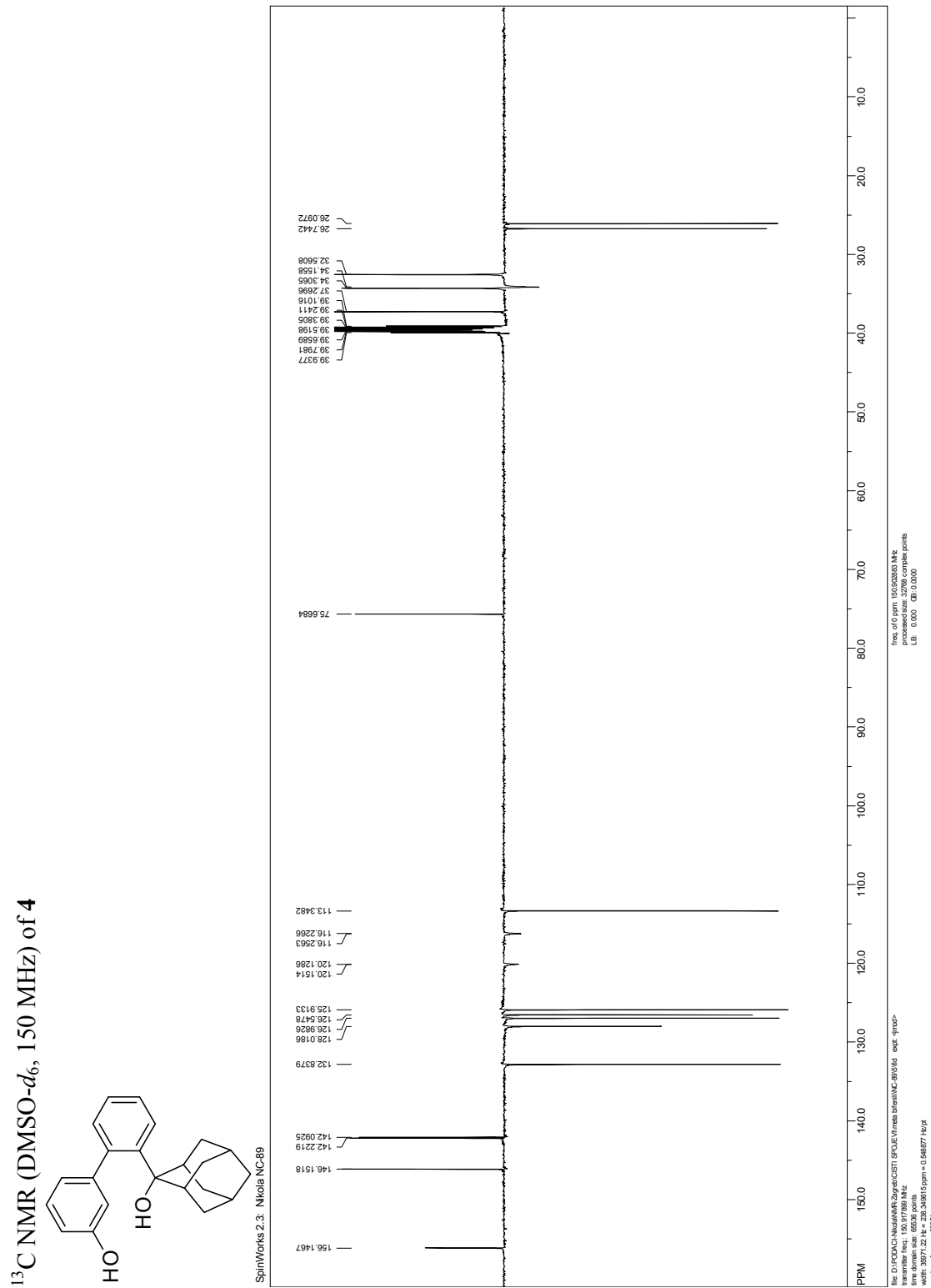


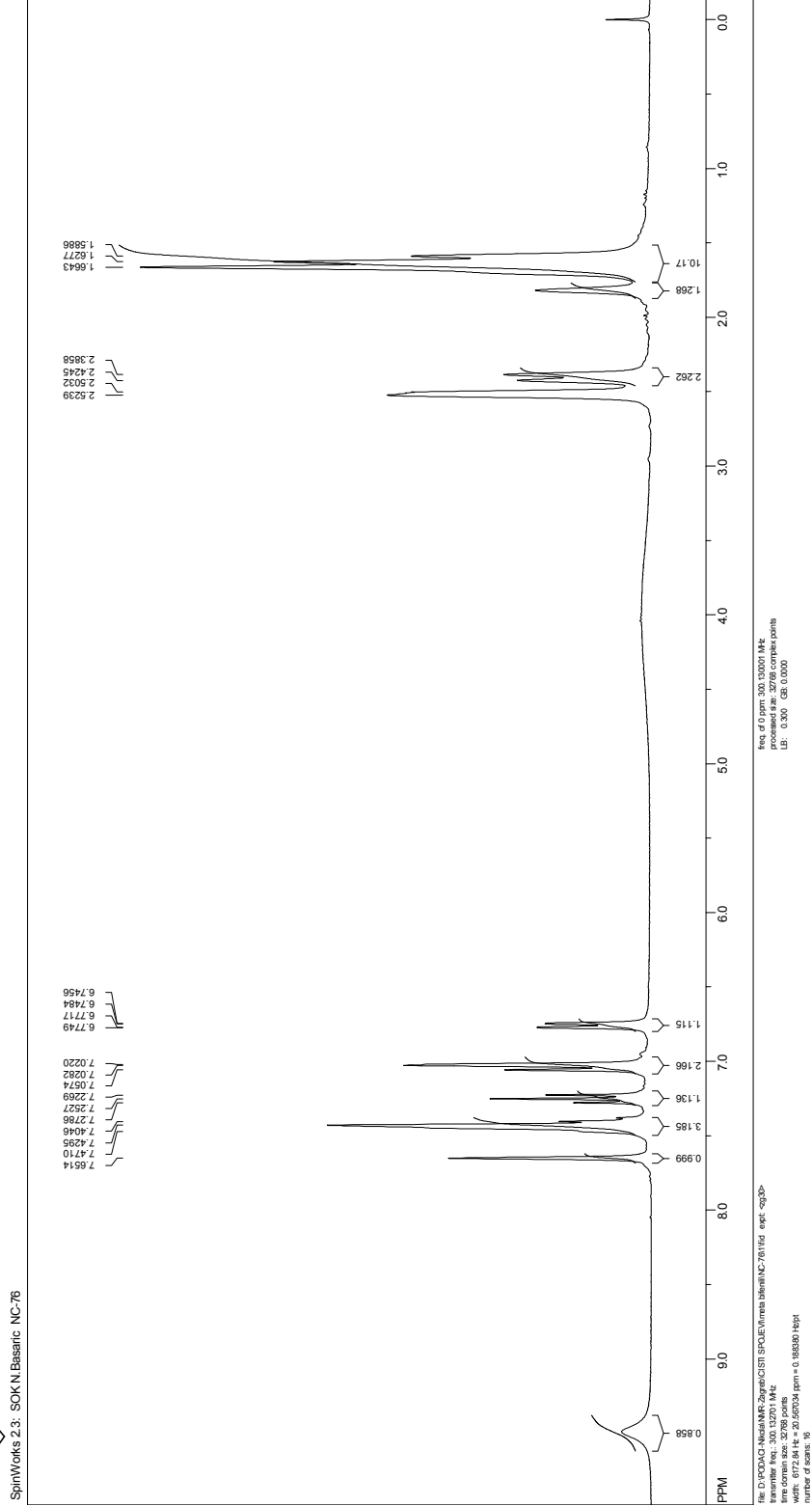
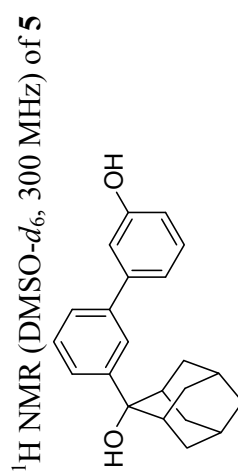


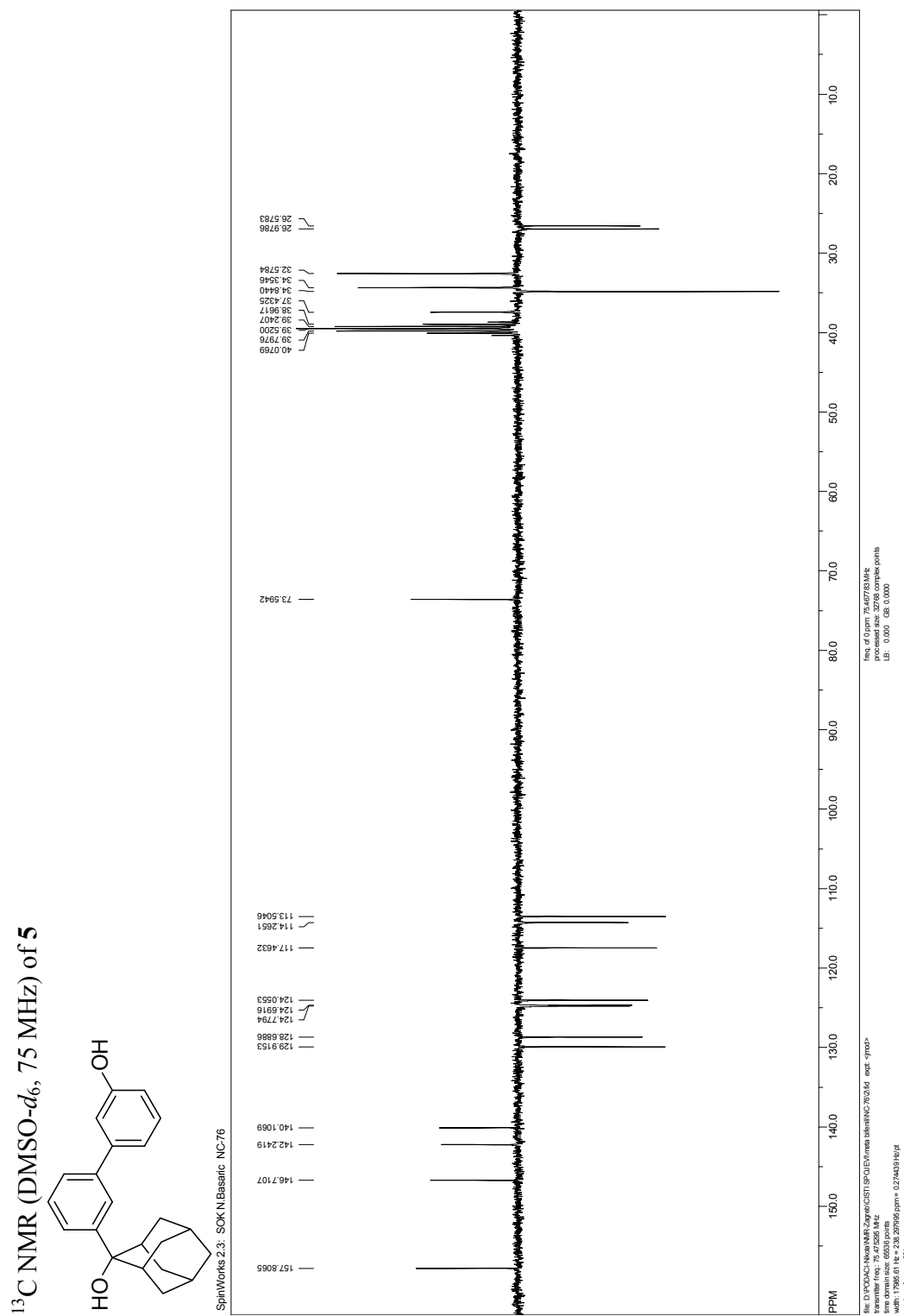


¹H NMR (DMSO-*d*₆, 600 MHz) of 4

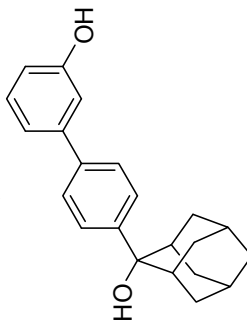




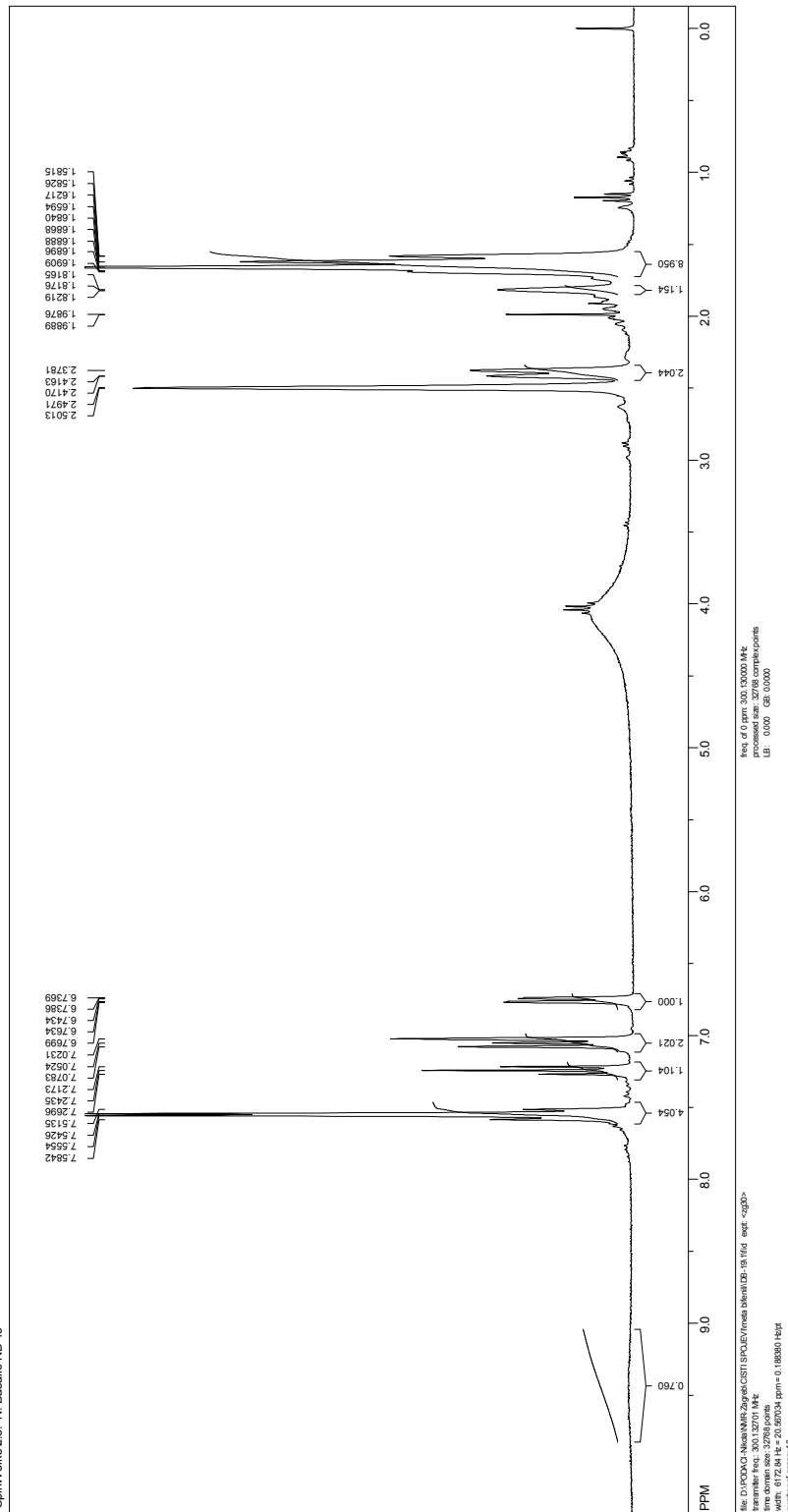




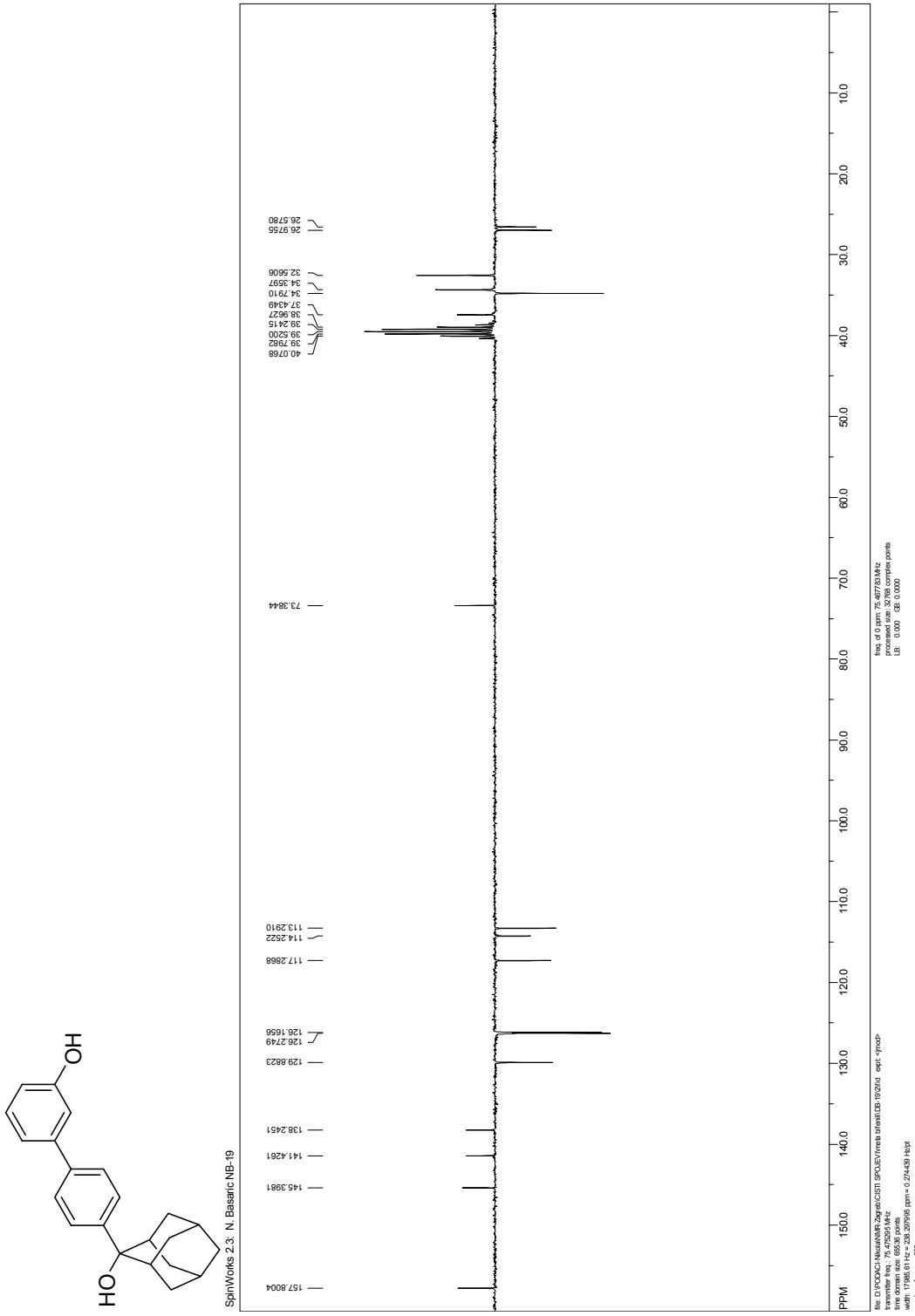
^1H NMR (DMSO- d_6 , 300 MHz) of **6**



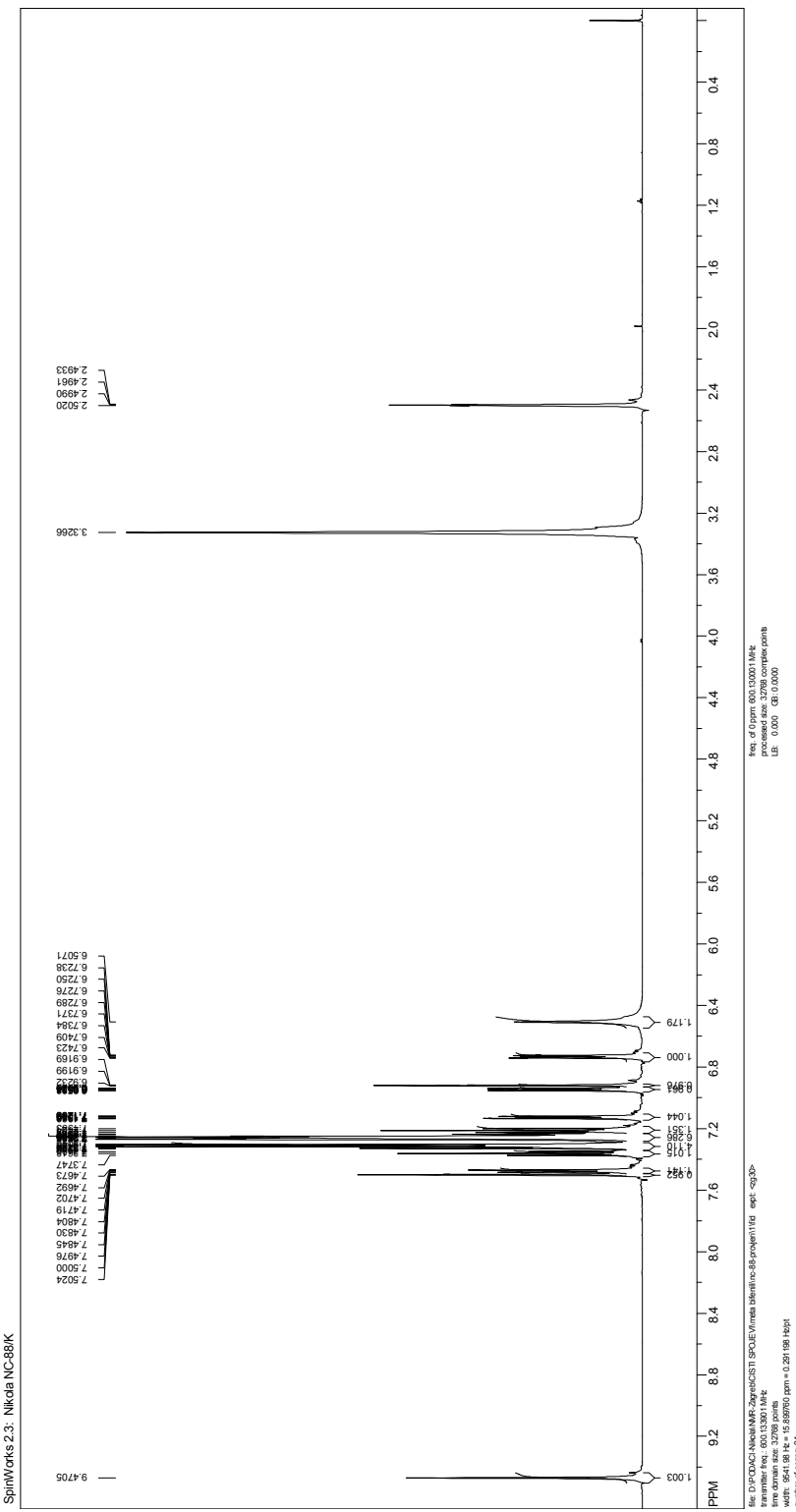
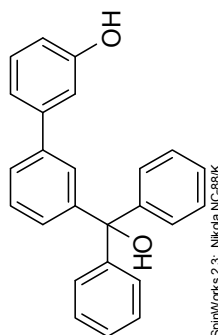
SpinWorks 2.3; N: Basic NB-19



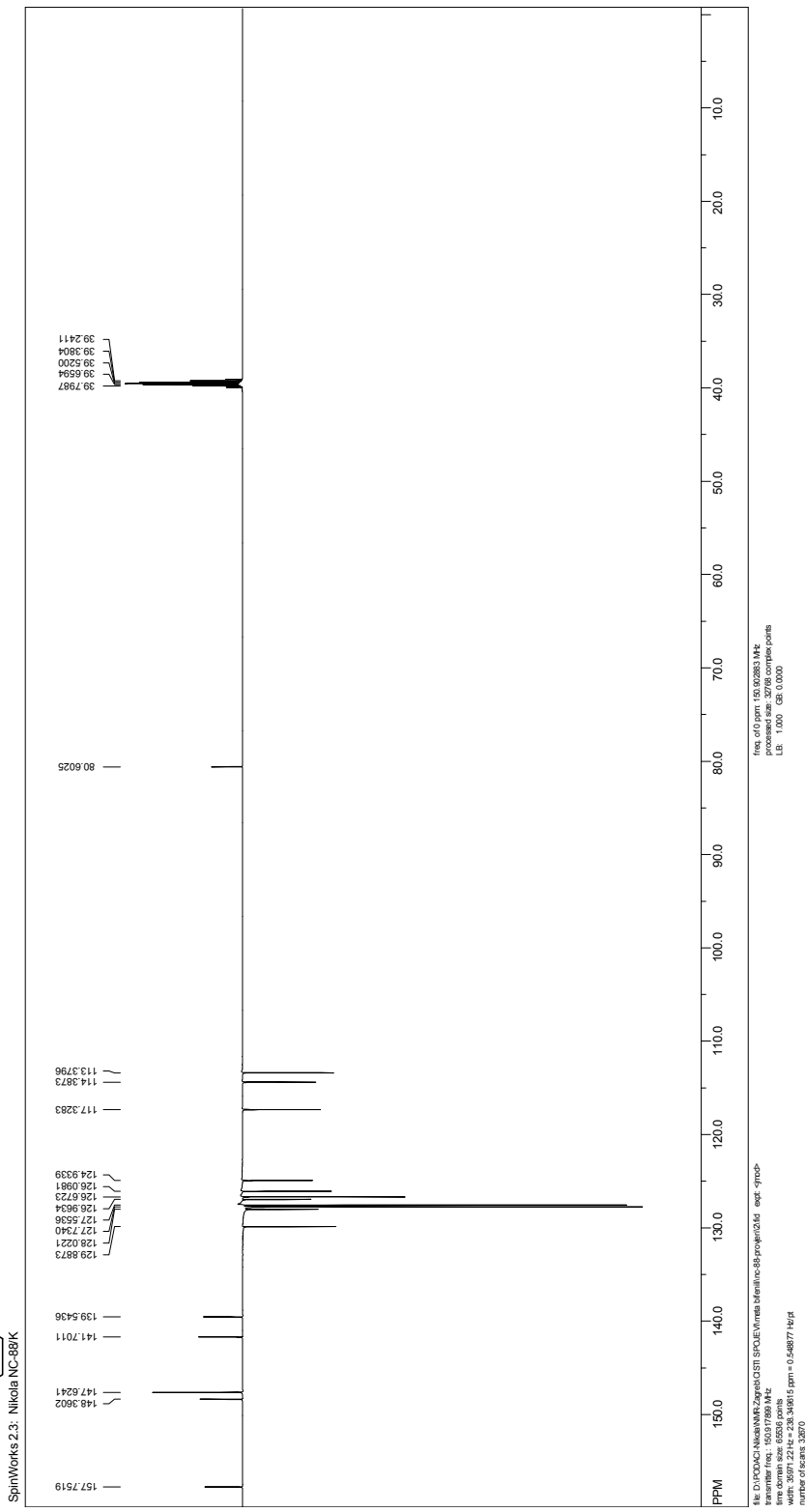
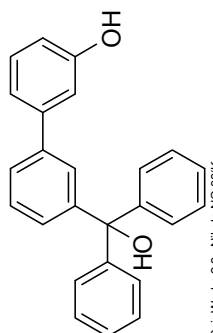
^{13}C NMR (DMSO- d_6 , 75 MHz) of **6**

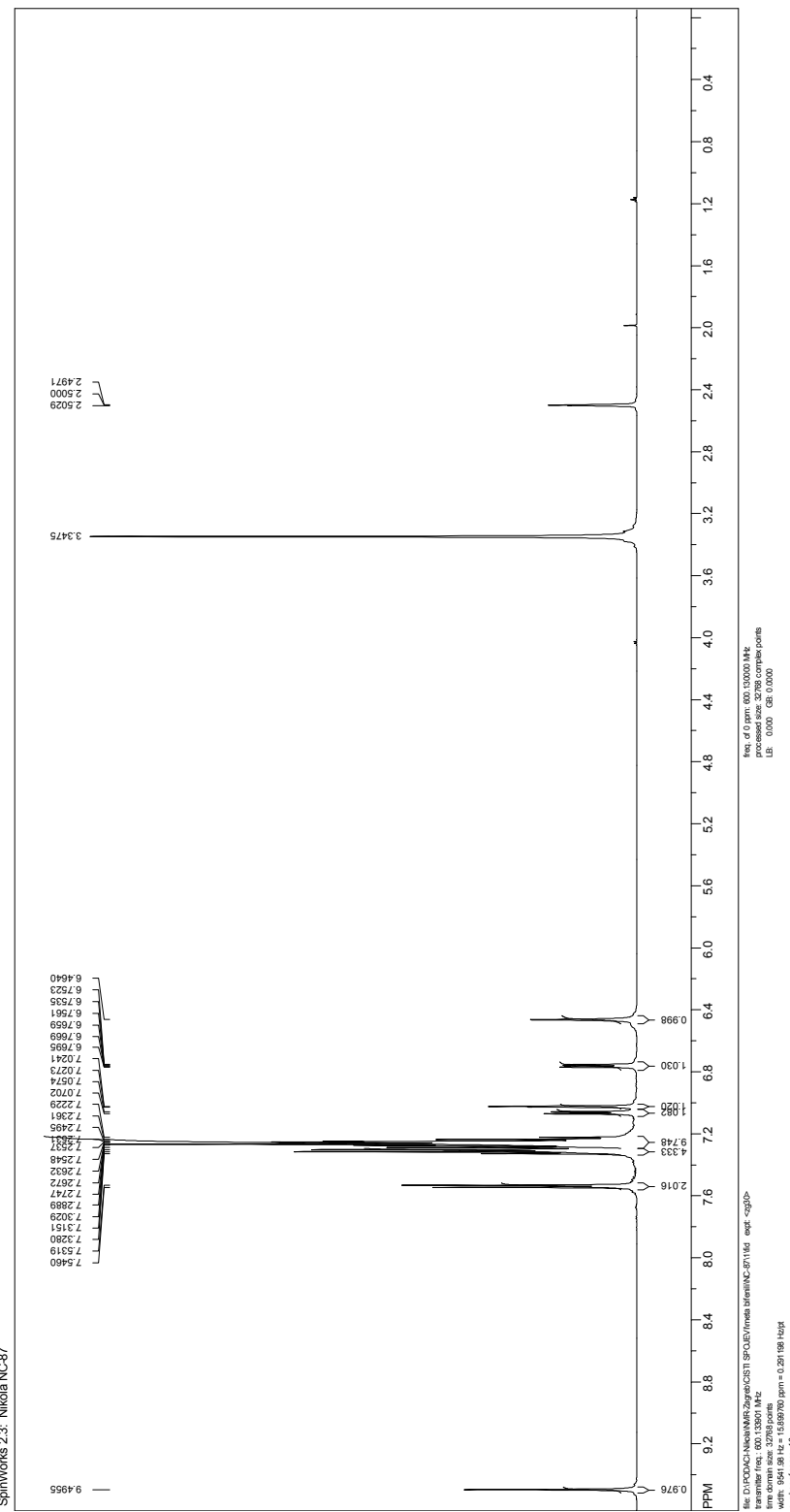
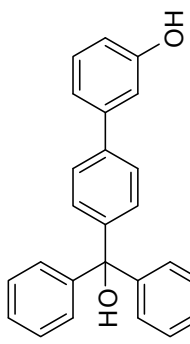


^1H NMR (DMSO- d_6 , 600 MHz) of 7

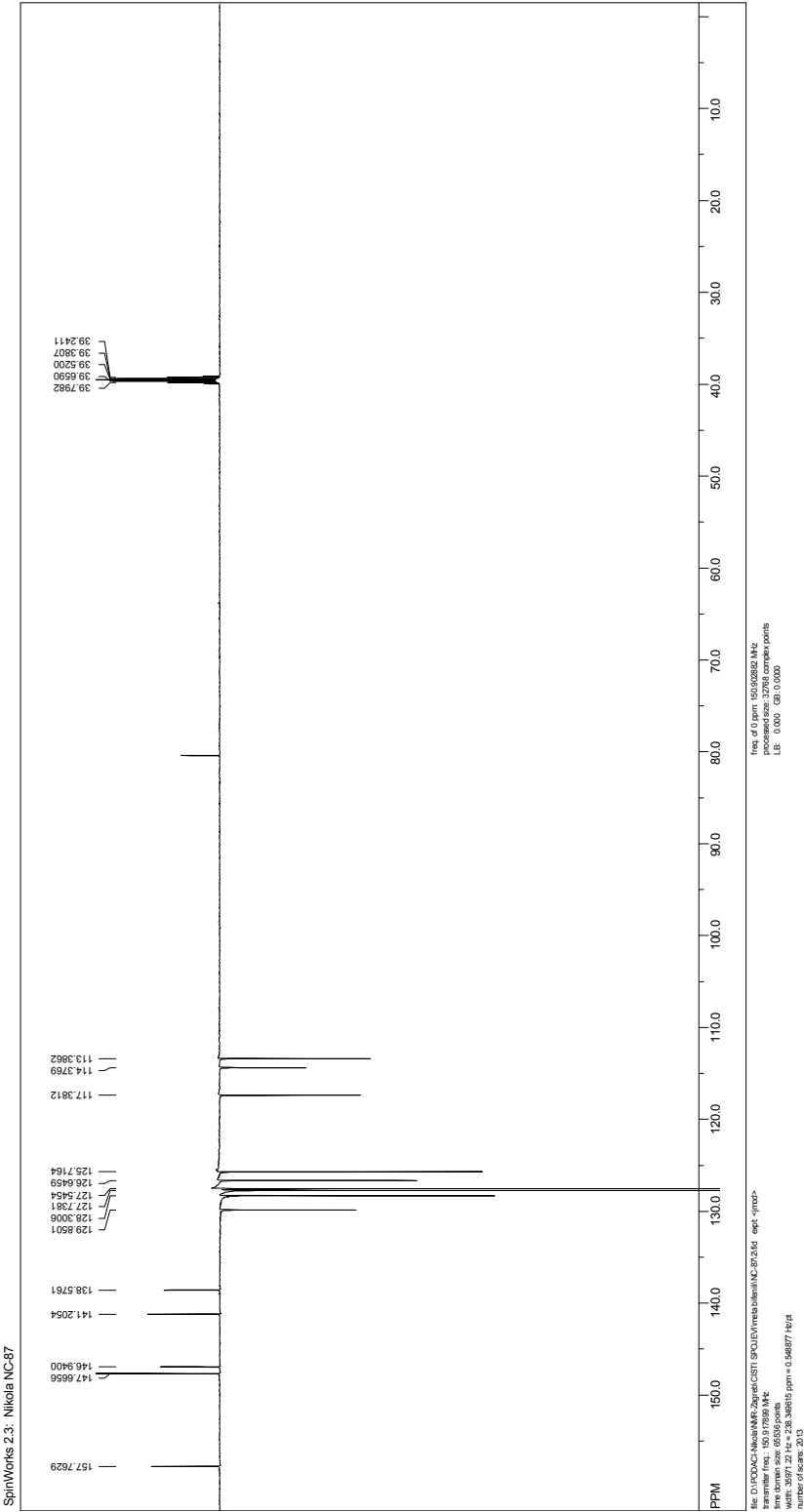
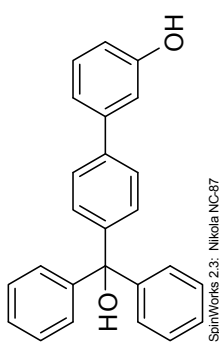


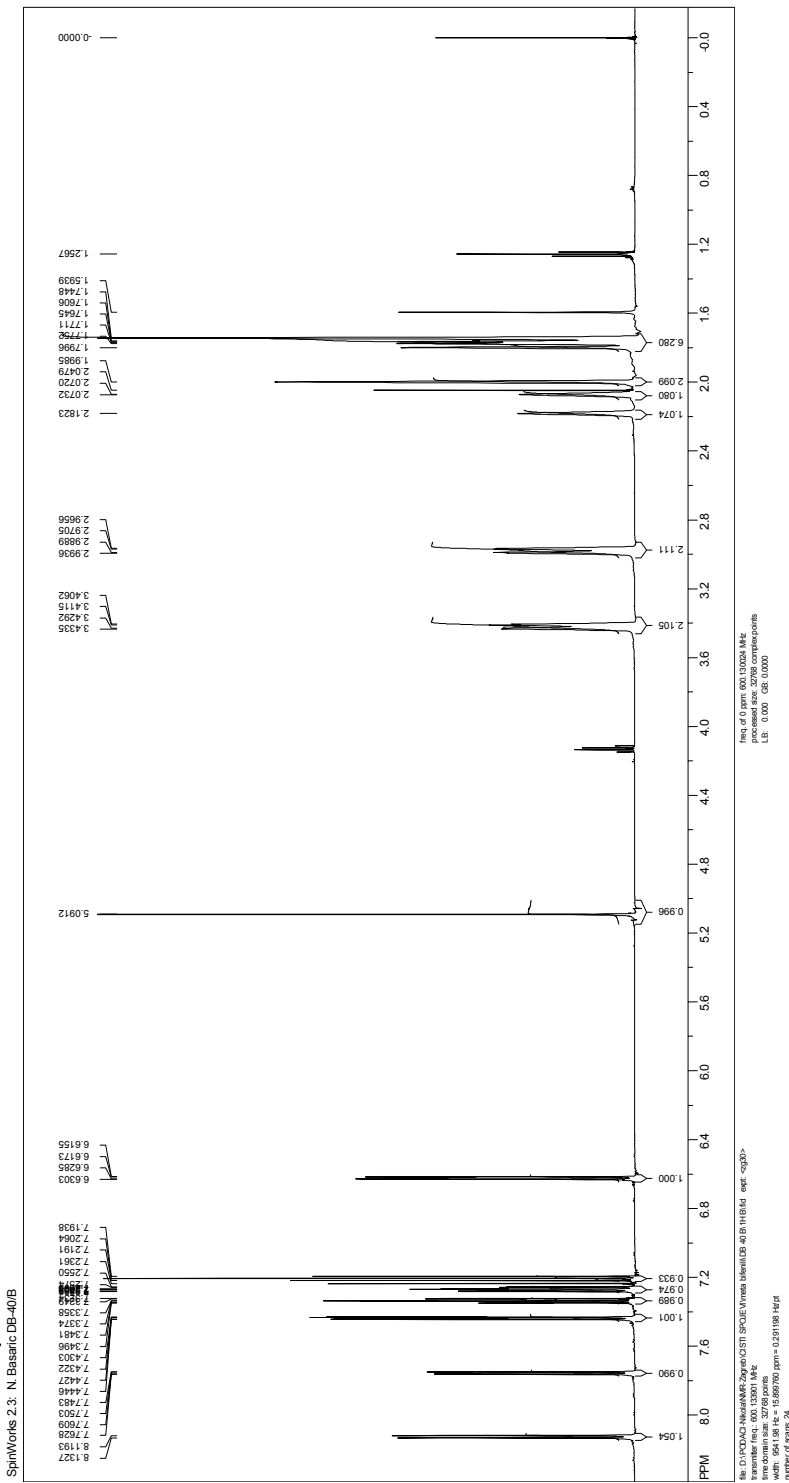
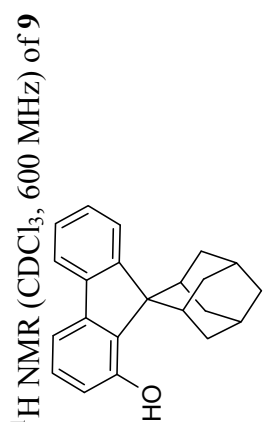
^{13}C NMR (DMSO- d_6 , 150 MHz) of 7



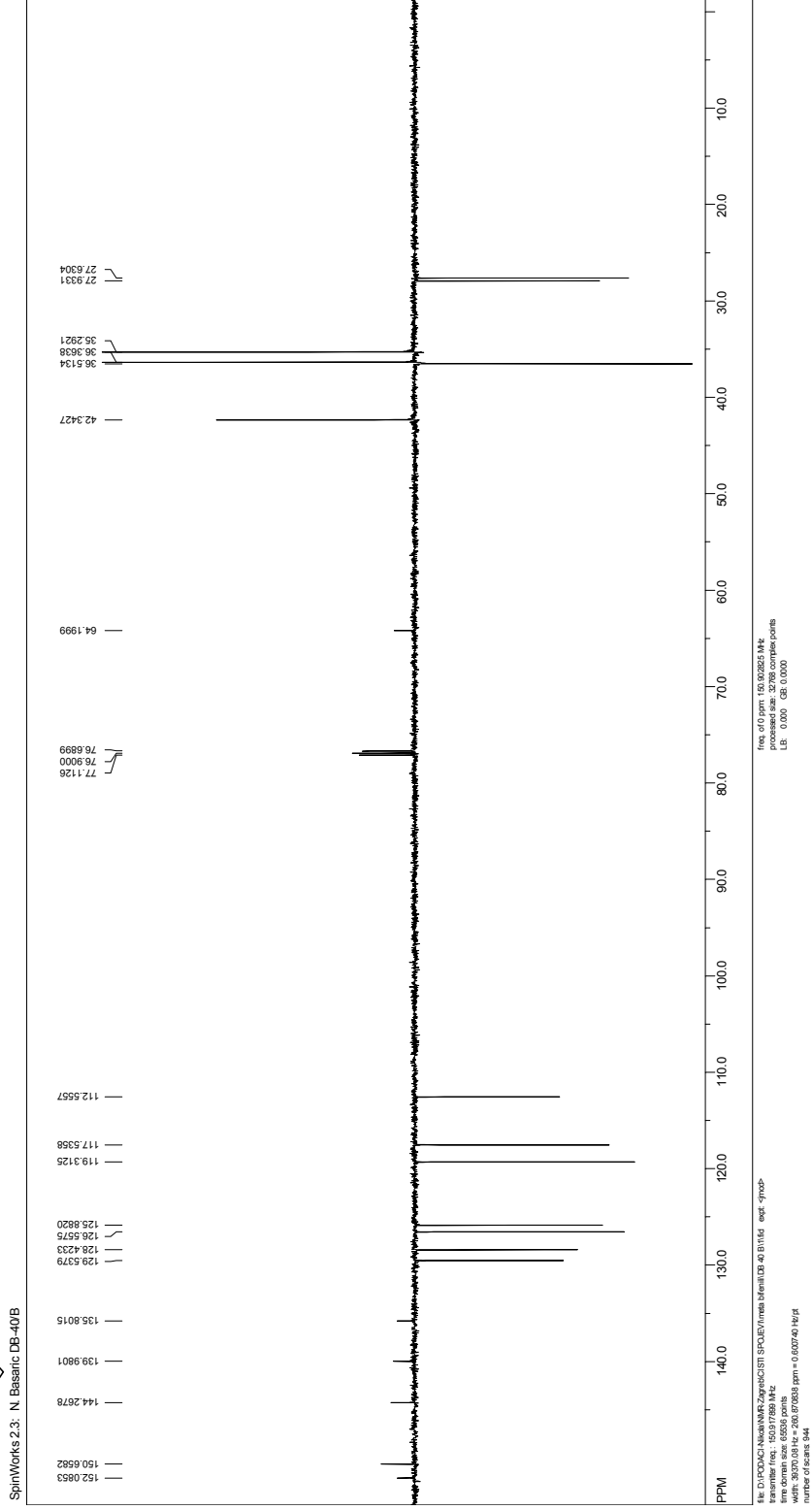
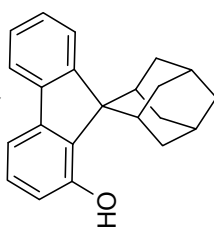


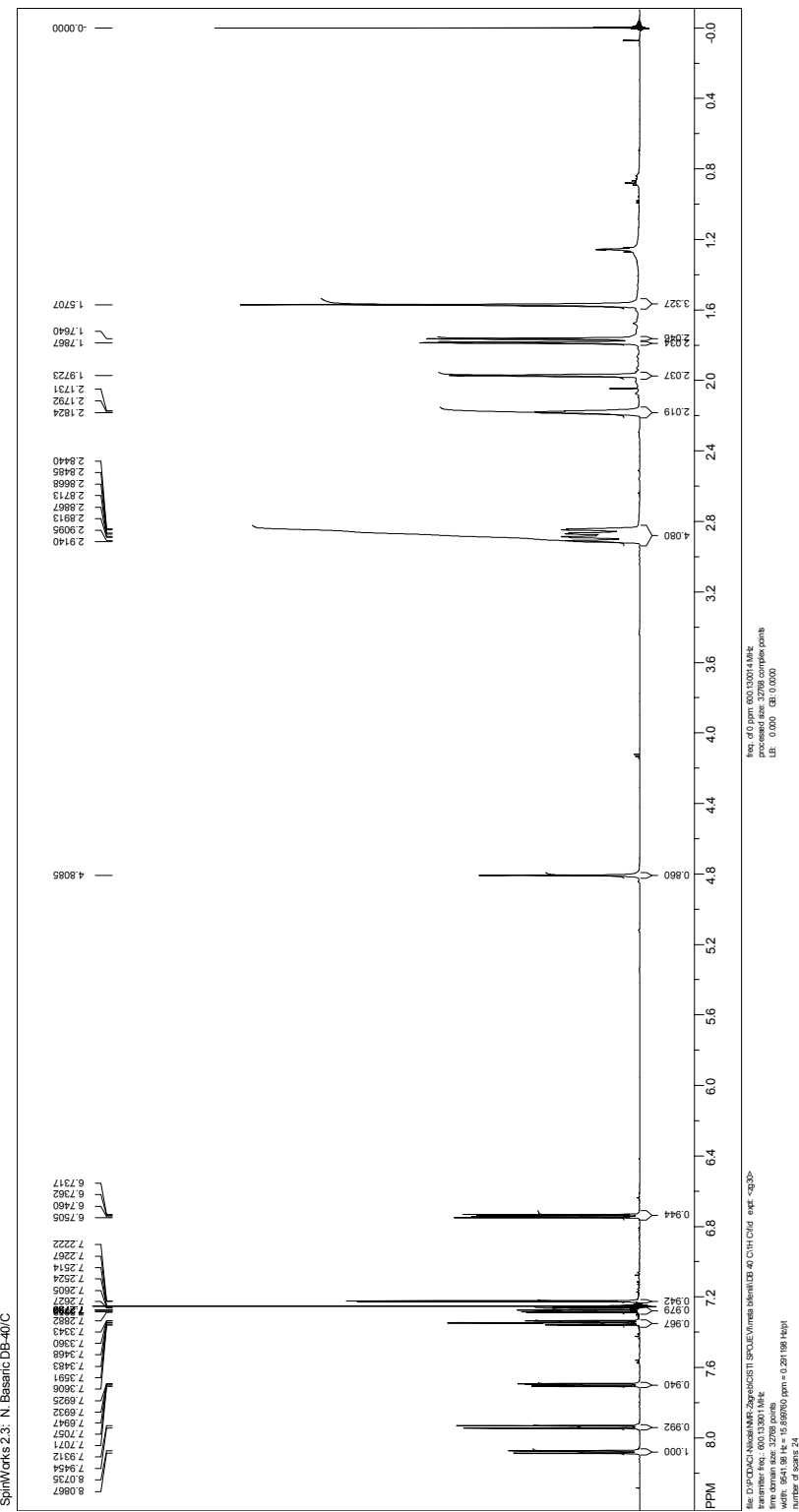
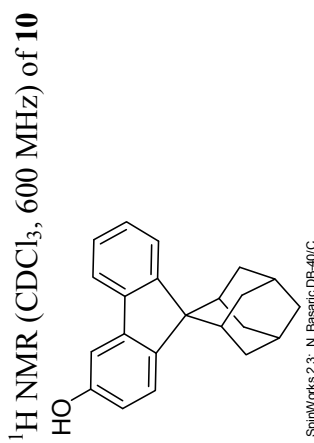
^{13}C NMR (DMSO- d_6 , 150 MHz) of 8



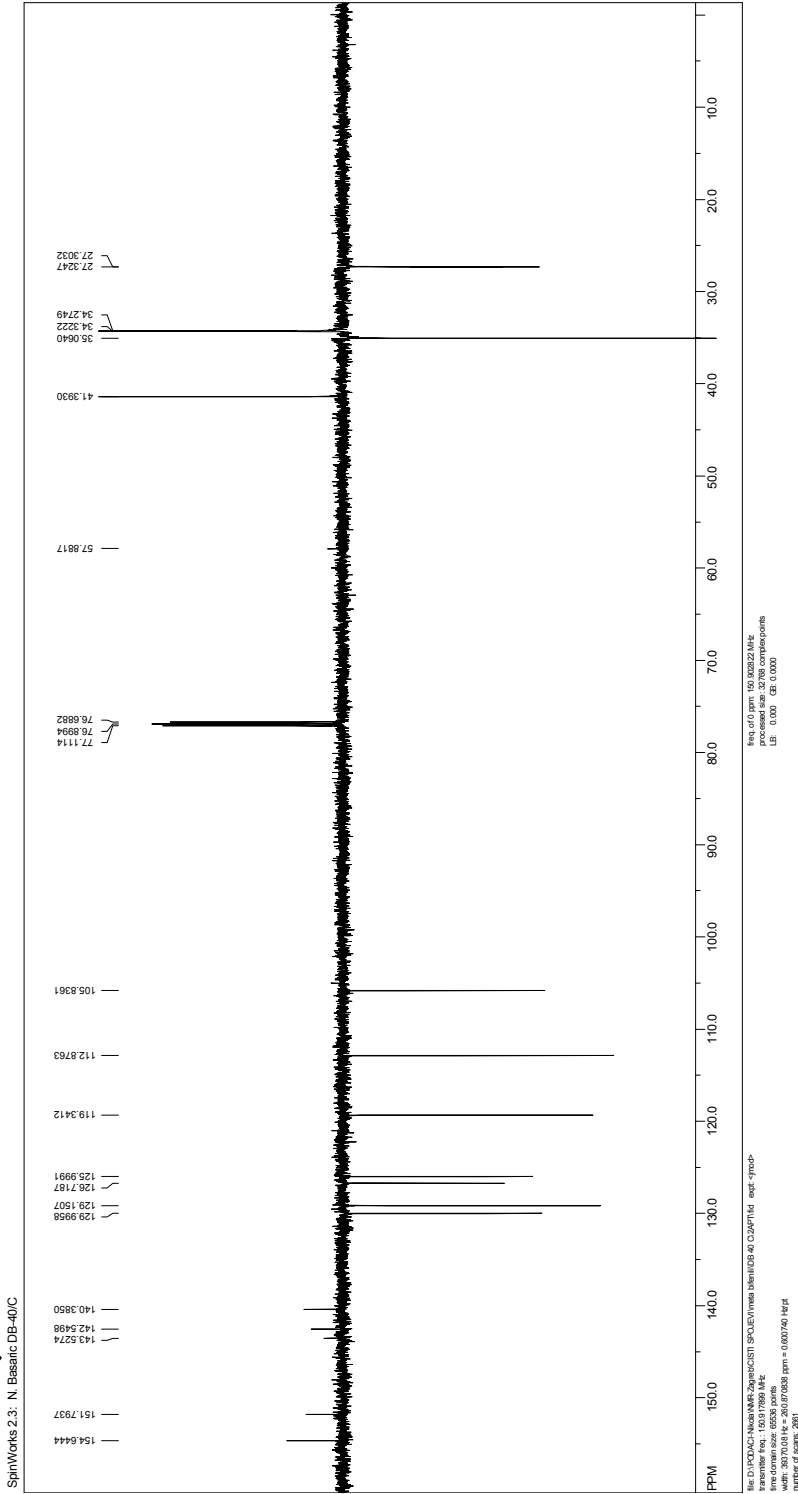
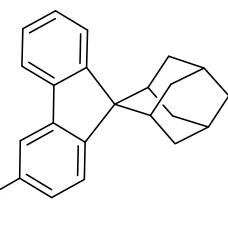


^{13}C NMR (CDCl_3 , 150 MHz) of **9**

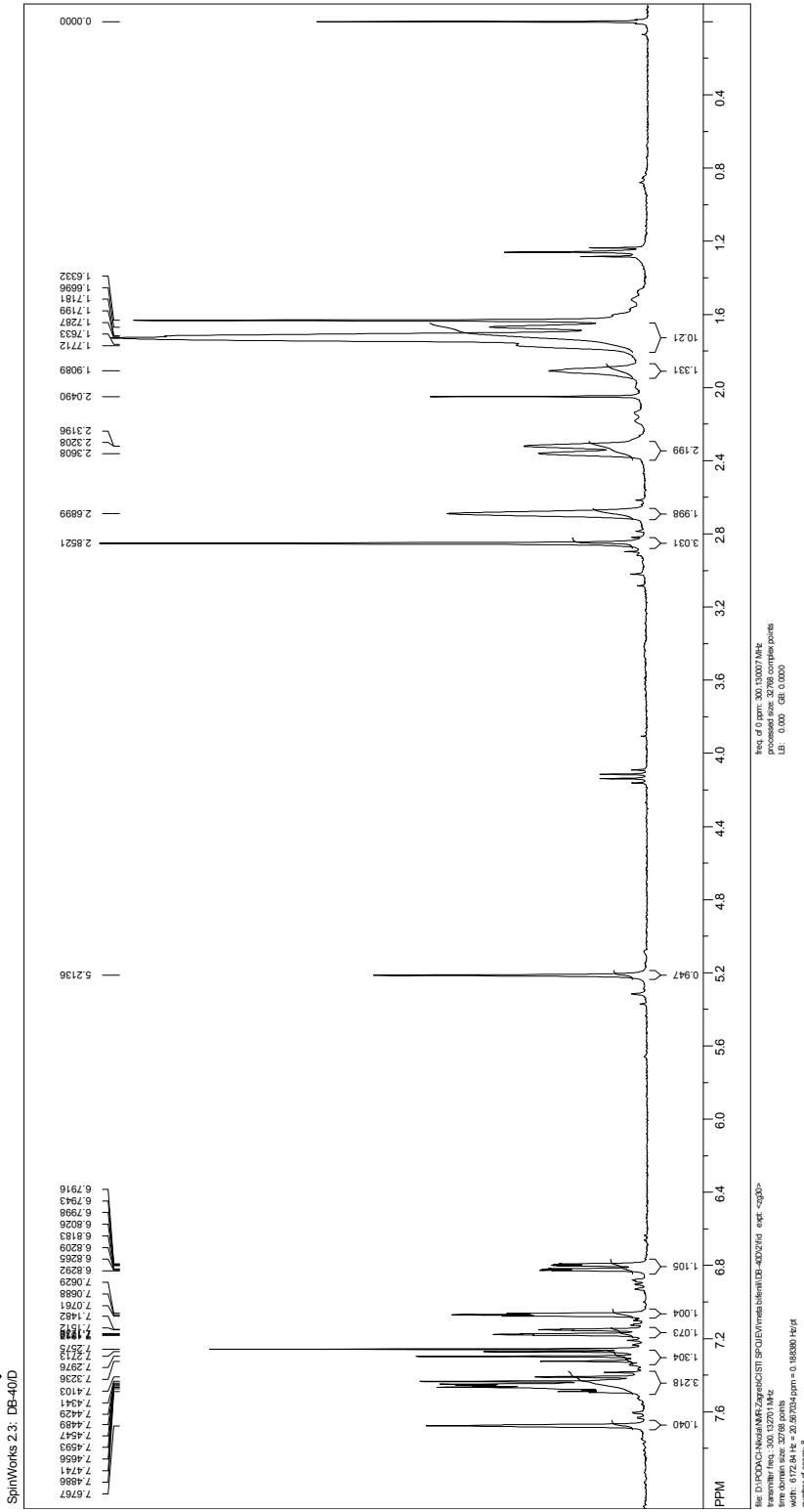
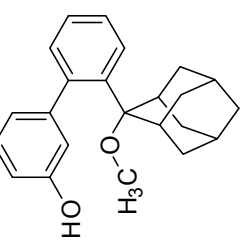




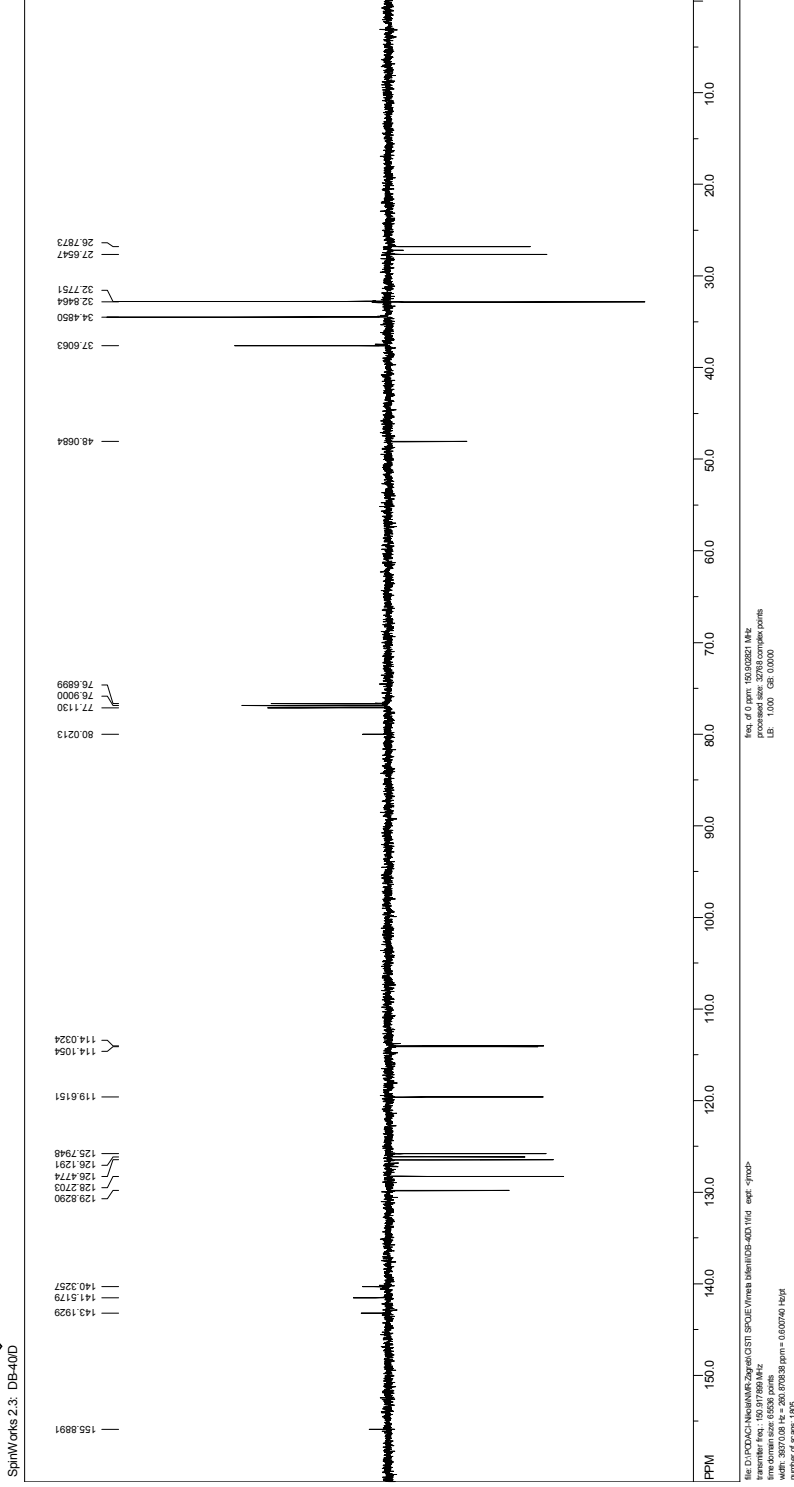
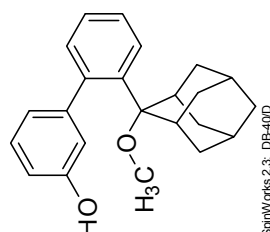
^{13}C NMR (CDCl_3 , 150 MHz) of **10**



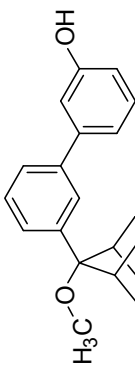
^1H NMR (DMSO- d_6 , 300 MHz) of 4b



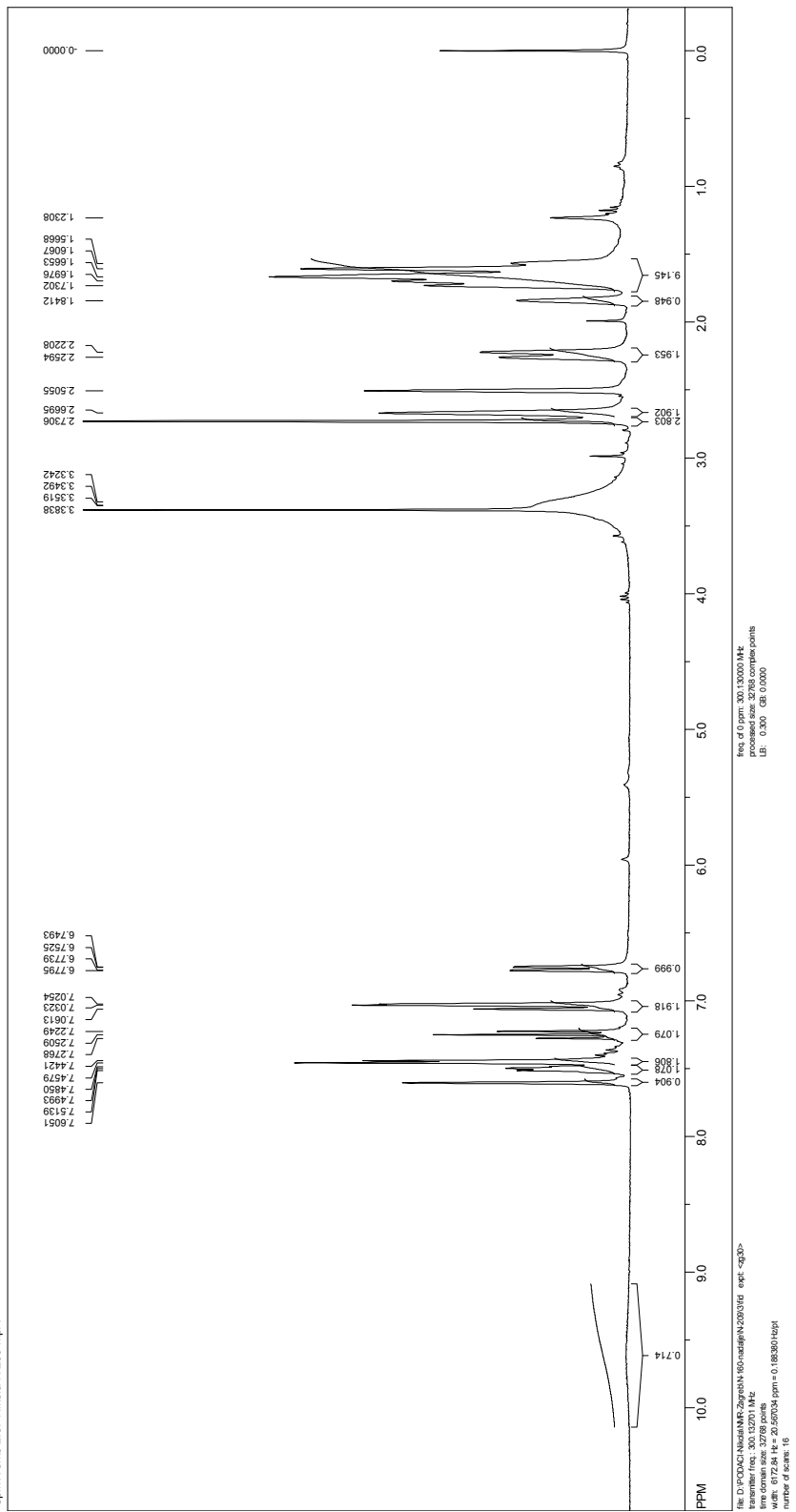
¹³C NMR (DMSO-*d*₆, 150 MHz) of 4b



^1H NMR (DMSO- d_6 , 300 MHz) of 5b

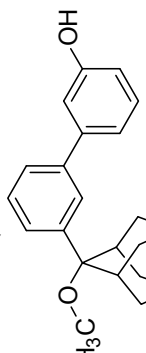


SpinWorks 2.3, NIKOLA N209 mPa

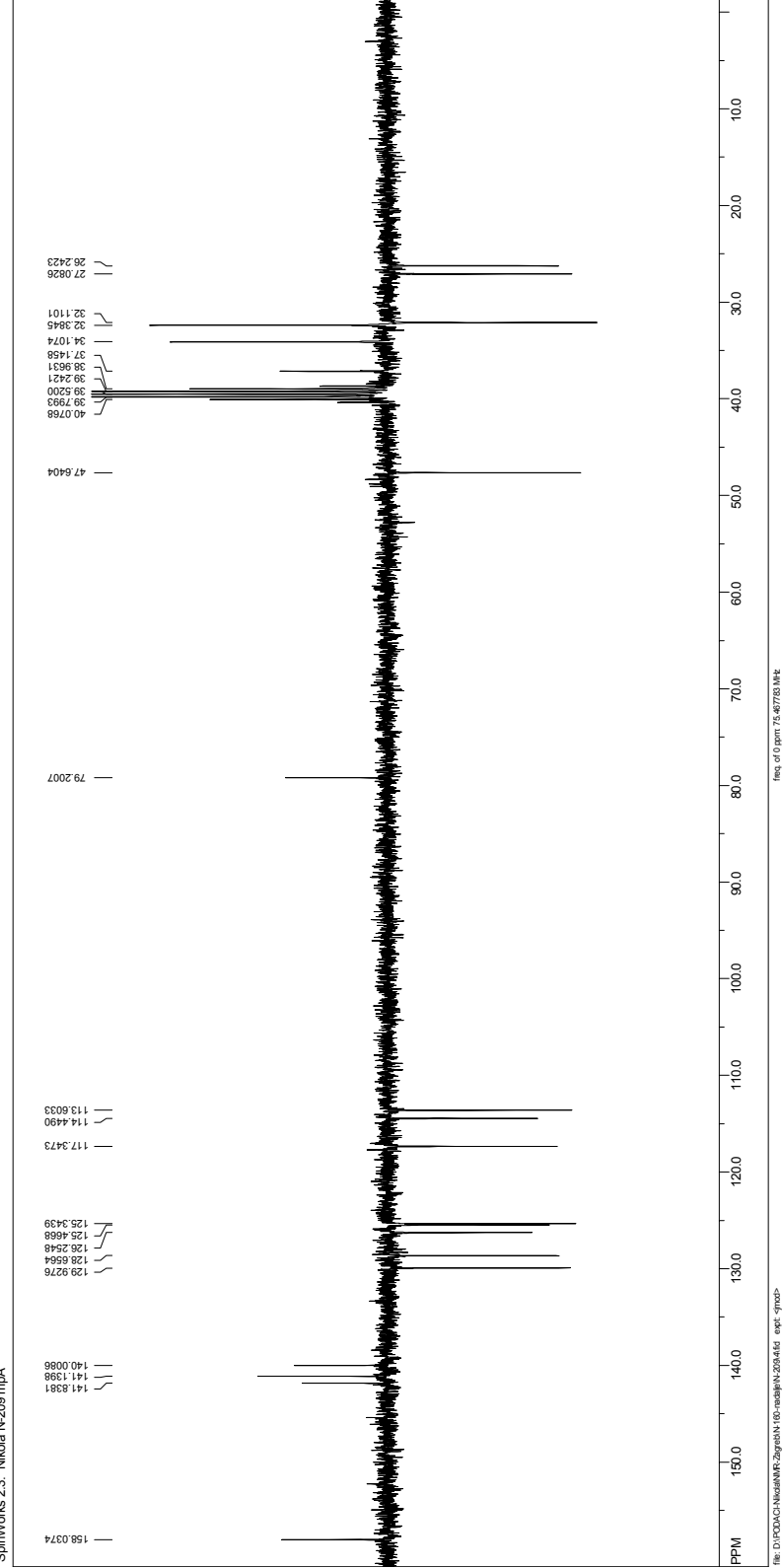


file: D:\POD4CN\NikolaN209\N209\3rd\1d\opt<>30-
transient free: 300, 52011 Hz
number of points: 2048000
width: 87.68 Hz
H_r = 20.20754 ppm, 0.188901 cps
number of scans: 16

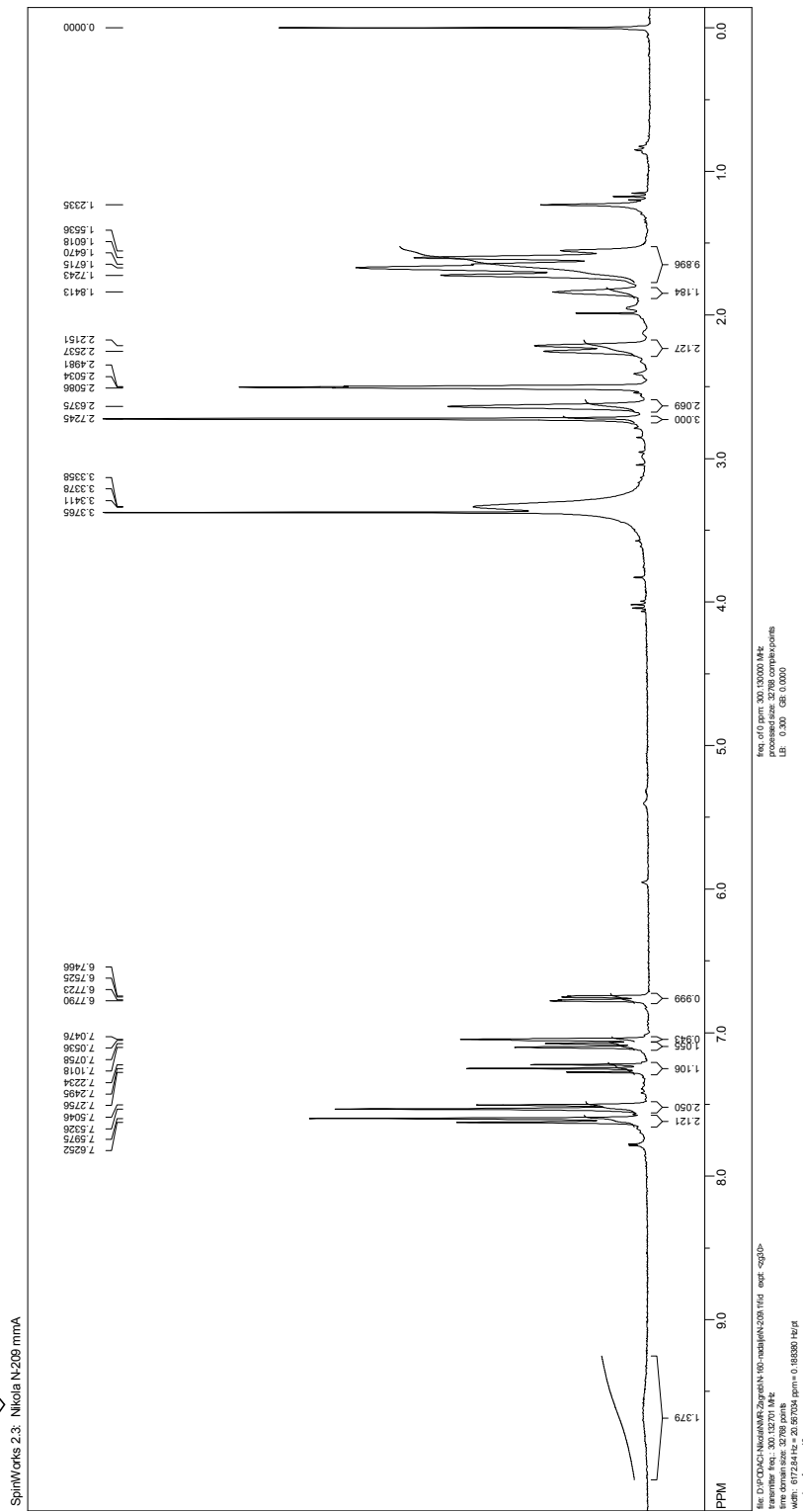
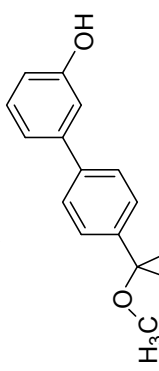
^{13}C NMR (DMSO- d_6 , 75 MHz) of 5b



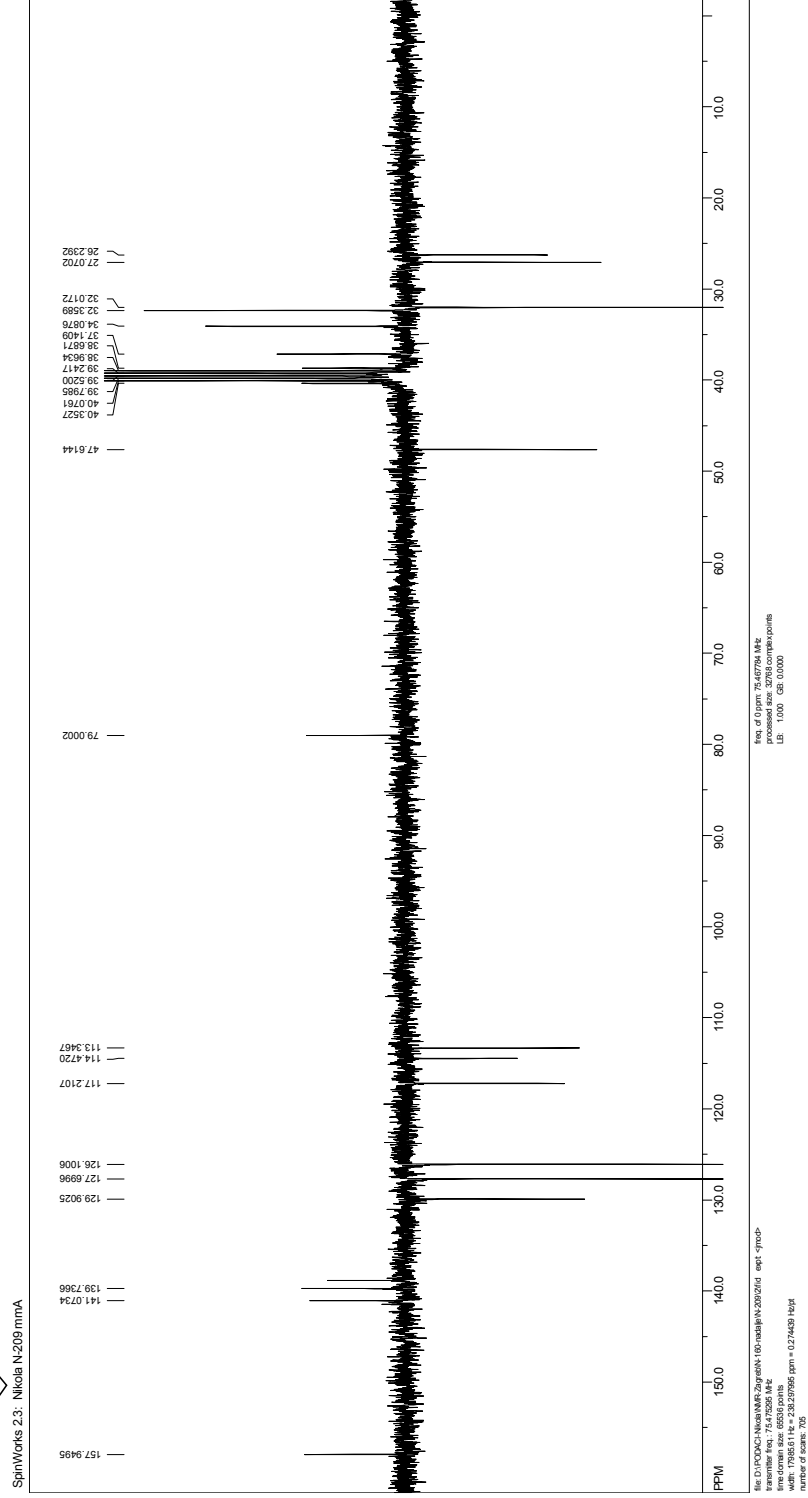
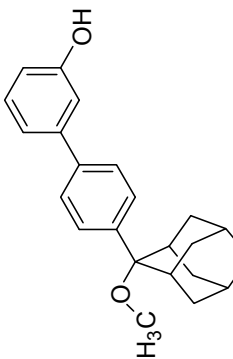
SpinWorks 2.3; Nikola N-209 mPa



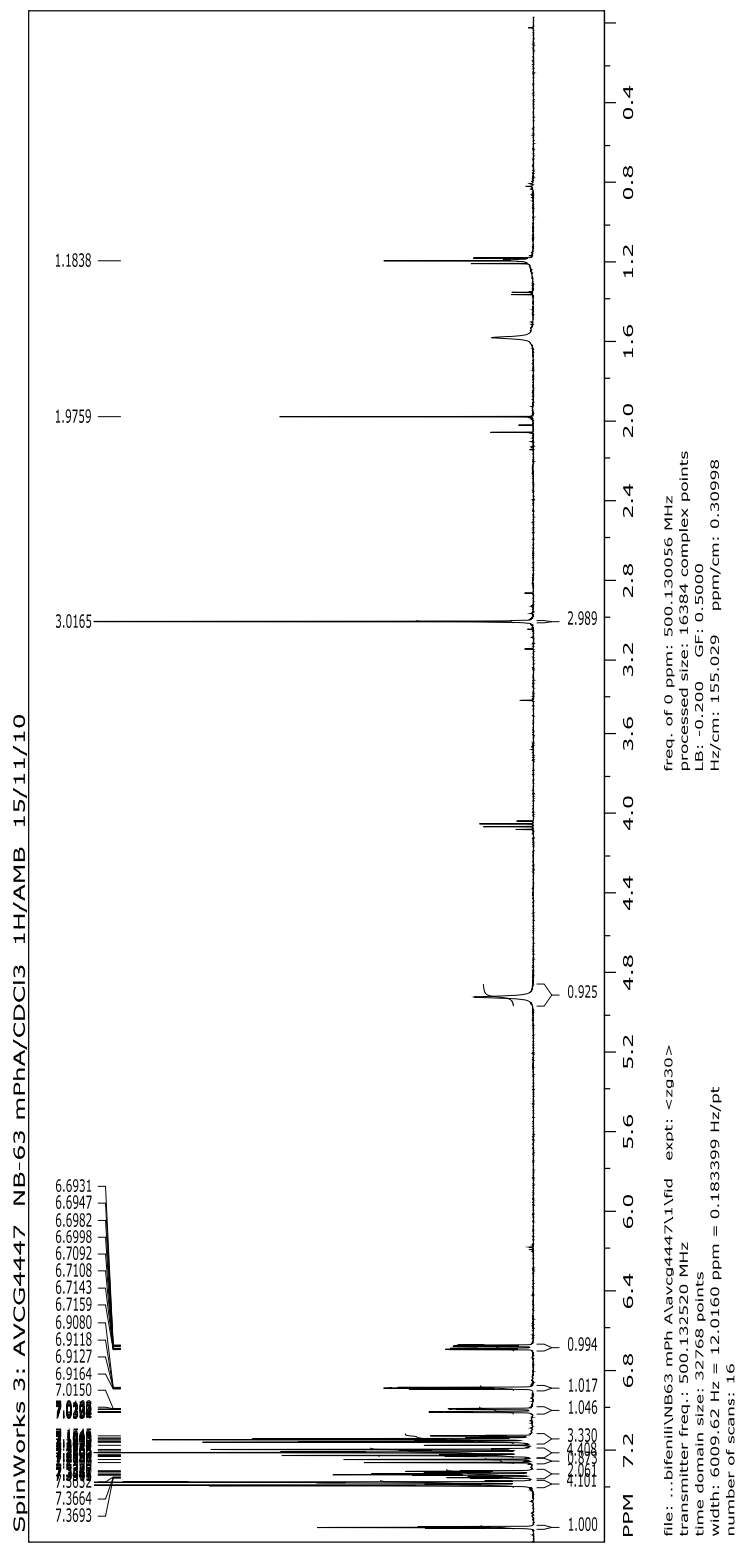
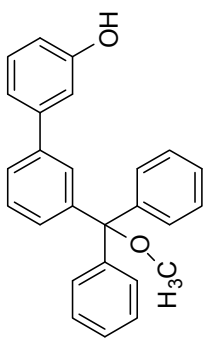
^1H NMR (DMSO- d_6 , 300 MHz) of **6b**



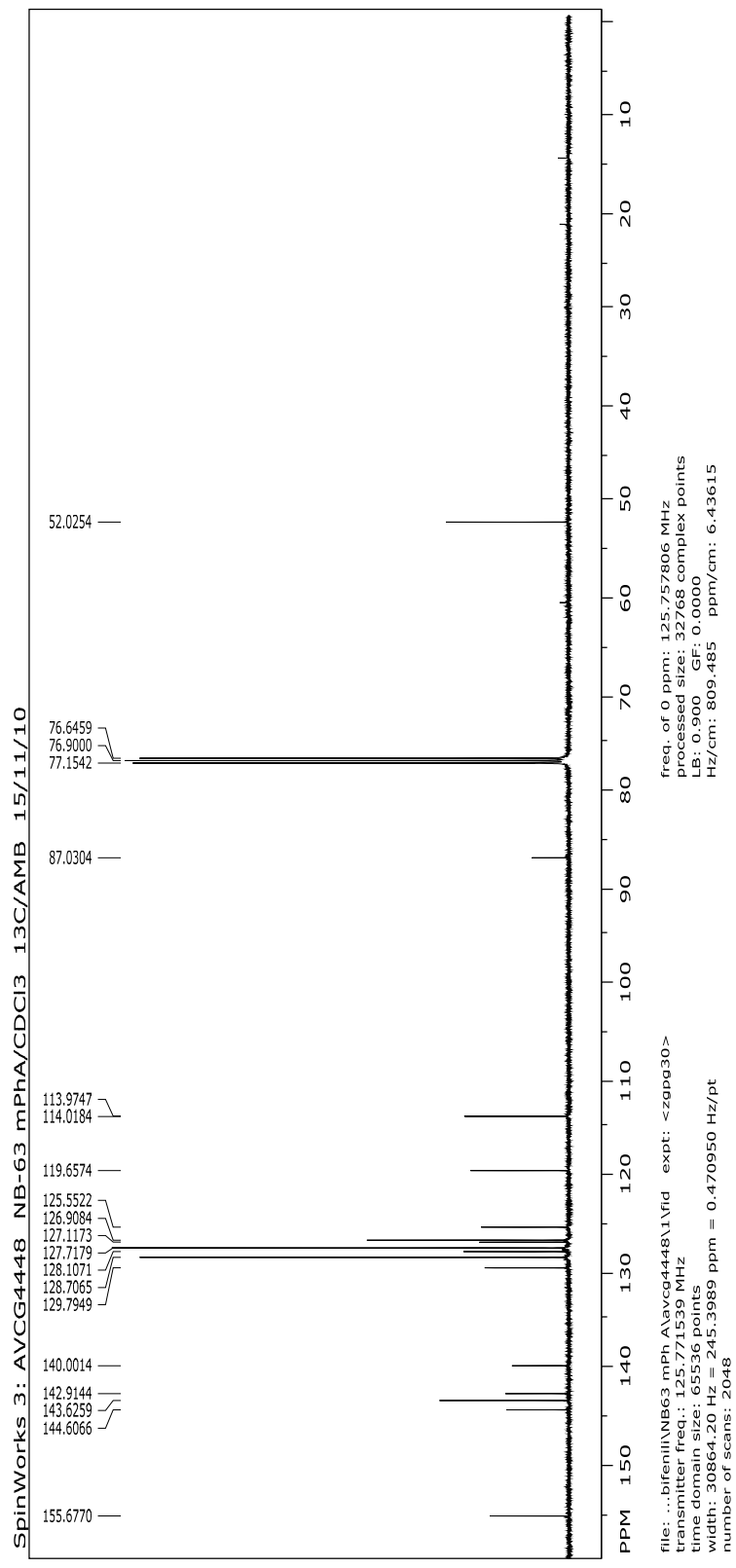
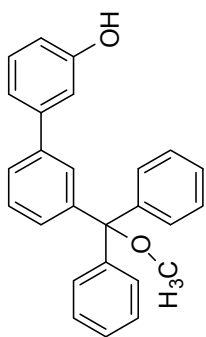
^{13}C NMR (DMSO- d_6 , 75 MHz) of **6b**



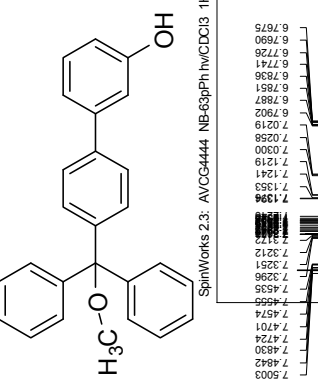
¹H NMR (CDCl₃, 500 MHz) of 7b



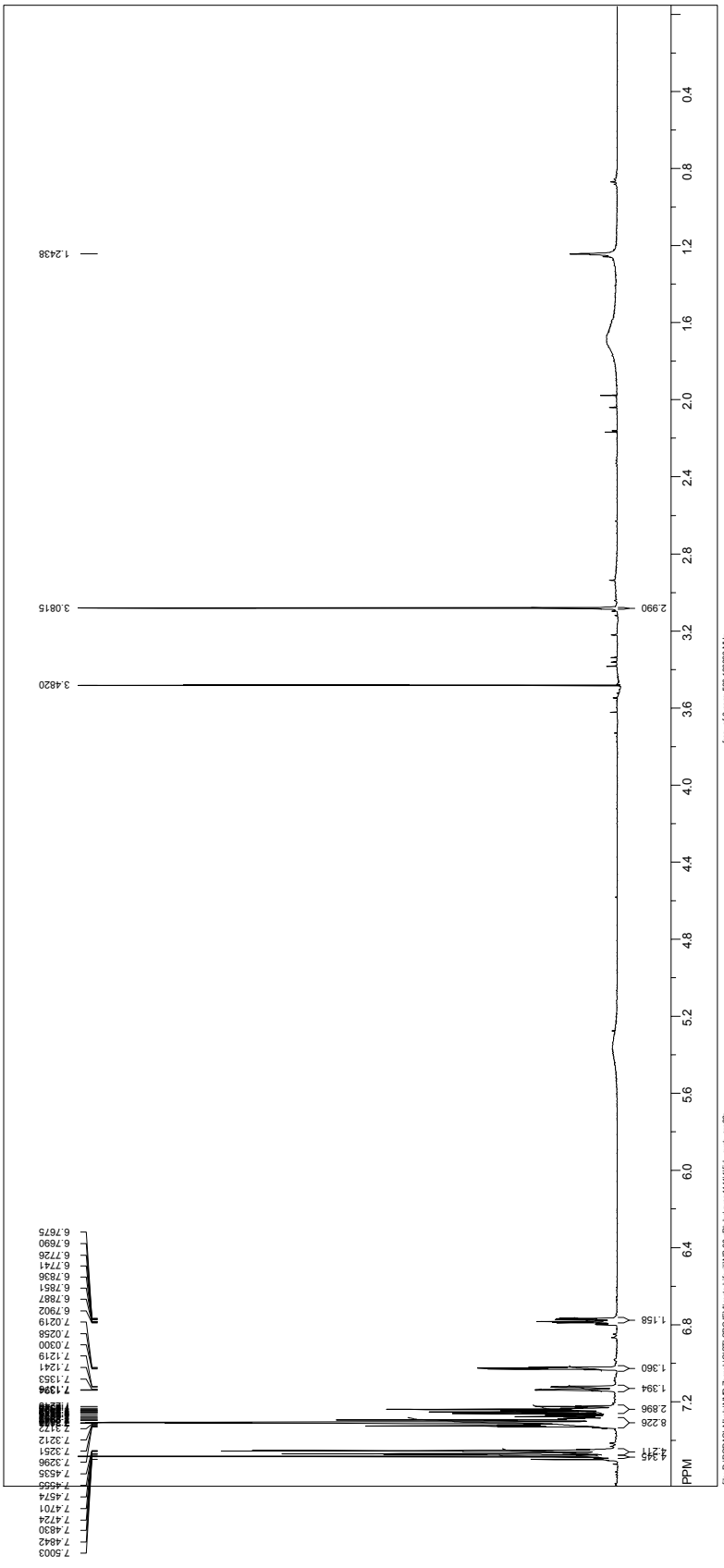
^{13}C NMR (CDCl_3 , 125 MHz) of 7b



¹H NMR (CDCl₃, 500 MHz) of 8b

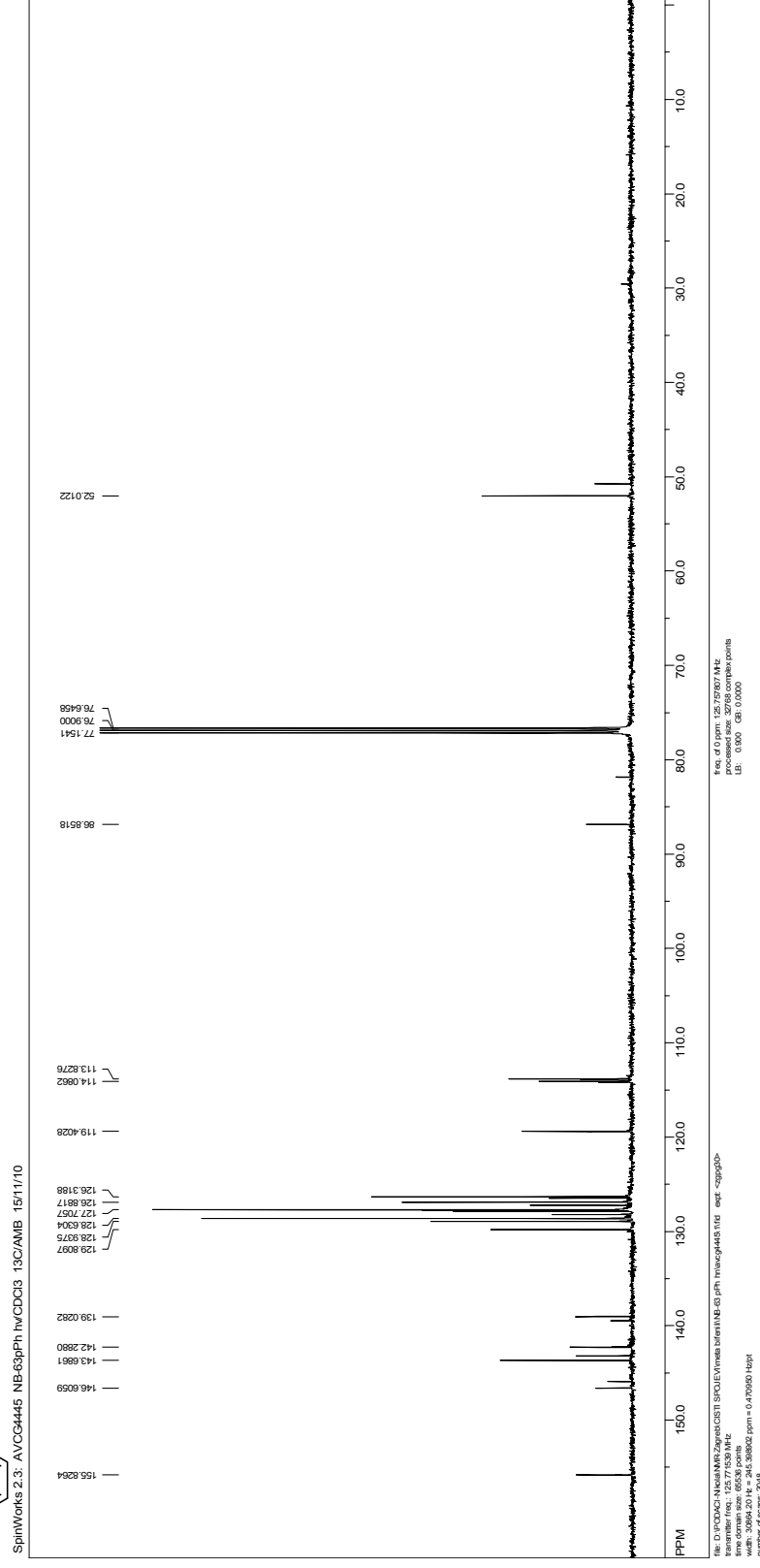
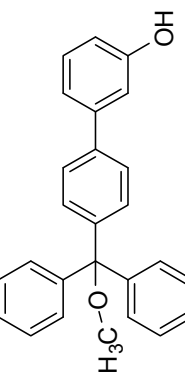


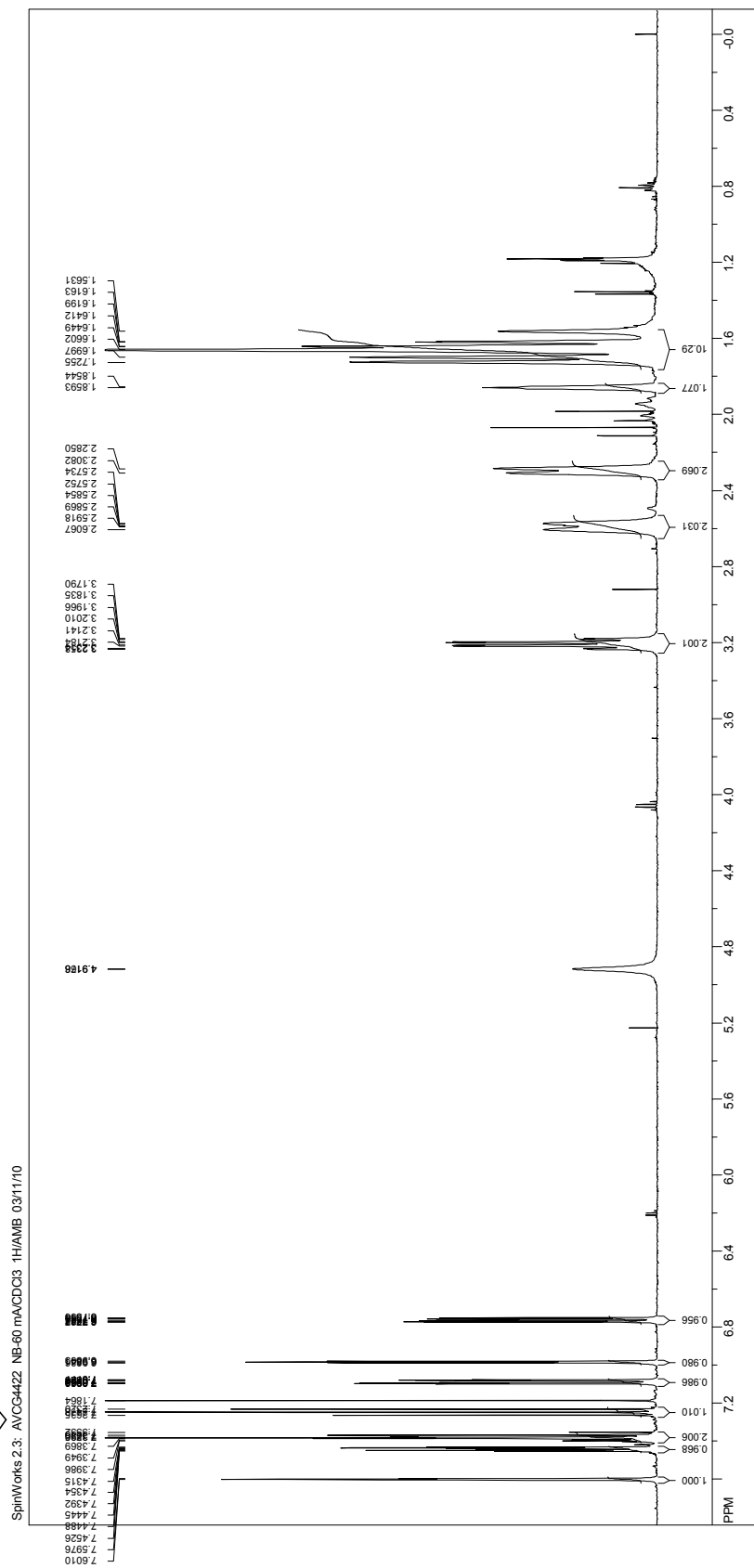
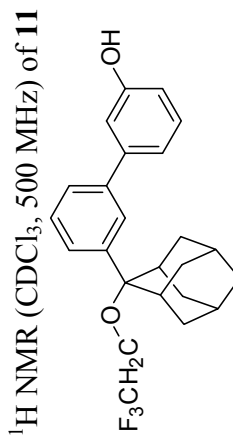
SpinWorks 2.3: AVCG4444 NB-63pPhhv/CDCl₃ 1H/AMB 15/11/10



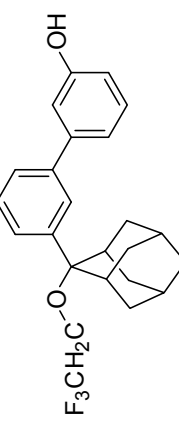
file: D:\POC\Ch-NMR\2\grnd\CDCl3\SP01\mrs_ben\mrs_b3.ppm\hdf\mrs_b3.hdf
transmitter freq.: 500.13252 MHz
time domain size: 27360 points
water: 6000.6214 = 0.07646 ppm = 0.183299 Hz/¹C
number of scans: 16
LB: -0.200 (GB: 0.000)

^{13}C NMR (CDCl_3 , 125 MHz) of **8b**

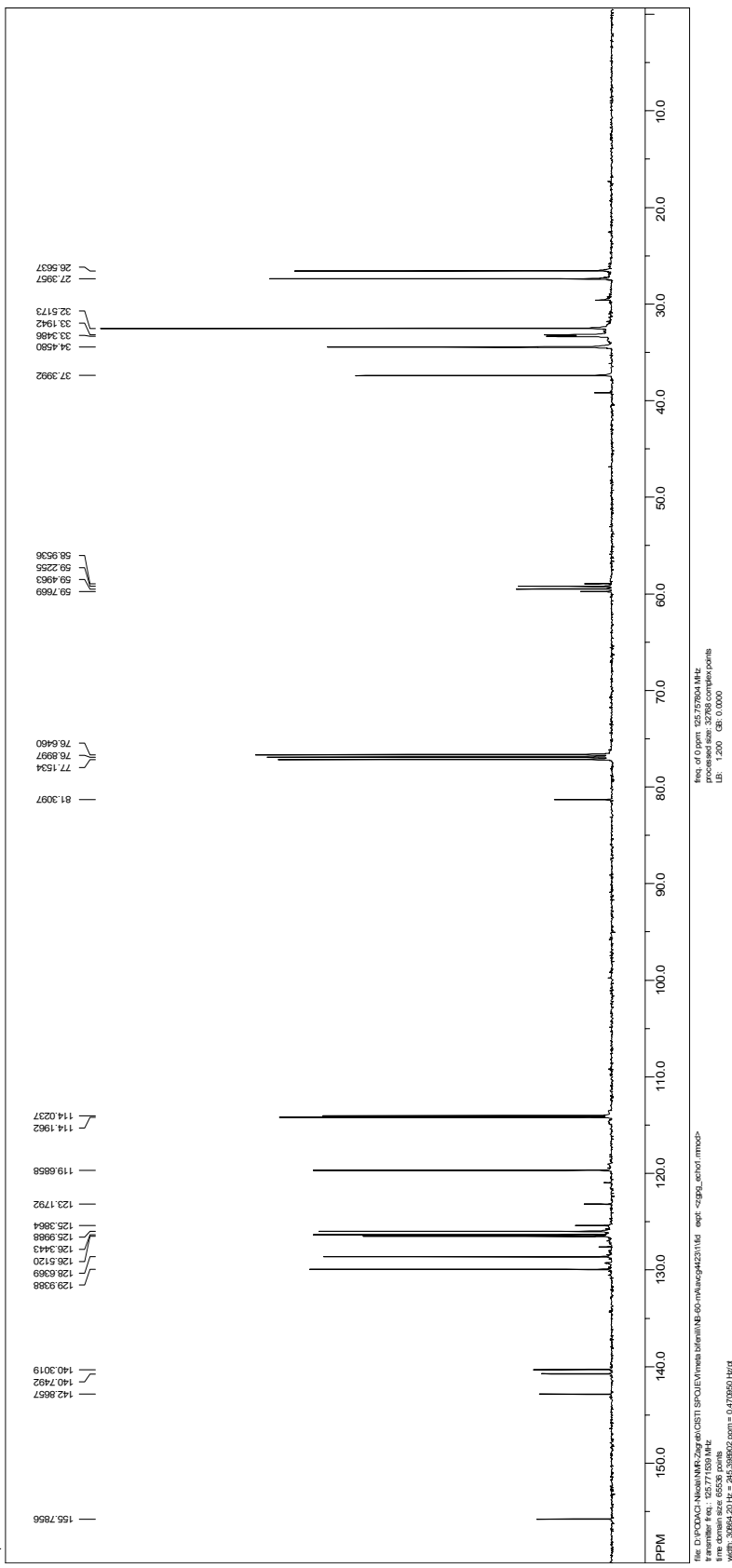




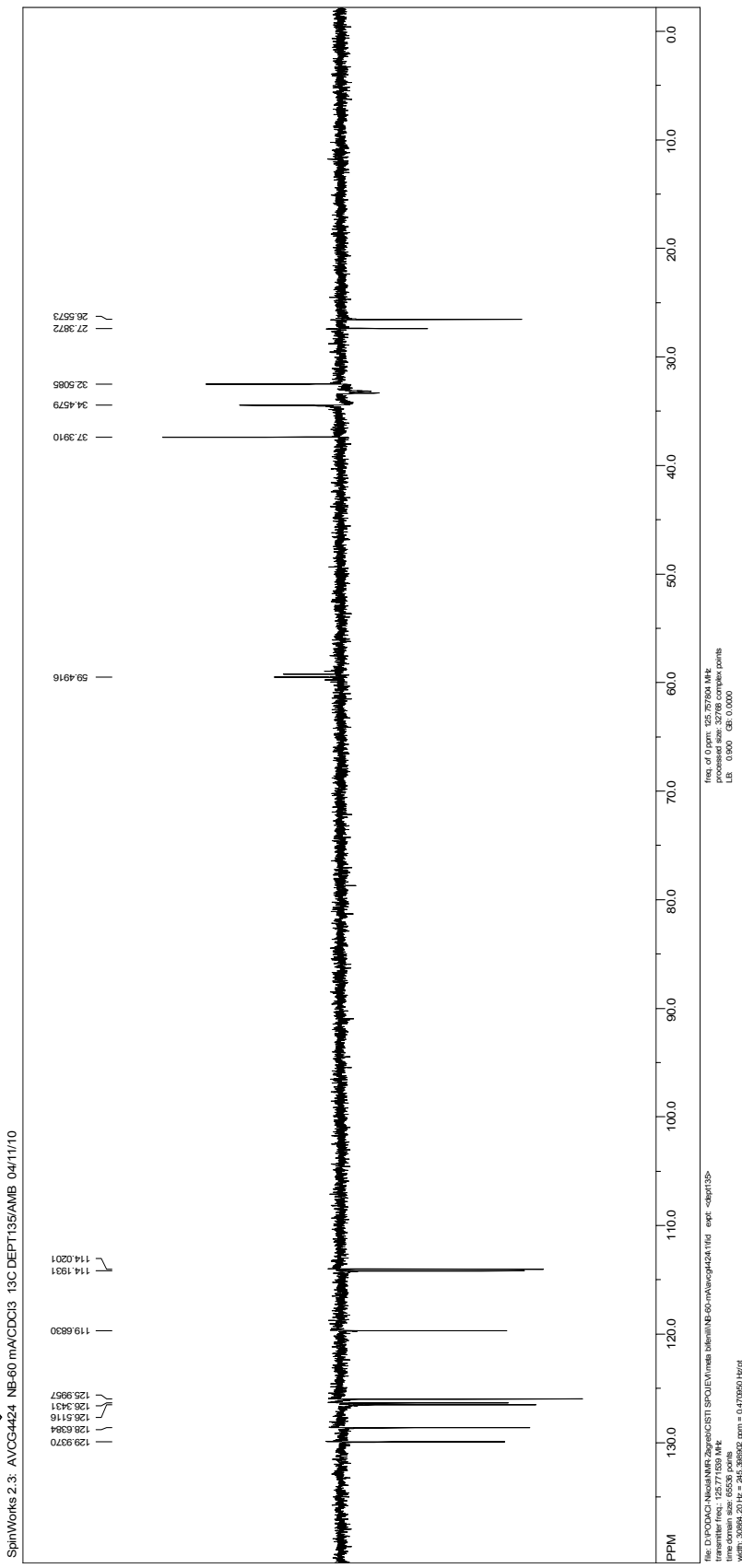
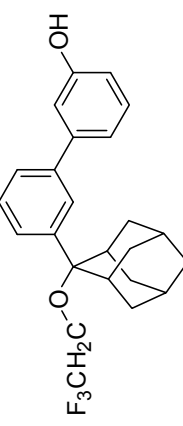
^{13}C NMR (CDCl_3 , 125 MHz) of 11



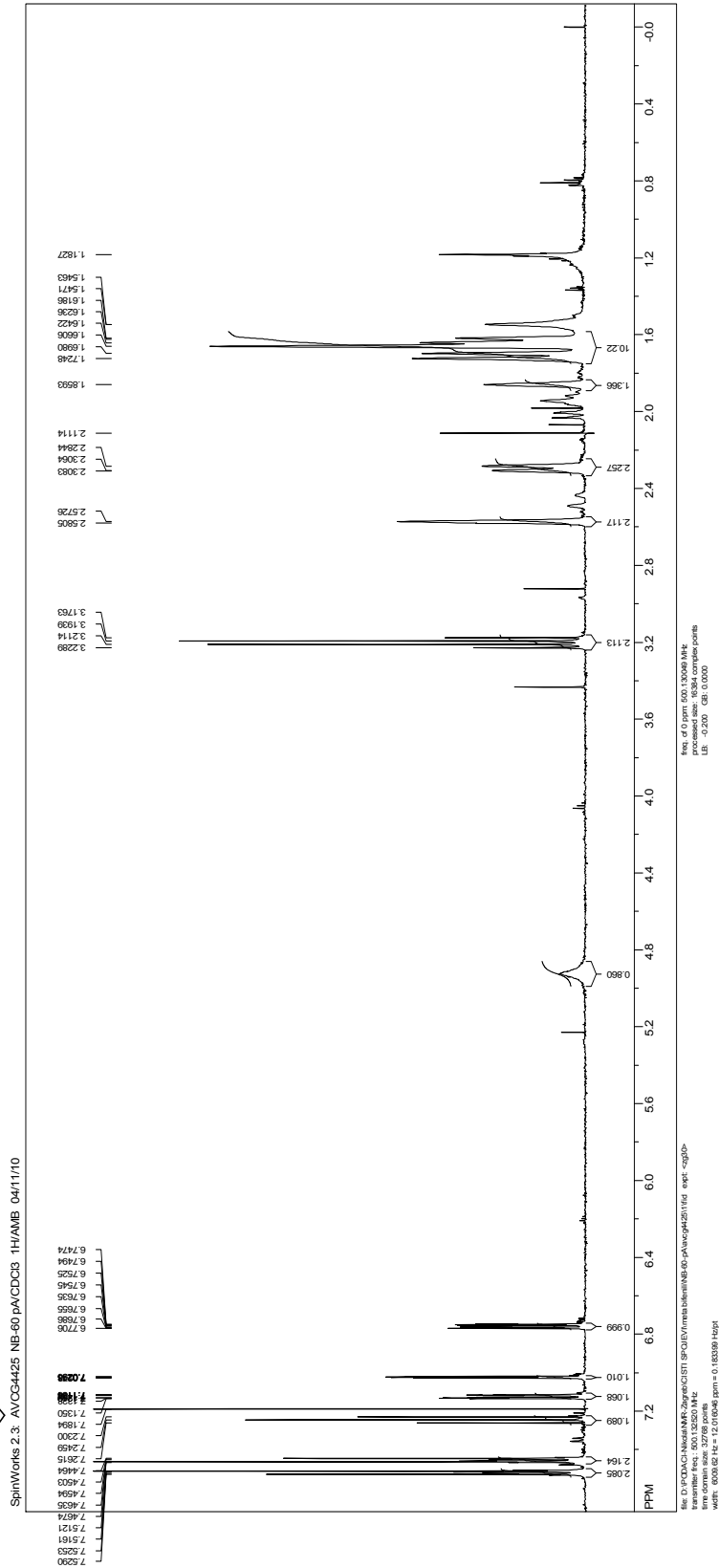
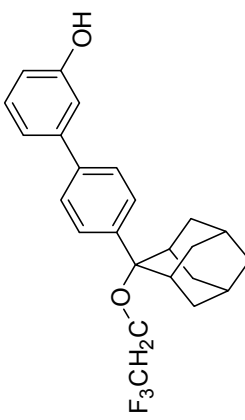
SpinWorks 2.3, AVCG4423, NB-60 mA/ODCIS 13C/AMB 03/11/10



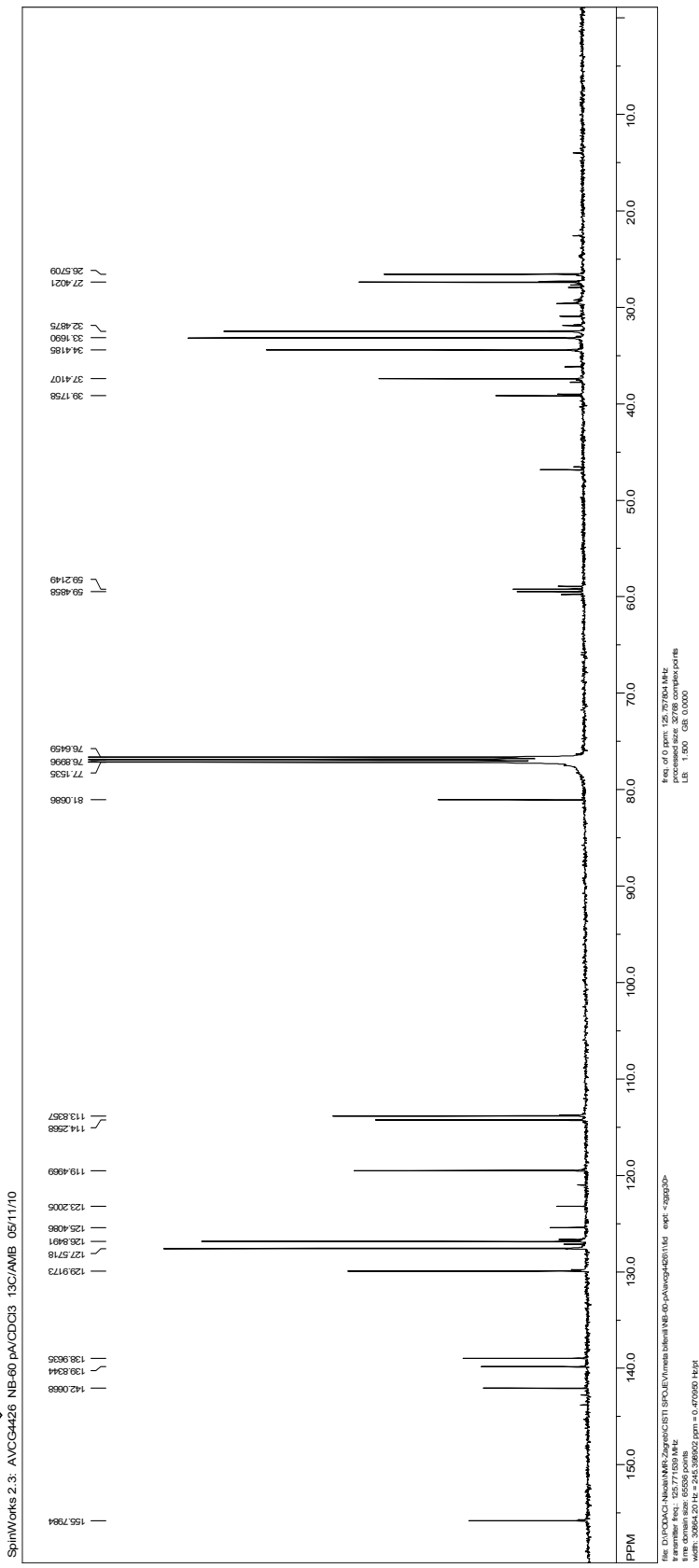
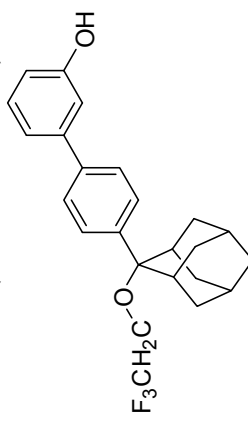
^{13}C NMR (CDCl_3 , 125 MHz, DEPT) of 11



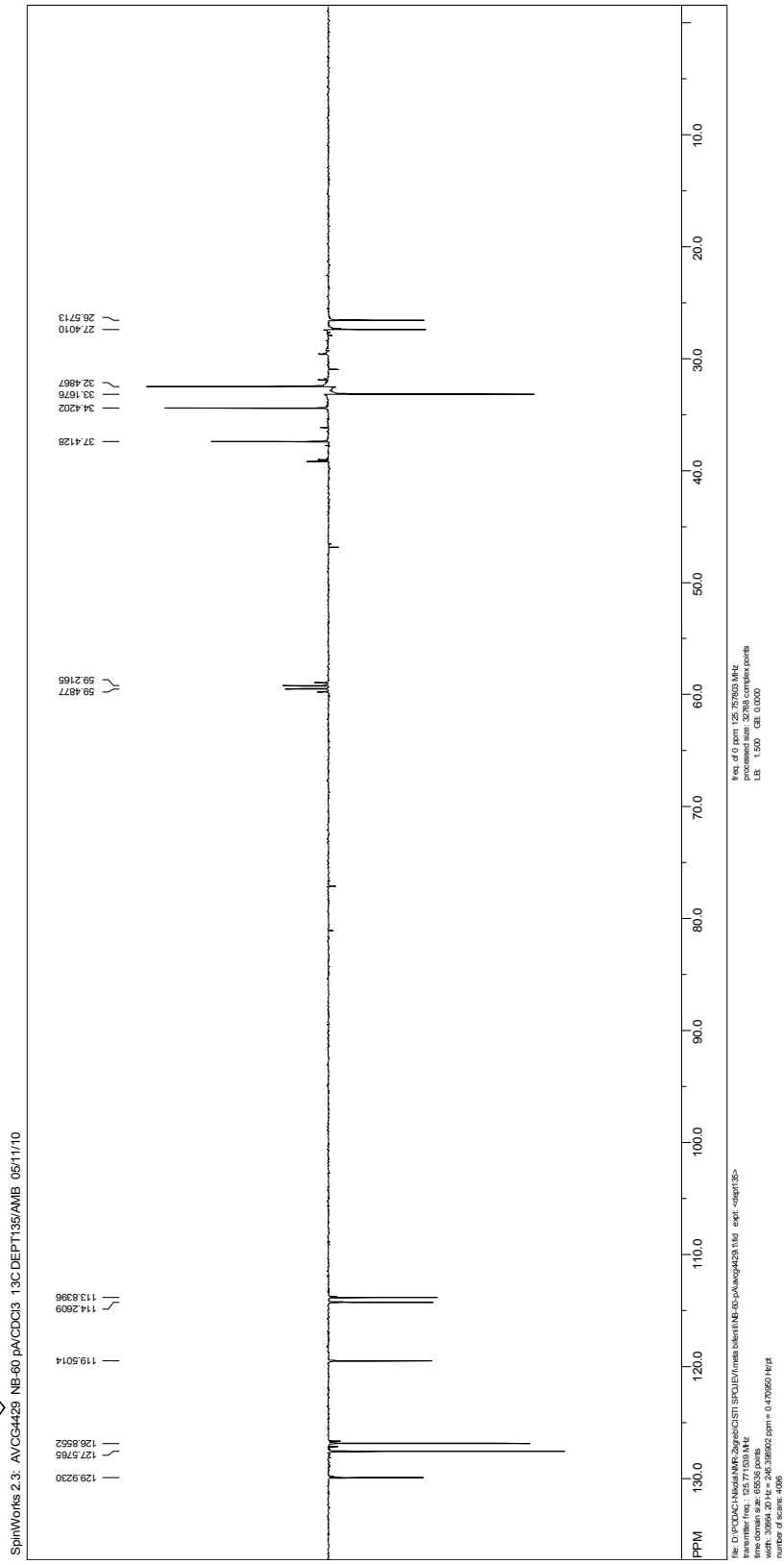
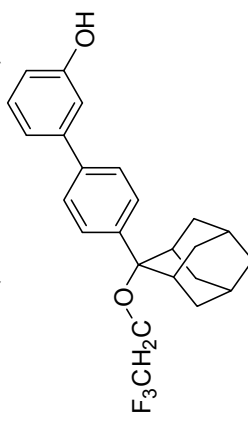
^1H NMR (CDCl_3 , 500 MHz) of 12



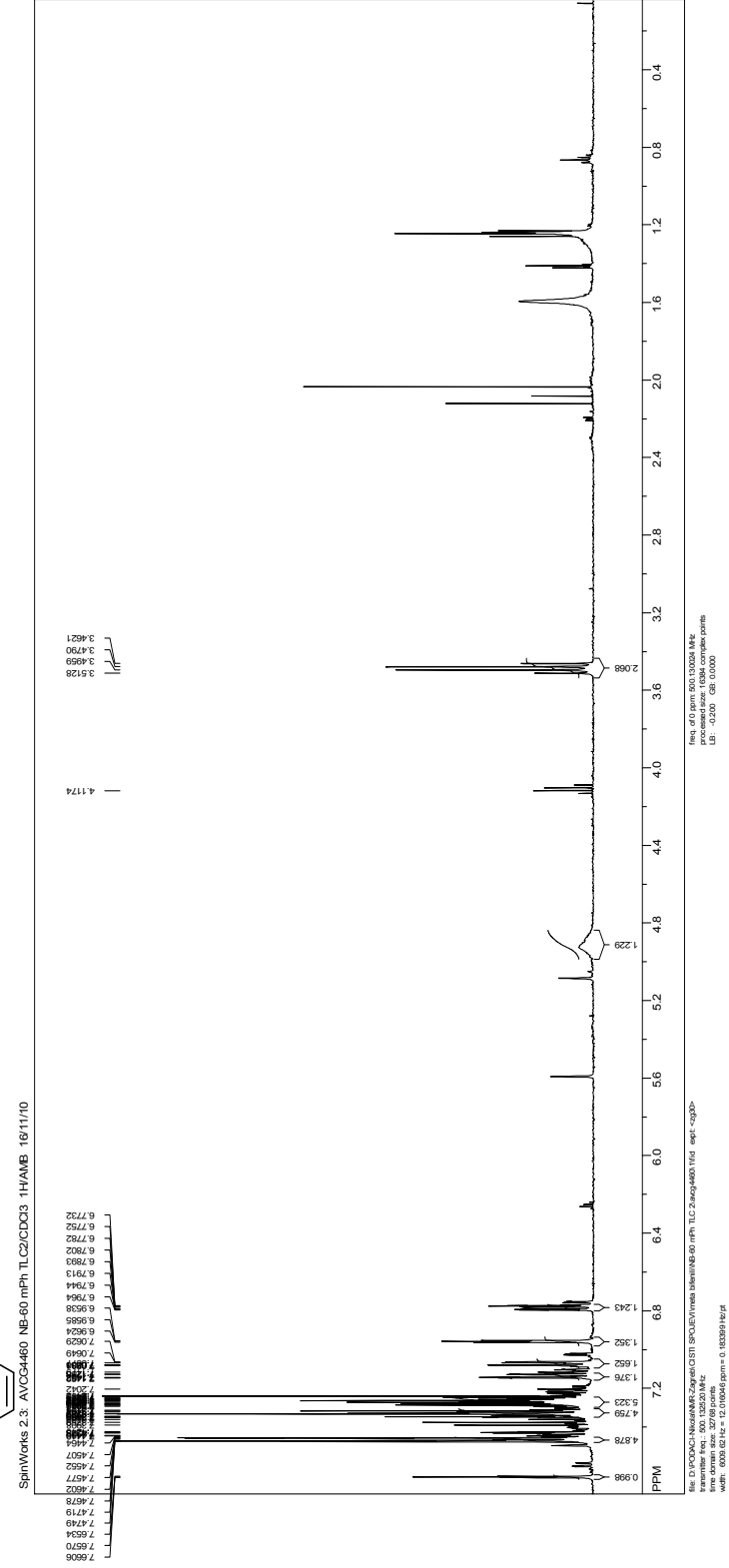
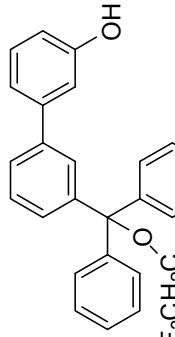
^{13}C NMR (CDCl_3 , 125 MHz) of 12



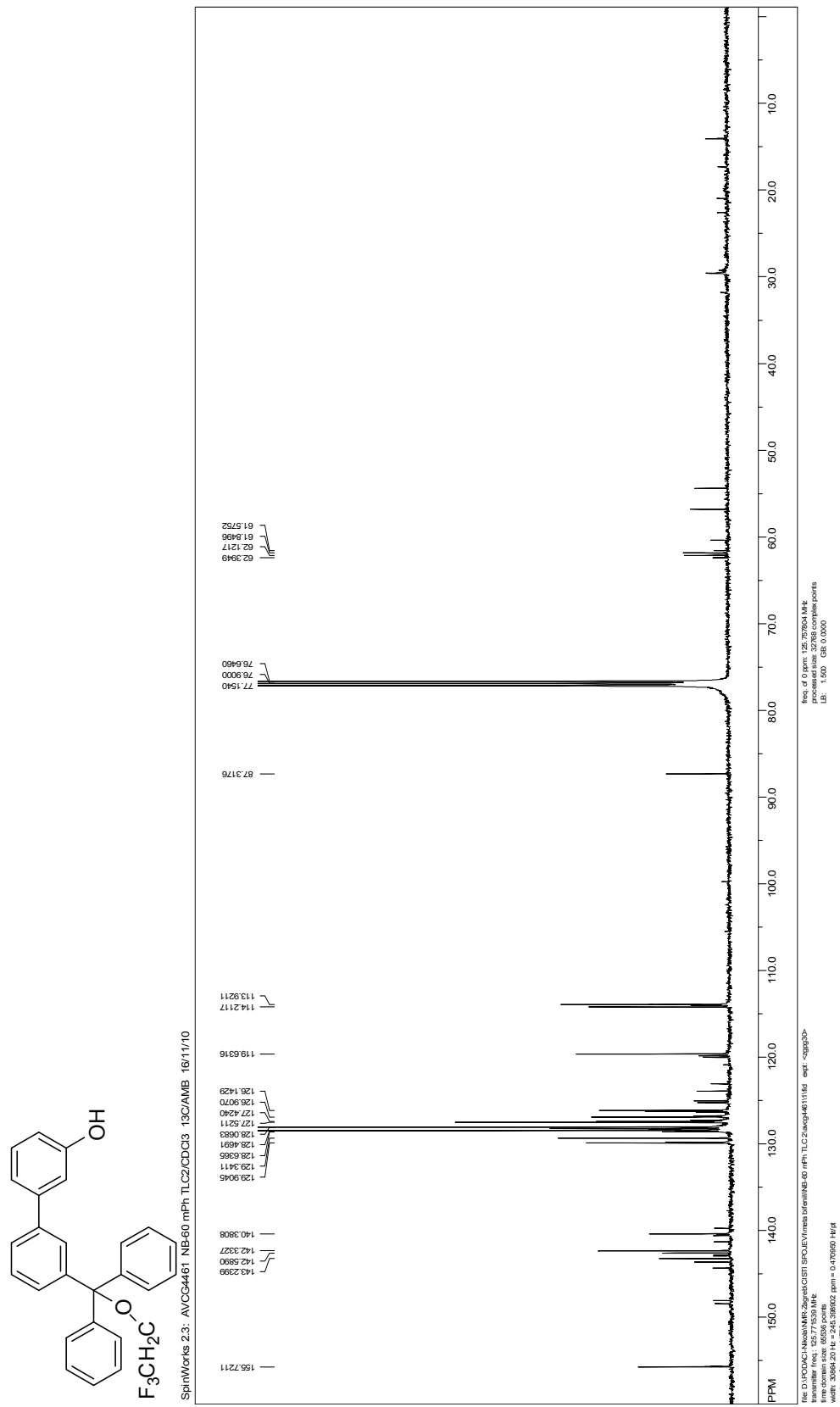
^{13}C NMR (CDCl_3 , 125 MHz) of 12



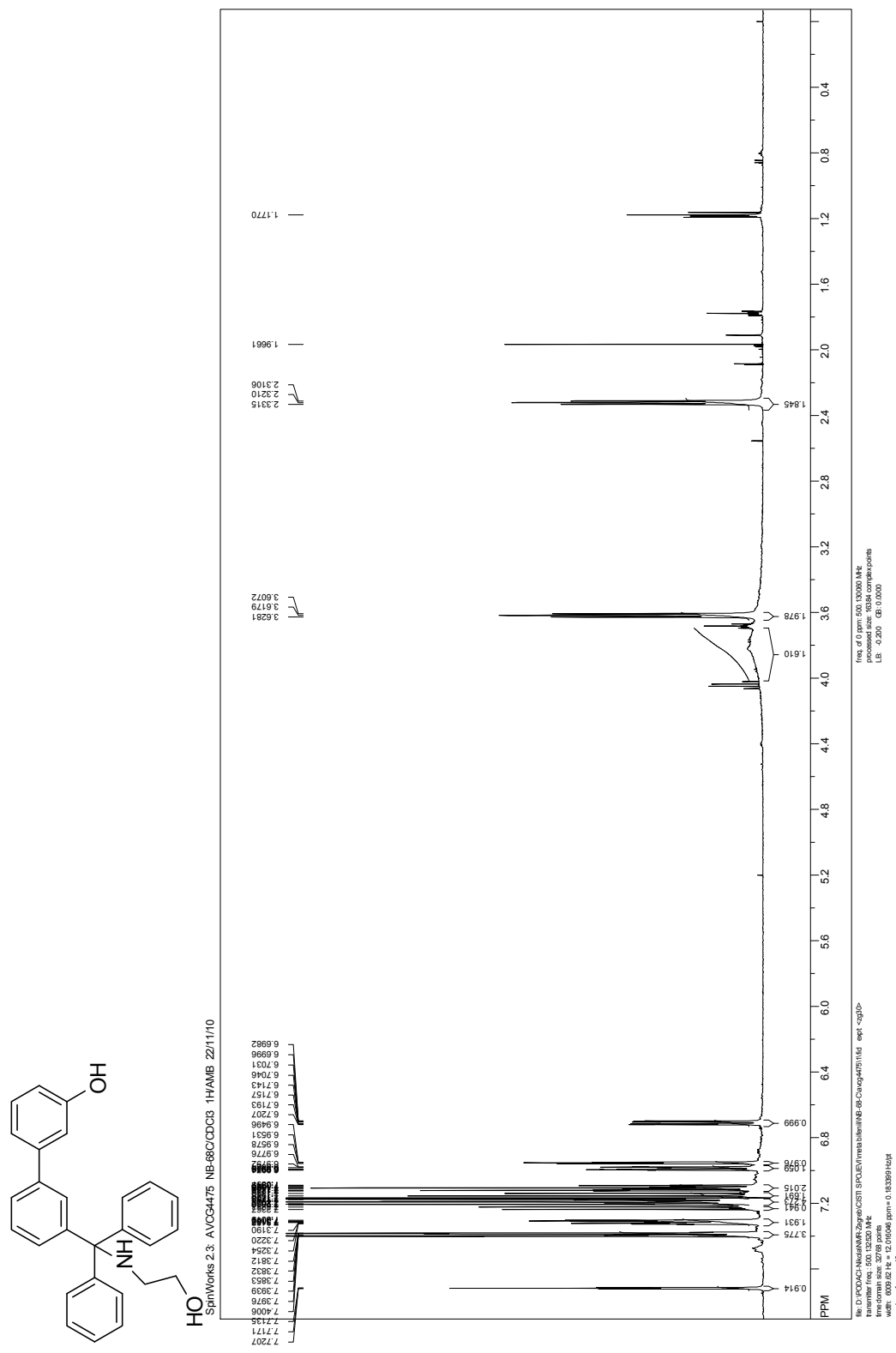
^1H NMR (CDCl_3 , 500 MHz) of 12



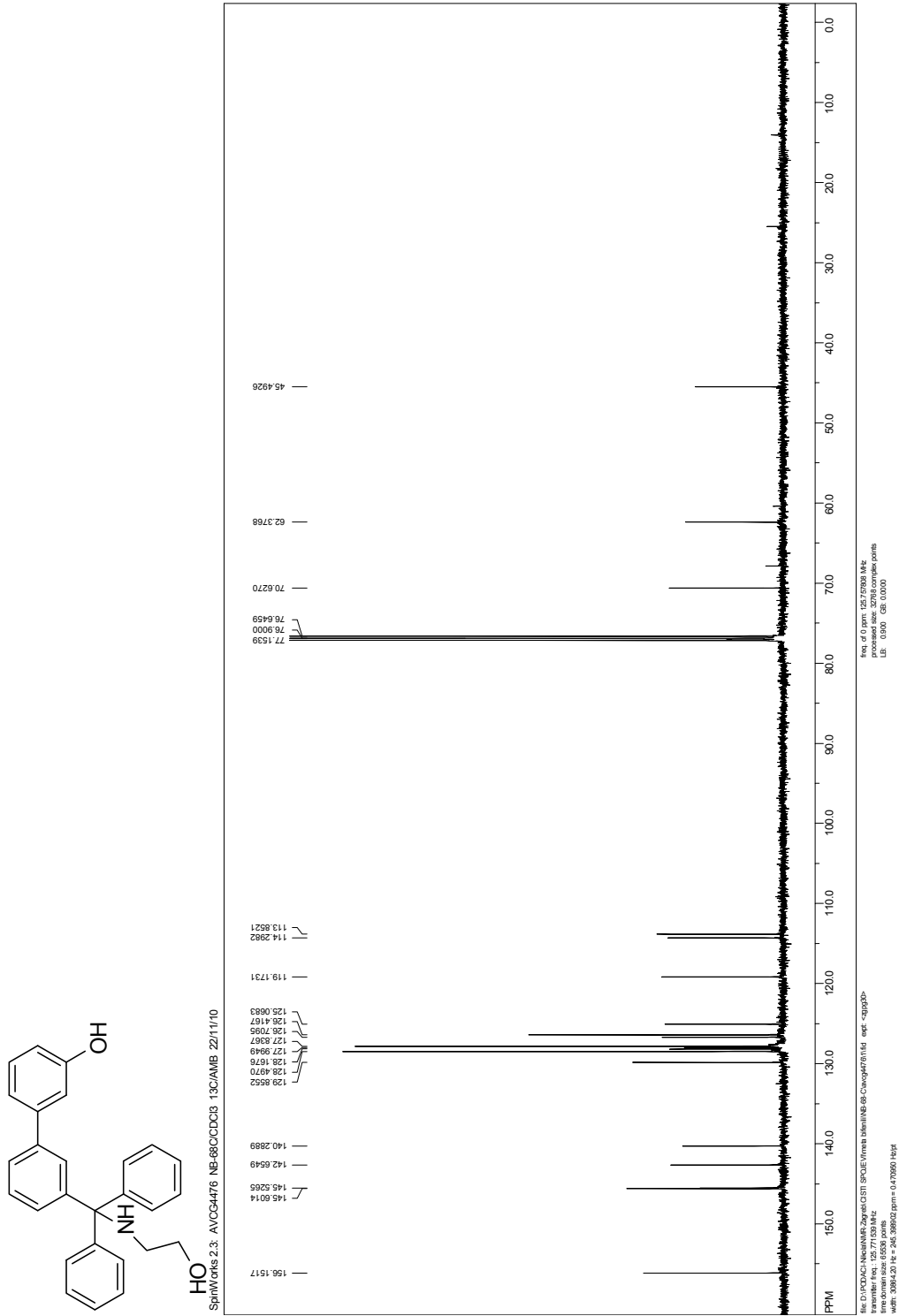
^{13}C NMR (CDCl_3 , 125 MHz) of 12



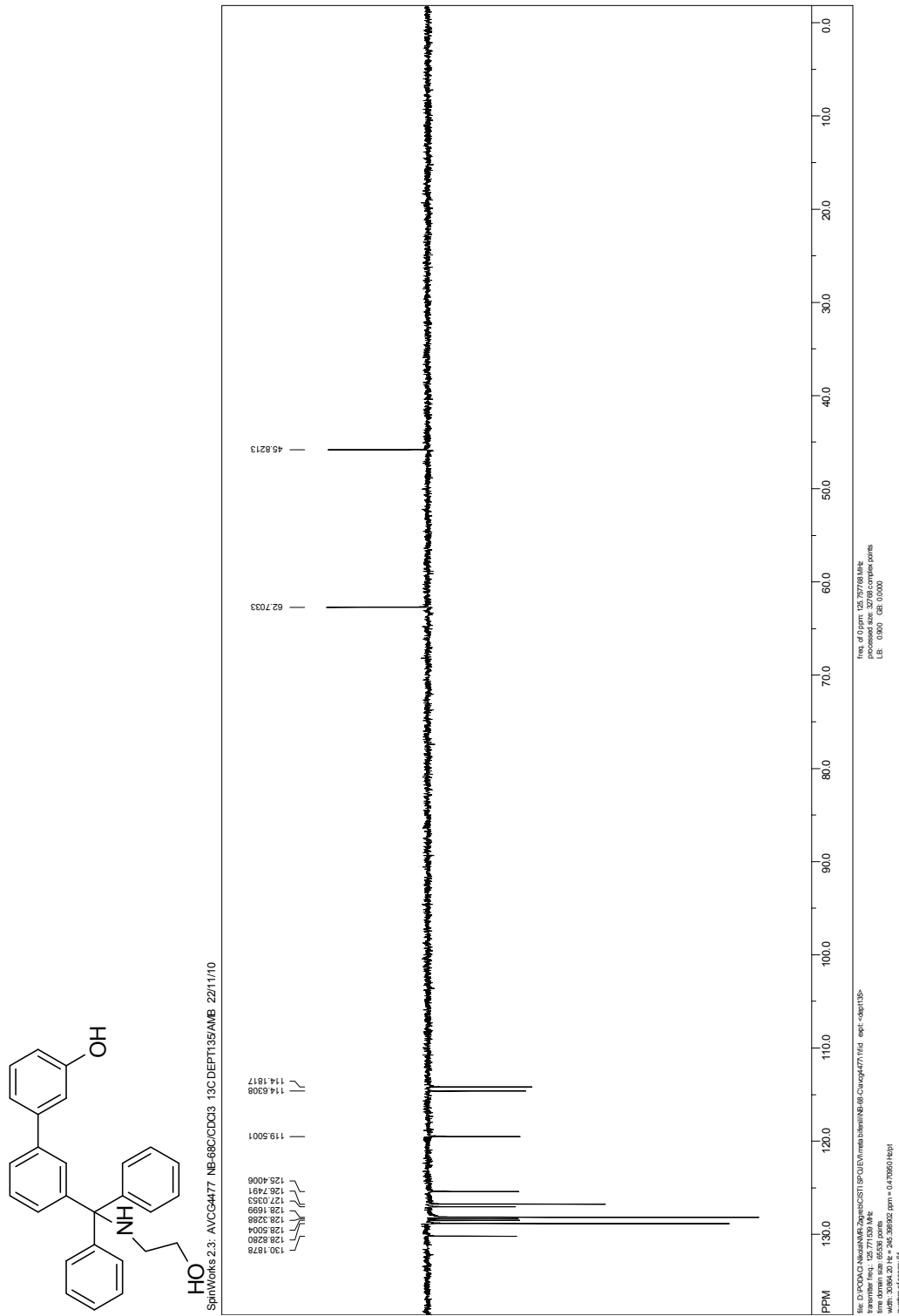
¹H NMR (CDCl₃, 500 MHz) of 14

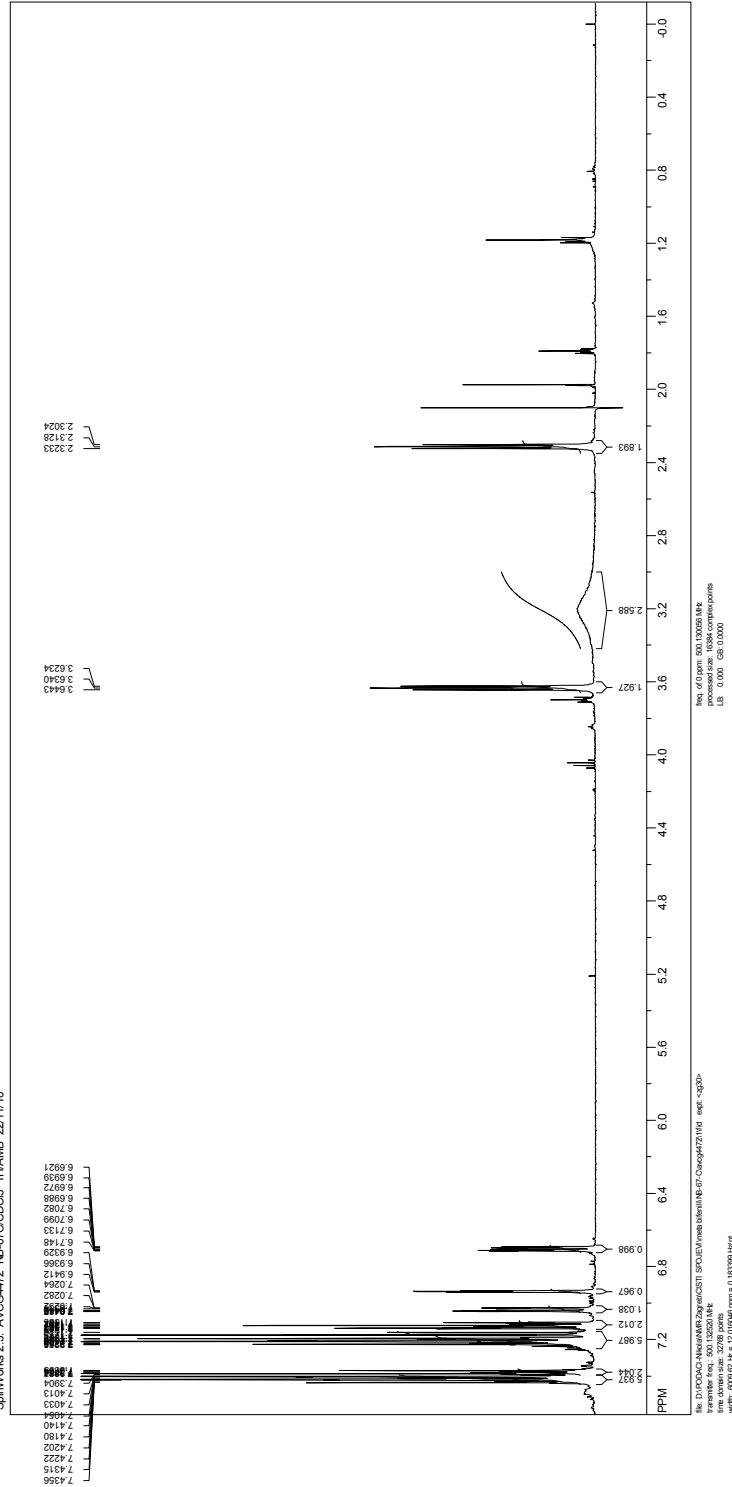
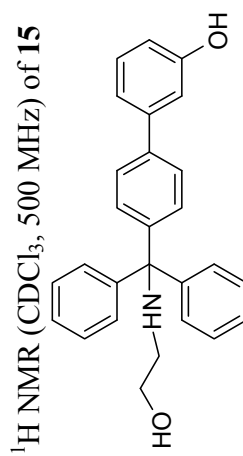


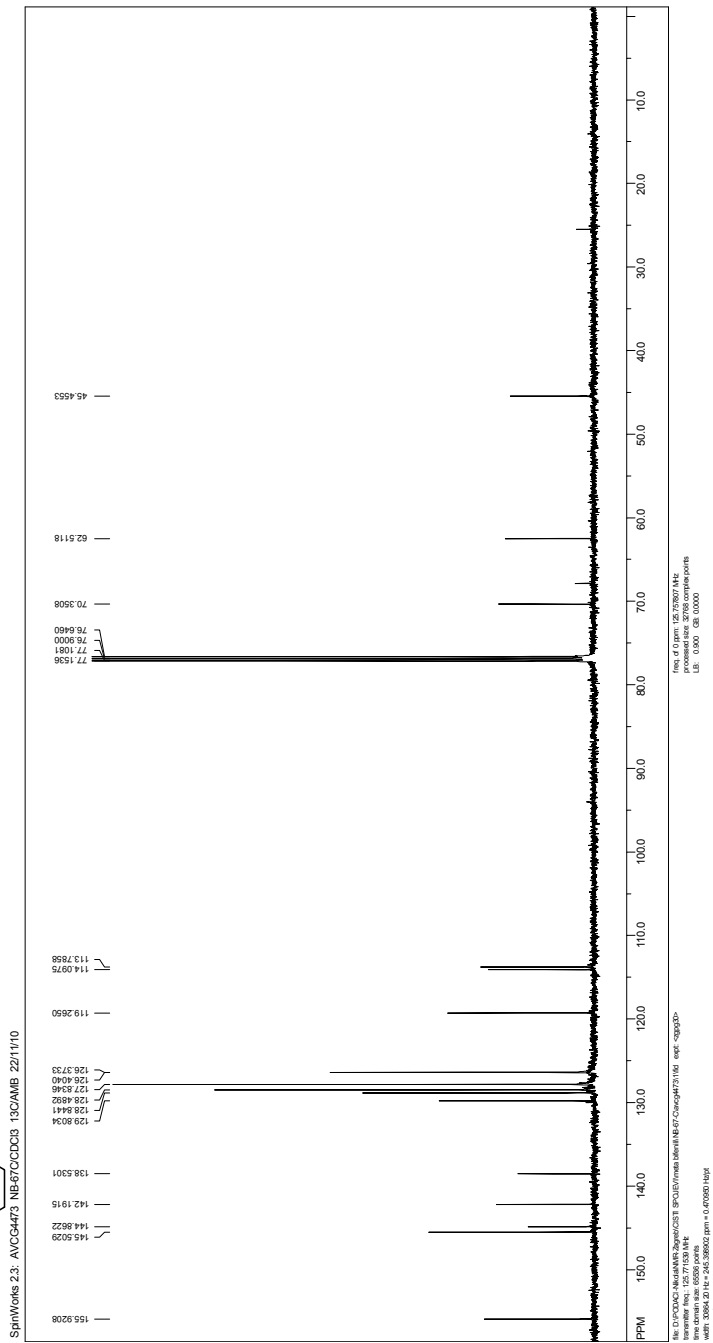
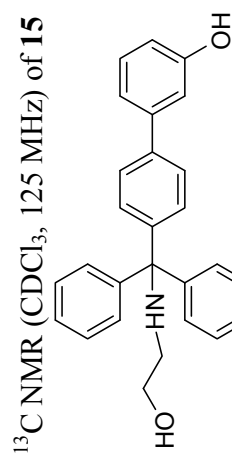
^{13}C NMR (CDCl_3 , 125 MHz) of 14



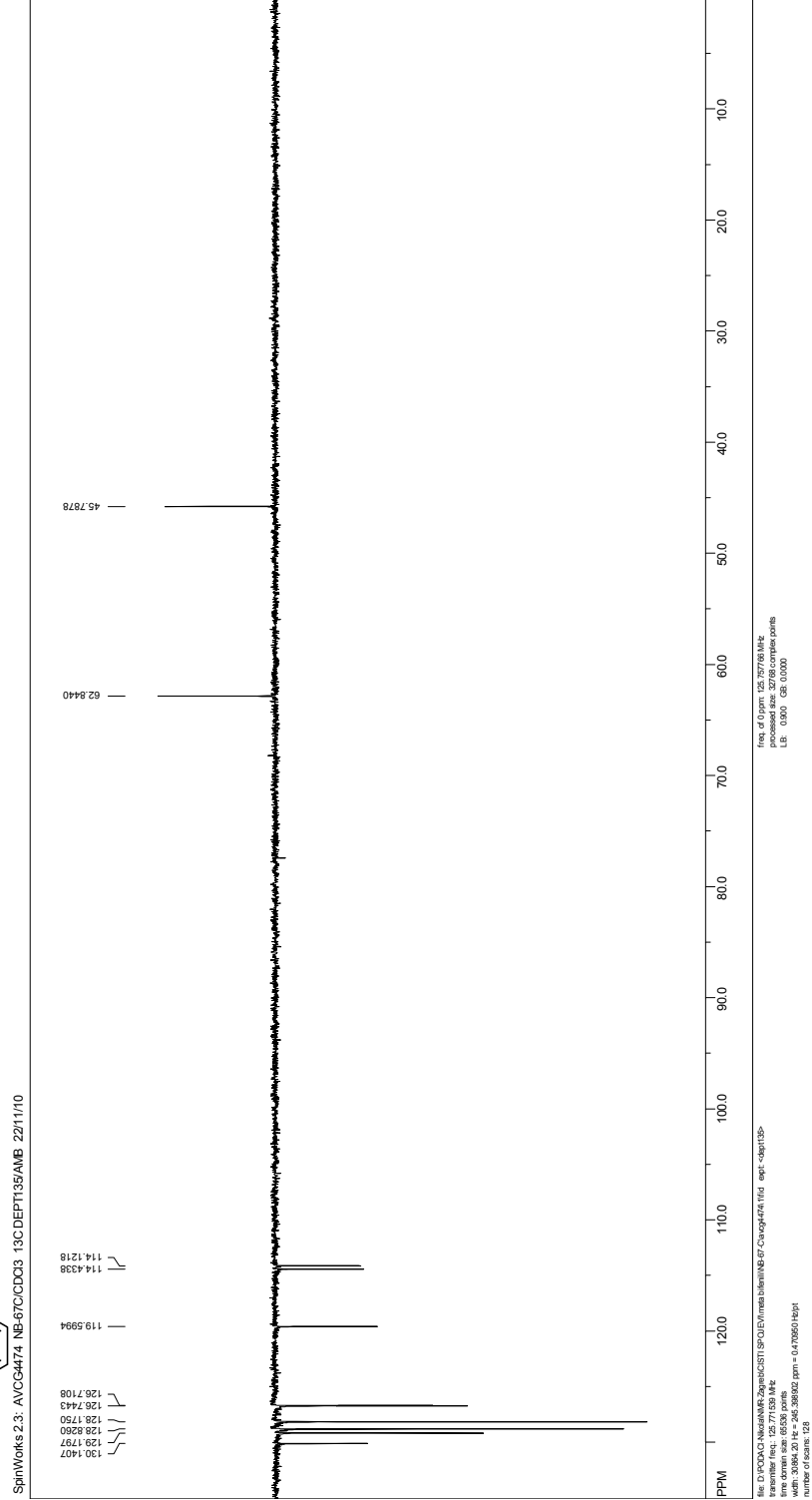
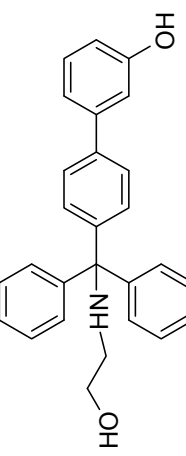
^{13}C NMR (CDCl_3 , 125 MHz, DEPT) of 14



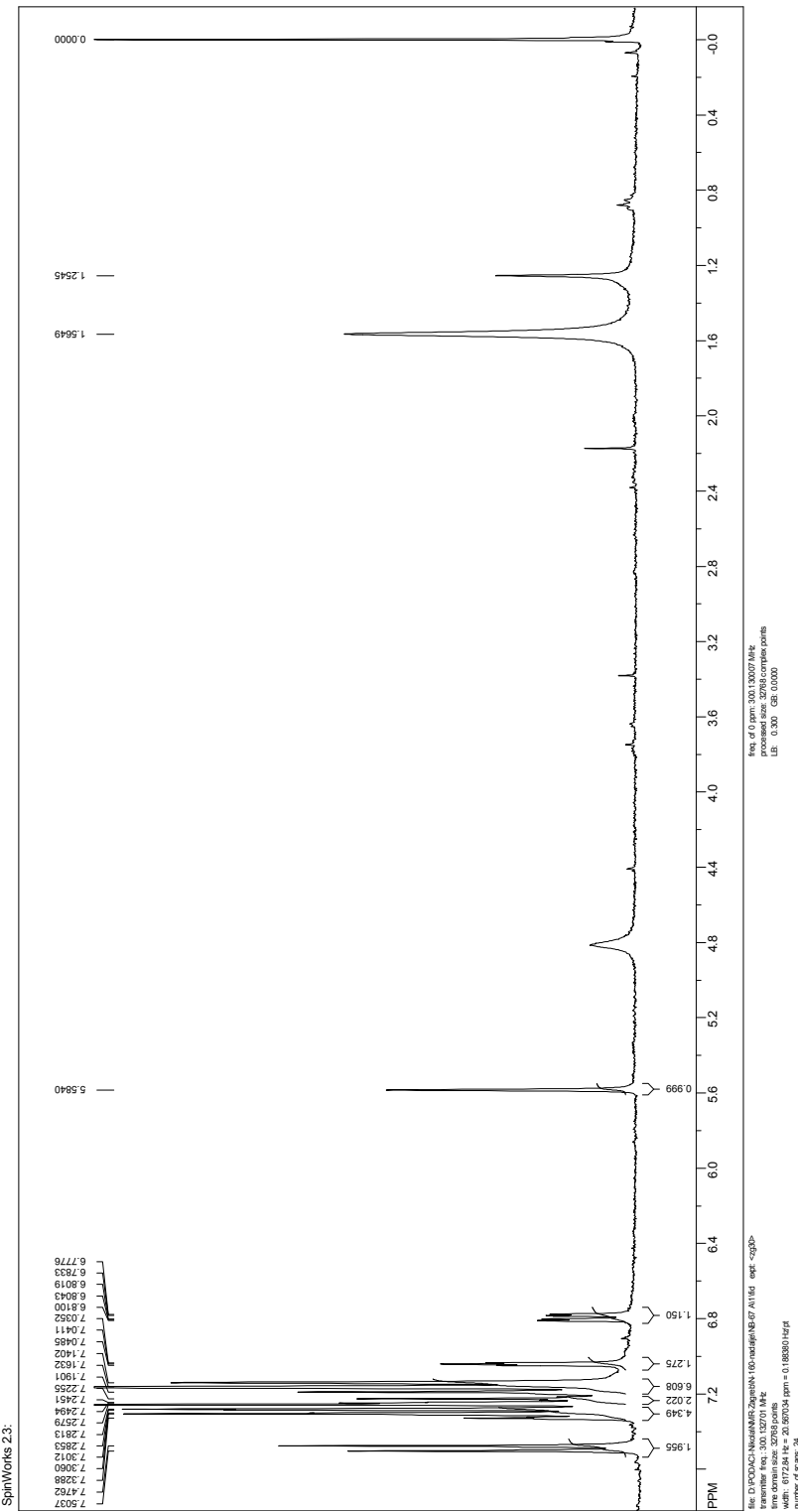
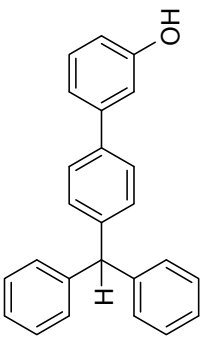


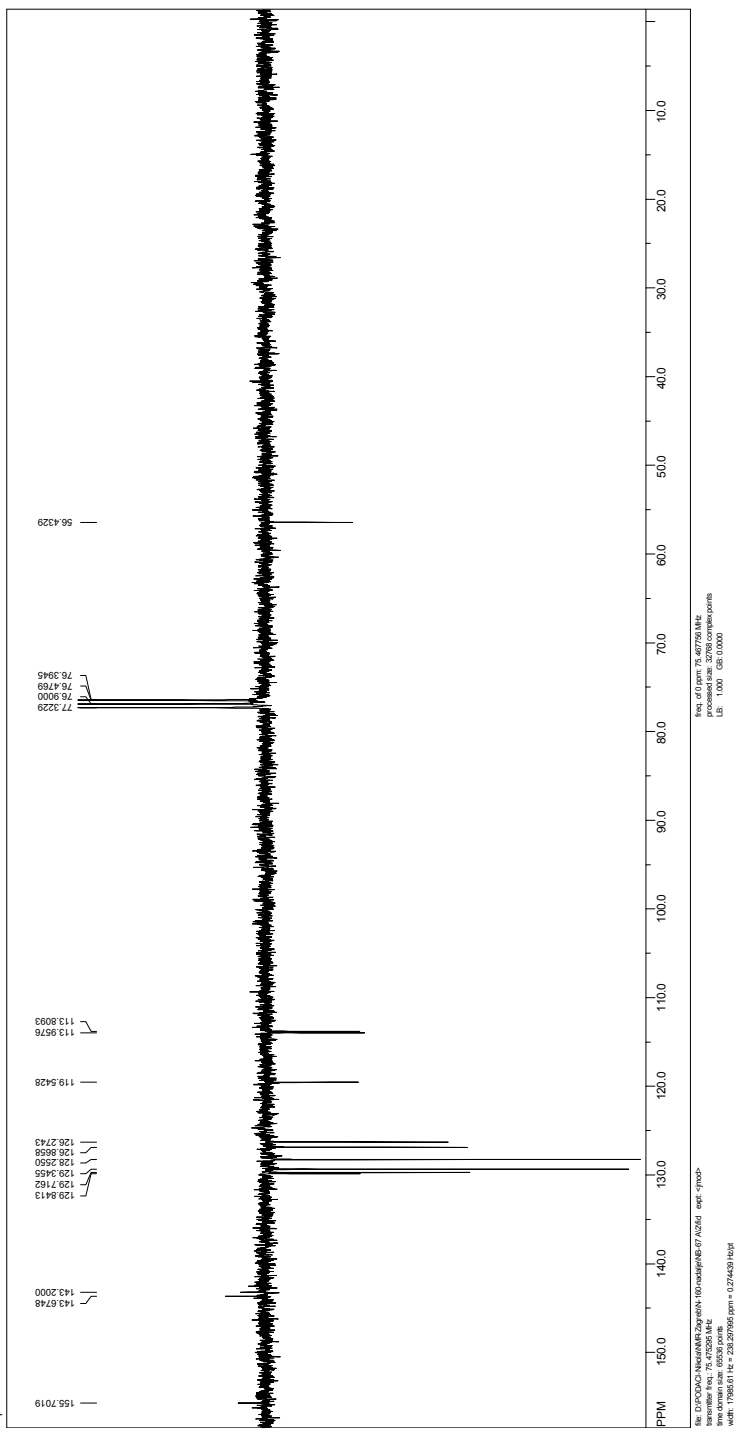
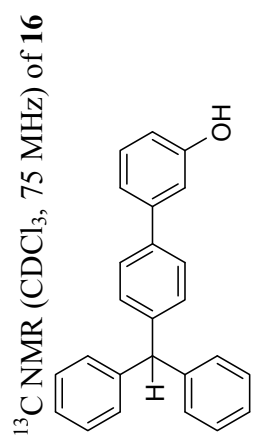


^{13}C NMR (CDCl_3 , 125 MHz, DEPT) of 15

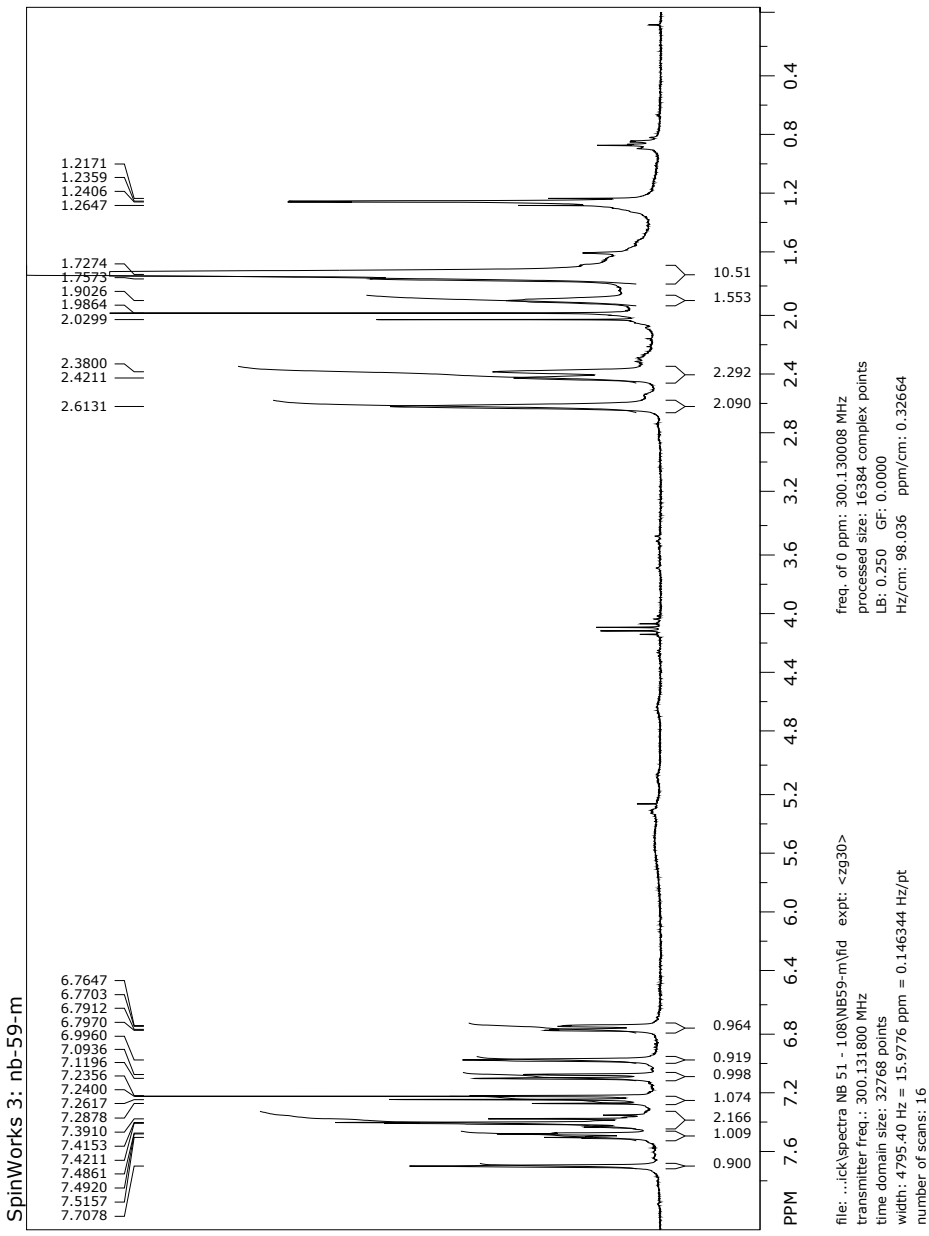


^1H NMR (CDCl_3 , 300 MHz) of 16





^1H NMR (CDCl_3 , 300 MHz) after photolysis of **5** in $\text{CH}_3\text{CN-D}_2\text{O}$



^1H NMR (CDCl_3 , 300 MHz) after photolysis of **6** in $\text{CH}_3\text{CN-D}_2\text{O}$

